



# **The Effect of Ultrasound on Nafion® Polymer in Proton Exchange Membrane Fuel cells (PEMFCs)**

**Haroon Momand**

A Thesis submitted to The University of Birmingham for the  
degree of

**Master of Research (MRes)**

The Centre for Hydrogen and Fuel Cell Research  
PEM Fuel Cell Research group  
School of Chemical Engineering  
College of Engineering & Physical Sciences  
The University of Birmingham

UNIVERSITY OF  
BIRMINGHAM

**University of Birmingham Research Archive**

**e-theses repository**

This unpublished thesis/dissertation is copyright of the author and/or third parties. The intellectual property rights of the author or third parties in respect of this work are as defined by The Copyright Designs and Patents Act 1988 or as modified by any successor legislation.

Any use made of information contained in this thesis/dissertation must be in accordance with that legislation and must be properly acknowledged. Further distribution or reproduction in any format is prohibited without the permission of the copyright holder.

## **Abstract**

The global energy demands are increasing year on year whilst at the same time the proven energy resources are dwindling. Fears over climate change and the rising fuel prices are pushing the industries to look for alternative fuels. Energy from alternative sources is increasingly being promoted as clean, reliable and potentially cheaper source of energy.

The need to understand degradation mechanisms in fuel cells has motivated many efforts to develop and apply advanced high-resolution techniques to characterize multi-scale transport and morphology, and to quantify the state of various chemical species and components before, during and after fuel cell operation. The aim of this study is to investigate whether there is a limiting parameter (time, frequency, power) in ultrasonic treatment that ensures Nafion®'s functionality in the PEMFC, the motivation for this work has arisen due to the wide scale use of Ultrasound in the fabrication of Catalysts inks and other fuel cells materials. The results and findings are listed and discussed in this thesis.

According to the results of this study it was found that ultrasound degrades the Nafion® polymer. The most extensive degradation was observed at the lowest frequency when the input power was above the cavitation threshold of 0.32 W. It was observed that above 11.28W, there was an increase in the number of bubbles produced this can be attributed to the decrease in the degradation rate. A possible explanation could be that it led to a decrease in ultrasonic efficiency through the solution thereby reducing the cavitation effect.

Sonication of Nafion® solutions over various periods of times revealed a steady decrease in viscosity however, at a minimum irradiation time and a fixed ultrasonic frequency an increase in the viscosity of Nafion® polymer was observed. This was attributed to the fact that scission of polymer bonds caused by ultrasound (i.e depolymerisation) supplies new chain carriers for polymerisation. Under carefully chosen conditions, it was possible to initiate polymerization reactions using ultrasound. 30 minutes ultrasound at 1.86 W using ultrasonic probe.

Various analytical methods were used such as Rheology to measure viscosity, Differential Scanning Calorimetry (DSC) and Spectroscopic methods (NMR and GC MS) to elucidate any changes in Nafion® structure, chemical and physical properties following ultrasound irradiation.

From DSC measurements it was found that sonicating Nafion® at various time periods at a specific ultrasound frequency resulted in an increase in the glass transition temperature (T<sub>g</sub>) by 8°C. For example after 30 minutes sonication using ultrasound probe at 1.86 W. DSC analysis also revealed that there were no changes in T<sub>g</sub> of Nafion® below, 10 minutes sonication using ultrasound probe at power of 3.84 W. For example the T<sub>g</sub> was 148°C analogous to the literature T<sub>g</sub> for Nafion®. It was established that the samples which showed sudden increase in viscosity also showed an increase in glass transition temperature due to improved morphology in the Nafion® structure. Therefore it was concluded that there is a link between ultrasound irradiation frequency at specific time intervals and the glass transition temperature.

The effect of high shear mixing showed very little degradation of Nafion® compared to ultrasound, and DSC results of high shear mixing showed no changes in T<sub>g</sub> values.

In addition GC/MS was used to characterize any possible degradation mechanisms and to observe any changes in the structure of Nafion® before and after sonication, however the results were inconclusive.

## **Acknowledgements**

I would like to begin by thanking Professor Bruno Pollet for encouraging me throughout the course. I am extremely grateful for having Bruno as my advisor. The amount of lab space which I was permitted to use is also gratefully acknowledged.

Bruno functioned as my main advisor and it was under his guidance that I carried out my research. Bruno was an absolutely outstanding advisor. He very kindly gave of his time during important meetings and was very tolerant in explaining concepts that were new to me. I am grateful for the freedom Bruno allowed me as I spent month long stretches doing experiments and, giving him updates. Furthermore, Bruno was quick in responding to my emails and proof-reading my work. Next, I would like to acknowledge and thank all the members of the Fuel cell group who welcomed my presence in the lab, and patiently explained various aspects. Fuel cell members during my tenure here include Dr Shangfeng Du, Oliver Curnick, Dr Aman Dhir, Jonathan Goh, Cheng Peng and James Courtney.

Jonathan has been a great labmate—being excellent at coming out with good ideas, insightful, fun, and offering significant advice when needed. Cheng Peng worked on related project and he was very generous about sharing ideas, time, supplies, journal, articles, etc. and was useful to work with. I am also extremely thankful to Professor Robert Steinberg and Dr Bushra-Al-Duri for their help.

Thanks to James Bowen of the chemical Engineering lab for teaching me how to use Rhemoeter. Thanks to Dr Shangfeng Du for teaching me how to operate DSC.

I am forever grateful of the support and love of my family. And most importantly I am extremely grateful to God for everything.

## LIST OF FIGURES

Figure 1 Showing crude oil production and demand (BP 2011) -----	14
Figure 2 showing annual mean CO <sub>2</sub> concentration from the Mauna Lao Observatory -----	15
Figure 3 Schematic Representation of PEM FUEL CELL (Leblanc 2010)-----	16
Figure 4 The various loses and resulting polarisation curves.(Barbir)-----	19
Figure 5 Cavitation bubble formation at various stages during alternating compression and rarefaction cycles of the ultrasonic wave and asymmetric bubble collapse on a surface leading to (i) high energy with temperature up to 5000 K and pressure of up to 200 atms and (ii) the sonolysis of water caused by the high energy where OH. are hydroxyl radicals, HO <sub>2</sub> are perhydroxyl radicals and H <sub>2</sub> O <sub>2</sub> is hydrogen peroxide. -----	25
Figure 6 Reaction mechanism of ultrasound-induced radical polymerization, assuming intrinsic polymerization and avoiding thermal initiation. -----	27
Figure 7 The molecular formula of Nafion® -----	29
Figure 8 Chemical structures and solid-state 19FNMRspectra of Nafion® 117. Asterisks indicate spinning side bands. The given spectra are normalized to the dominant peak of the backbone CF2 groups. -----	35
Figure 9 Solid-state 19FNMRspectra of Nafion® 117 samples after treatment with 0.1M Fe <sup>2+</sup> in 30 v/v% H <sub>2</sub> O <sub>2</sub> . The line widths, $\frac{1}{2}$ , of the peak at -121 ppm, referring to the backbone CF2 groups, are shown. Exposure times are given to the left of the figure.-----	36
Figure 10 Solid-state 19F NMR spectra of Nafion® 117 samples after 3 h of with different Fe <sup>2+</sup> concentrations, as indicated, in 30 v/v% H <sub>2</sub> O <sub>2</sub> solutions. The line widths, $\frac{1}{2}$ , of the peak due to the backbone CF2 groups are shown. -----	37
Figure 11 . Solid-state 19F NMR spectra of Nafion® 117 samples after Fenton tests with 0.0002M Fe <sup>2+</sup> in 30 v/v% H <sub>2</sub> O <sub>2</sub> . Exposure times are given to the left of the figure. -----	39
Figure 12 ATR-IR spectra of Nafion® 117 samples after Fenton tests with 0.0002M Fe <sup>2+</sup> in 30 v/v% H <sub>2</sub> O <sub>2</sub> . -----	39
Figure 13 Total ion chromatograms obtained with SPME/GC–MS of (a) the reaction mixture at time zero containing 40 µg l <sup>-1</sup> of each phthalate (i.e. initial overall phthalates concentration of 240 µg l <sup>-1</sup> ) where (1)-----	42
Figure 14 Chromatograms of Mowilith® 50 obtained by Py–GC/MS analysis: (a) 300 °C;(b) 400 °C; (c) 500 °C; (d) 600 °C; (e) 700 °C; mixture: CO, CO <sub>2</sub> and H <sub>2</sub> O; CPT, 1-3- cyclopentadiene. (Wei 2012)-----	43
Figure 15 Sonochemical [(a) Sonics 20KHz ultrasonic probe system; (b) Sonomatic 40KHz ultrasonic bath system used for Sonication studies on Nafion® . (Pollet 2010)-----	46
Figure 16 Showing complete setup of AR 2000 Rhemoeter -----	50
Figure 17 Complete Perkin Elmer Pyris 1 Differential Scanning Calorimeter Setup -----	52
Figure 18 Schematic representation of High Shear Mixer-----	54
Figure 19 showing jacketed reactor-----	55
Figure 20 Graph showing viscosities (η) of different concentration Nafion® solutions at no ultrasound and constant temperature of 25°C-----	57
Figure 21 Graph showing Tg of Nafion® of control experiment with no ultrasound and no high shear mixer. -----	58
Figure 22 Showing The Effect of Temperature On 2.5% Nafion® at 60 Minutes at Various Temperature-----	60
Figure 23 Graph Showing change in Viscosity for 5% Nafion® At Shear Rates of 5000 rpm -----	62

Figure 24 Graph Showing change in Viscosity ( $\eta$ ) for 5% Nafion® At Shear Rates of 10,000 rpm --	63
Figure 25 Graph showing No change of Tg for Nafion® 10% In THF 5 Minutes High Shear Mixer (HSM) 5000 rpm-----	64
Figure 26 Graph showing No change of Tg for Nafion® 10% In THF 30 Minutes High Shear Mixer (HSM) 5000 rpm-----	64
Figure 27 Graph showing Decrease in Tg for Nafion® 10% In THF 10 Minutes High Shear Mixer (HSM) 10,000 rpm -----	65
Figure 28 Graph Showing Decrease inTg for Nafion® 10% In THF 5 Minutes High Shear Mixer (HSM) 10,000 rpm -----	65
Figure 29 Showing effect of ultrasound on Different Nafion® Concentrations at 30 minutes using ultrasound Probe %20amp at 25°C-----	67
Figure 30 Showing Change in Viscosity $\eta$ of 5% Nafion® solution Using Ultrasonic bath and Probe Over 120 minutes at 25°C-----	70
Figure 31 Showing Change in Viscosity ( $\eta$ ) of 2.5% Nafion® Solution Using Ultrasonic Probe at 20%, 40 %, 60% and 80 % AMP Over 120 minutes at 25°C -----	71
Figure 32 Showing Change in Viscosity ( $\eta$ ) of 5% Nafion® Solution Using Ultrasonic Probe at 20%, 40 %, 60% and 80 % AMP Over 120 minutes at 25°C-----	75
Figure 33 Showing Change in Viscosity ( $\eta$ ) of 7.5% Nafion® Solution Using Ultrasonic Probe at 20%, 40 %, 60% and 80 % AMP Over 120 minutes at 25°C -----	78
Figure 34 Showing Comparison between Changes in Viscosity ( $\eta$ ) of 10% Nafion® Using Ultrasonic Probe vs Ultrasound Bath Over 120 minutes at 25°C-----	82
Figure 35 Showing Change in Viscosity ( $\eta$ ) of 10% Nafion® Solution Using Ultrasonic Probe at 20%, 40 %, 60% and 80 % AMP Over 120 minutes at 25°C-----	83
Figure 36 Graph showing comparison between change in viscosity ( $\eta$ ) for different concentration Nafion® solutions sonicated with 20%AMP ultrasound probe over 120 minutes at 25°C-----	85
Figure 37 Showing Difference in Viscosity ( $\eta$ ) of 5% Nafion® Using Ultrasonic Bath Over 120 minutes vs Overnight Sample at 25°C-----	87
Figure 38 Bar Chart showing comparison between fresh and overnight Nafion® Solution in water and THF -----	87
Figure 39-----	90
Figure 40 Graph Showing Increase in Tg for 5wt% Nafion® Sonicated for 30min with US Probe 20AMP% Fast Scan -----	90
Figure 41 Graph Showing Increase in Tg of Nafion® 5% wt Sonicated for 30min with US Probe 20% Fast Scan 2 <sup>nd</sup> sample -----	91
Figure 42 Graph Showing Increase in Tg for Nafion® 5% wt Sonicated for 30min with US Probe 20%AMP Fast Scan 3 <sup>rd</sup> sample -----	91
Figure 43 Graph Showing Increase in Tg for Nafion® 5% wt sonicated for 60min using US Probe 40 AMP% Fast Scan sample 1 -----	92
Figure 44 Graph showing Increase in Tg for Nafion® 5% wt Sonicated for 60min using US Probe 40%AMP Slow Scan sample 2 -----	92
Figure 45 Graph Showing Increase in Tg for Nafion® 5% wt Sonicated for 60min using US Probe 40%AMP Slow Scan sample 3 -----	93
Figure 46 Graph Showing no change in Tg for Nafion® 10% in THF Sonicated for 20 Min with Us Probe 40%AMP -----	93
Figure 47 Graph showing no change in Tg for Nafion® 10% in THF Sonicated for 20 Min with Us Probe 40%AMP 20hr Dry -----	94

Figure 48 Graph Showing No change in Tg for Nafion® 10% in THF Sonicated for 10 Min Using US Bath 18hr Dry-----	94
Figure 49 Graph Showing No change in Tg for Nafion® 10% in THF Sonicated for 10 Min Using Us Probe 40%AMP -----	95
Figure 50 Graph Showing Decrease in Tg for 10% Nafion® in THF Sonicated for 120 Min Using Us Probe 20% AMP -----	95
Figure 51 Graph Showing Decrease in Tg for 10% Nafion® in THF Sonicated for 60 Min Using Us Probe 20% AMP -----	96
Figure 52 graph of ln A vs Sonication time For 2.5% Nafion® Solution-----	106
Figure 53 Graph showing the relationship between the calculated Rate constant and Reverse Concentration-----	107

## LIST OF TABLES:

Table 1 Showing the parameters and variables used during the experiments .....	48
Table 2 Showing the viscosity of different Nafion® solution's under controlled conditions .....	57
Table 3 Showing The Effect of Temperature On 2.5% Nafion® at 60 Minutes at various temperatures .....	60
Table 4 The effect of high shear mixer on 5% Nafion® At Shear Rates of 5000 rpm .....	61
Table 5 The effect of high shear mixer on 5% Nafion® At Shear Rates of 10,000 rpm .....	62
Table 6 Showing effect of ultrasound on Different Nafion® Concentrations at 30 minutes using ultrasound Probe %20AMP at 25°C.....	67
Table 7 Showing change in viscosity for 5% Nafion® solution using ultrasonic bath and Probe over 120 minutes at 25°C .....	69
Table 8 Showing Change in Viscosity ( $\eta$ ) of 2.5% Nafion® Solution Using Ultrasonic Probe at 20%, 40 %, 60% and 80 % AMP Over 120 minutes at 25°C .....	71
Table 9 Showing Change in Viscosity ( $\eta$ ) of 5% Nafion® Solution Using Ultrasonic Probe at 20%, 40 %, 60% and 80 % AMP Over 120 minutes at 25°C .....	75
Table 10 Showing Change in Viscosity ( $\eta$ ) of 7.5% Nafion® Solution Using Ultrasonic Probe at 20%, 40 %, 60% and 80 % AMP Over 120 minutes at 25°C .....	78
Table 11 Showing Comparison between Changes in Viscosity ( $\eta$ ) of 10% Nafion® Using Ultrasonic Probe vs Ultrasound Bath Over 120 minutes at 25°C.....	82
Table 12 Showing Change in Viscosity ( $\eta$ ) of 10% Nafion® Solution Using Ultrasonic Probe at 20%, 40 %, 60% and 80 % AMP Over 120 minutes at 25°C .....	83
Table 13 Showing variations in Viscosity ( $\eta$ ) of 5% Nafion® Using Ultrasonic Bath Over 120 minutes vs Overnight Sample at 25°C.....	86
Table 14 Table showing increase and decrease in Tg for different Nafion® samples at different experimental condition .....	97
Table 15 showing the calculated rate constants for Nafion® at various concentrations .....	106
Table 16 Showing reverse concentratin vs K values .....	106



## Table of Contents

1. CHAPTER 1 .....	12
1.1. Motivation for this work .....	12
1.2. Introduction.....	13
1.3. Theory.....	17
1.4. Membrane Electrode Assembly (MEA) .....	20
1.5. Function Of The Nafion® Membrane In MEA .....	20
2. CHAPTER 2 ULTRASOUND AND SONOCHEMISTRY .....	22
2.1. What Is Ultrasound .....	22
2.2. Sonochemistry and Applications .....	22
Applications .....	23
2.3. Effect of Sonication on Polymers.....	24
2.4. Sonochemical Degradation of Nafion® .....	24
2.5. Polymerization Due To Ultrasound Induced Cavitation .....	26
2.6. Degradation Mechanism of Nafion® .....	28
2.7. Sonochemical Degradation of Polymers Quantified by GC/MS .....	41
2.8. Degardation of Polymers Quantified by GC/MS.....	43
3. CHAPTER 3 EXPERIMENTAL METHODS AND MATERIALS .....	45
3.1. Experimental Plan .....	45
3.2. Experimental Setup .....	46
3.3. Experimental Procedures.....	46
3.3.1. Ultrasound bath 40kHz.....	46
3.3.2. Ultrasound probe 20kHz .....	47
3.4. Experimental Apparatus.....	47
3.5. Materials List .....	47
3.6. Nafion® Sample Preparation .....	48
3.7. Experimental Parameters and Variables.....	48
3.8. Power Measurements .....	48
3.9. Depth of the Horn .....	49
3.10. Equipment setup.....	49
A. Ultrasonic bath.....	49
B. Ultrasonic Probe.....	49
C. Rheometer .....	50
D. Sample Preparation for DSC Analysis .....	51

E.	Differential Scanning Calorimetry Apparatus .....	51
F.	GC/MS Analysis .....	53
	Gas chromatography (GC) .....	53
	Mass Spectrometer (MS) .....	53
	Computer .....	54
G.	High shear mixer .....	54
3.11.	Temperature Control .....	55
3.12.	Volume Used .....	55
4.	CHAPTER 4 RESULTS AND DISCUSSION .....	56
4.1.	Silent Conditions.....	56
4.1.1.	The Effect of Ultrasound on Nafion® At Various temperatures .....	56
4.1.2.	Effect of Nafion® Concentration .....	57
4.1.3.	The Effect of Temperature on Nafion® .....	58
4.1.4.	Effect of High Shear Mixing on Nafion® in the Absence of Ultrasound .....	61
4.1.5.	DSC measurement Of High Shear mixed Nafion samples .....	63
4.2.	Ultrasonic Conditions .....	66
4.2.1.	Effect of Nafion® Concentration.....	66
4.2.2.	5% Nafion® Solutions Sonicated at 0.32 W (Bath) .....	68
4.2.3.	2.5 Nafion® Solution Sonicated at Different Powers With US (Probe) .....	71
4.2.4.	5% Nafion® Solution Sonicated at Different Powers With US (Probe).....	75
4.2.5.	7.5% Nafion® Solution Sonicated at Different Powers With US (Probe) .....	78
4.2.6.	10% Nafion® Solutions Comparison between Bath and Probe.....	81
4.2.7.	10% Nafion® Solution Sonicated at Different Powers With US (Probe) .....	83
4.2.8.	Viscosity Variations between Overnight and Fresh samples .....	85
4.2.9.	DSC ANALYSIS.....	88
	Differential Scanning Calorimetry (fig 39 to fig 45 shows increase in Tg).....	90
	Nafion® 10% in THF 20 Min Us Probe 40% (Fig 46 to Fig 49 no change in Tg) .....	93
	Nafion® 10% in THF 60 And 120 Min Us Probe 20% (Fig 50 to Fig 51 Decrease in Tg) .....	95
4.2.10.	Summary of the 4 different Nafion® concentrations at 4 different powers .....	96
4.2.11.	Advantage of Increase in Tg of Nafion® .....	98
4.2.12.	GC/MS Analysis of Sonicated Samples .....	99
5.	CHAPTER 5 KINETICS .....	101
5.1.	Kinetics of Degradation .....	101
5.2.	Calculation of Rate Constants for Different Ultrasound Powers .....	102

5.3.	Viscosity and Molecular Weight Relationship .....	104
5.4.	Sample Calculation of Rate Constant .....	105
6.	CHAPTER 6 FURTHER WORK .....	108
6.1.	MEA Preparation for Ultrasound Effects .....	108
6.2.	Testing Of MEA with Nafion® Incorporated Membrane.....	109
6.3.	Structural Changes following Ultrasonic Treatment of Nafion® .....	109
6.4.	Determination of Mechanical properties After Sonication .....	110
6.5.	Additional Work .....	110
7.	CHAPTER 7 CONCLUSION.....	111
7.1.	Conclusions.....	111
	References .....	113

## Nomenclature and Abbreviations

*MEA – Membrane Electrode Assembly*

*GDE – Gas Diffusion Electrode*

*ORR – Oxygen Reduction Reaction*

*PAFC – Phosphoric Acid Fuel Cell*

*PEM – Proton Exchange Membrane*

*PEMFC – Proton Exchange Membrane Fuel Cell*

*SOFC – Solid Oxide Fuel cell*

*$P_A$  – Acoustic Pressure (kPa)*

*$P_M$  – Amplitude (Pa)*

*– Frequency kHz*

*$P$  – Pressure (Pa)*

*$V_R$  – wall velocity ( $\text{ms}^{-1}$ )*

*$R_m$  – maximum bubble radius ( $\mu\text{m}$ )*

*$P_h$  – External Pressure (kpa)*

*$R$  – Instantaneous radius ( $\mu\text{m}$ )*

*$M$  – Total Molar Concentration ( $\text{mol/m}^3$ )*

*$k$  – Rate constant ( $\text{min}^{-1}$ )*

*$M_0$  – initial total molar concentration ( $\text{mol/m}^3$ )*

*$M_n$  – number average molecular weight (g/mol)*

*$M_v$  – average viscometric molecular weight (g/mol)*

*$\eta$  – Intrinsic viscosity (pa.s)*

*$M_t$  – average molecular weight at irradiation time  $t$  (g/mol)*

*$E$  – Electrode potential (V)*

*$E_{rev}$  – Reversible Potential (V)*

*$b$  – Tafael slope ( $\text{V dec.}^{-1}$ )*

*$i$  – Current density ( $\text{A.m}^{-2}$ )*

*$i_0$  – exchange current density ( $\text{A.m}^{-2}$ )*

*$n$  – Number of electrons transferred in the redox reaction*

## 1. CHAPTER 1

### 1.1. Motivation for this work

The motivation for this work has arisen due to the wide scale use of Ultrasound in the fabrication of Catalysts inks and other fuel cells materials. It is shown that the sonochemical production of carbon supported mono- and bi-metallic catalysts gives excellent electrochemical activity due to surface functionalization of the support and better dispersion induced by ultrasound. These observations are mainly due to enhanced mass-transfer caused by asymmetrical collapse of cavitation bubbles at the surface support leading to the formation of high velocity jets of liquid being directed toward its surface. This jetting, together with acoustic streaming, is thought to lead to random punctuation and disruption of the mass transfer at the surface. The search for new polymers with better properties is of great research interest, the polymer industry requires constant advances in existing materials. Due to this large efforts are carried out for modifying existing polymers. i.e, the interaction of an object with its environment is significantly determined by its surface properties. The capability to alter the surface properties of a low-cost commodity polymer is therefore of great importance for economical aspect. Similarly, improvement in the properties of a bulk polymer by incorporating little amounts of other compounds is an economical way of producing extremely functional materials. Additionally, the material properties shown by a particular polymer depend seriously on its molecular weight and chain structure so these must be accurately controlled. Sonochemistry has a part to play in each of these areas. The effect of ultrasound on other polymers has shown some interesting results such as increase in the glass transition temperature which will increase the durability of the Nafion polymer. Ultrasound has been used as method to control the polymerization rate and hence the properties of the resulting polymer. Consequently the effect of ultrasound was investigated to see if there is a limiting parameter in ultrasonic treatment (time, frequency, power) that ensures Nafion® functionality in the PEMFC.(Pollet 2010)

## 1.2. Introduction

There is no doubt that the world economies are inextricably linked to energy usage. Since the 1980's; for every 1% growth in GDP in any region, there has been 0.3% increase in primary oil demand. Most of the Western economies have already developed and have reached a stable phase, whereas economically poorer countries such as China and India for example, are now growing at an alarming rate. The problem they are faced with is resource scarcity. China and India have two of the largest populations on the planet and as the number of middle class people in those countries increase, they will require more luxury and hence their energy usage will increase. This problem is not unique to developing countries as populations in the Western world also demand an increase in living standards which, in the current paradigm, come with increasing energy usage.(BP 2011)

Transportation is the lifeblood of the world economy. Each day, millions of goods are delivered from one place to another whether by road, air or sea – consuming vast amounts of energy in the process. This energy mainly comes from crude oil derivatives such as petroleum, diesel and kerosene. Whilst crude oil is abundant, the world economy can continue to expand as more and more transactions are able to be performed but once crude oil gets scarce, the prices rise, leading to a price increase in derivatives and straining the global transportation system. Evidence is now emerging that shows that conventional crude oil is beginning to plateau, whilst the demand continues to rise.

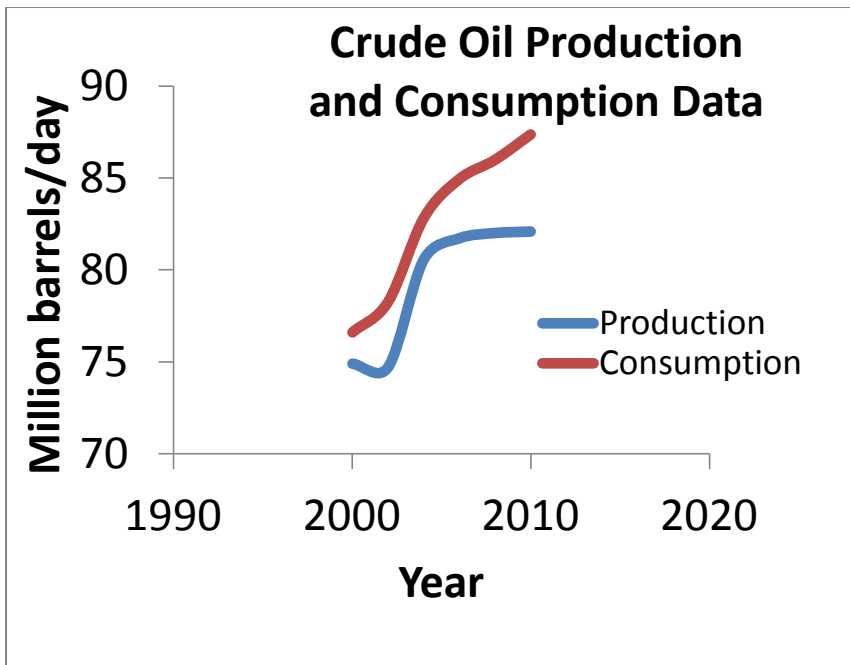


**Figure 1 Showing crude oil production and demand (BP 2011)**

According to the BP statistical review 2011, the gap between supply and demand is being offset by biofuels, coal to liquids, Liquefied Natural Gas and unconventional sources such as oil from tar sands and ‘tight oil’ from shale fields. BP also claims that the world has 46.2 years of crude oil supply left assuming that the current consumption rates remain as they are and no new oil fields are found. (BP 2011)

Apart from crude oil depletion, another major concern is climate change. The continuous burning of fossil fuels has released vast amounts of greenhouse gases such as CO<sub>2</sub> into the atmosphere and these gases absorb infrared radiation, which would normally radiate out into space. The heat energy thus remains on Earth thus heating up the planet. The concentration of CO<sub>2</sub> has steadily increased since records first began in 1959 as shown by Figure 2. The concentration has increased from 315.97 to 391.57 ppm in 2011, making it the highest concentration of CO<sub>2</sub> in the atmosphere in the last 420’000 years.(J. R. Petit 1999)

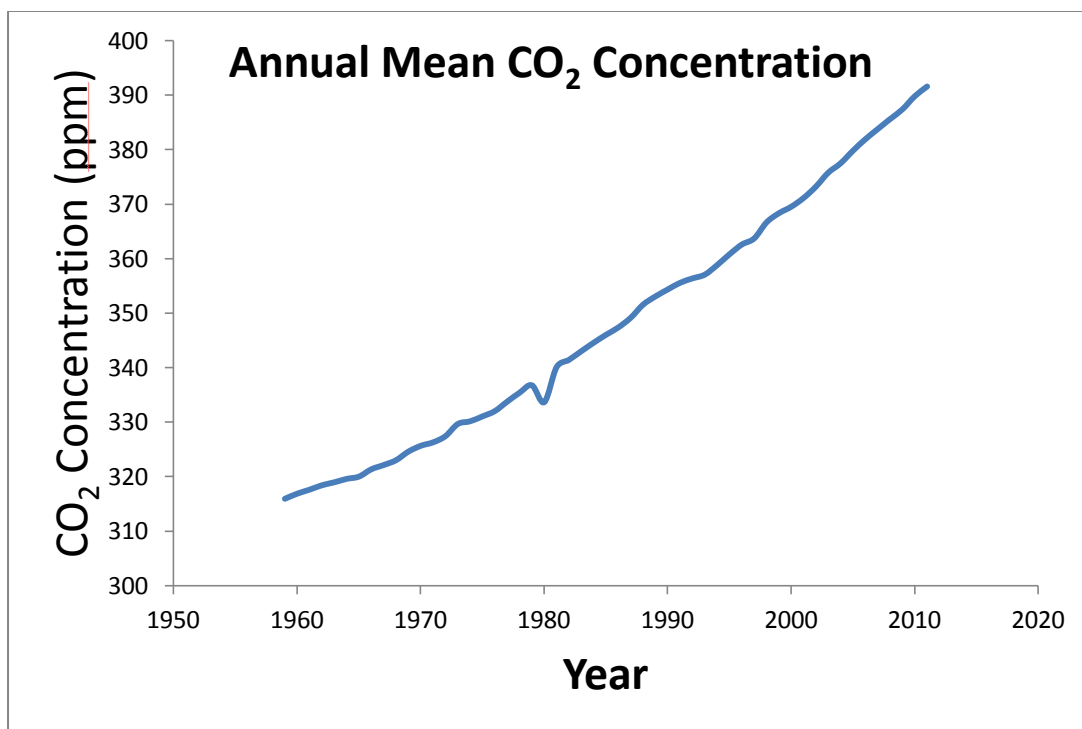
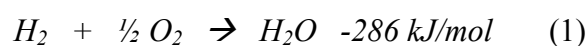


Figure 2 showing annual mean CO<sub>2</sub> concentration from the Mauna Lao Observatory

The biggest challenge, by far, is how to adapt to a ‘post oil’ world. A post oil world would consist of a world that is not fuelled by fossil fuels but rather by technologies that can be sustained for a long period of time and ones which would cause minimal damage to the environment. Hydrogen is one such alternative as it meets all the criteria – it is abundant so there is no problem of scarcity and it produces water via the reaction below meaning that no polluting substances are formed. To use Hydrogen for transportation purposes, the most efficient method is via a fuel cell – in particular, a Proton Exchange Membrane Fuel Cell or PEMFC.





Currently PEM fuel cells show a lot of promise but they have issues such as durability and the costs are high which present barriers to the commercialization. Although the on-going research in fabrication methods have shown promising future for the commercialization of PEM fuel cells.

Proton exchange membrane fuel cells (PEMFCs) are used in the automotive and domestic sectors. (PEMFCs) are characterized by their polymer electrolyte membrane and their low temperature range of 50 to 100°C. Below is a schematic representation of a PEM Fuel Cell.(Leblanc 2010)

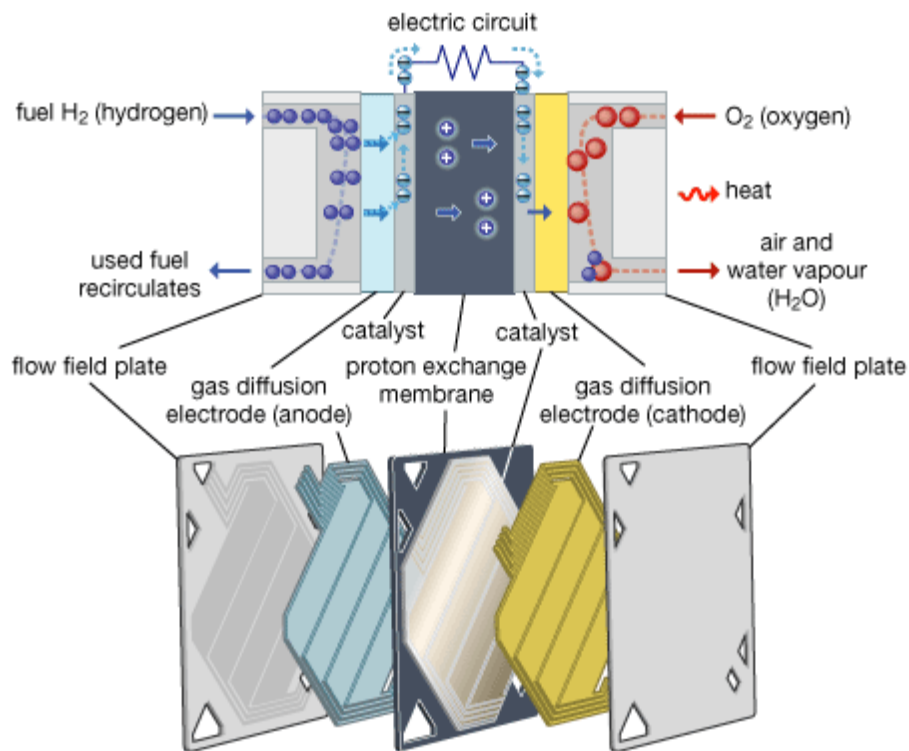
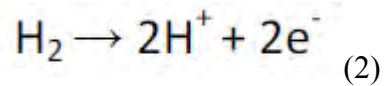


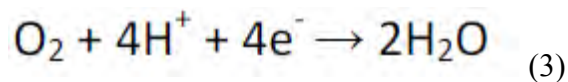
**Figure 3 Schematic Representation of PEM FUEL CELL (Leblanc 2010)**

### 1.3. Theory

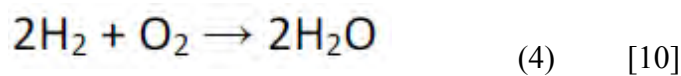
Hydrogen is oxidized at the anode side of the electrode to give 2 protons and 2 electrons as shown by the reaction below:



The electrolyte is specially designed to allow the passage of ions but not electrons and therefore the free electrons from the reaction have to flow through a wire producing the electrical current, while the ions formed travel through the electrolyte. At the cathode the two free species react with oxygen to produce water and that is why this is considered as a clean energy. The following reaction shows what happens:



Thus the overall reaction is as follows:



Using the Gibbs free energy equation (Eq 5), the theoretical efficiency for the conversion of chemical energy into electrical energy can be found.

$$\Delta G = \Delta H - T\Delta S \quad \dots(5)$$

where:

G = Gibbs Function in kJ/mol

$\Delta H$  = Free Energy of Formation W/m<sup>2</sup>K

T = Absolute Temperature K

$\Delta S = \text{Entropy kJ/K}$

Gibbs Function = 237.340 kJ/mol

The theoretical potential of a fuel cell can then be calculated:

$$E = \frac{\Delta G}{nF} \quad (6)$$

Where: n = number of electrons involved in the reaction

F = Faraday's constant, 96485 C/mol

$$E = \frac{237.340 \text{ kJ/mol}}{2 * 96485 \text{ As/mol}} = 1.23 \text{ V}$$

At 25°C and 1atm, the theoretical potential of a PEM FC is 1.23V

The maximum theoretical efficiency of the fuel cell can be calculated using the following equation:

$$\eta = \frac{\Delta G}{\Delta H} \quad (7)$$

$\Delta H = \text{Higher Heating Value of Hydrogen} = 286.02 \text{ kJ/mol}^1$

$$\eta = \frac{237.340}{286.02} = 83\%$$

At 25°C and atmospheric pressure of 101.325 Kpa.

The actual potential from a fuel cell is always smaller than the theoretical one due to the irreversible losses that occur. The main causes for the loss of potential are listed below and their effect can be seen in Figure 4.

- Activation losses
- Internal electrical and ionic resistance
- Mass transportation limitations
- Internal (stray) currents
- Crossover of reactants

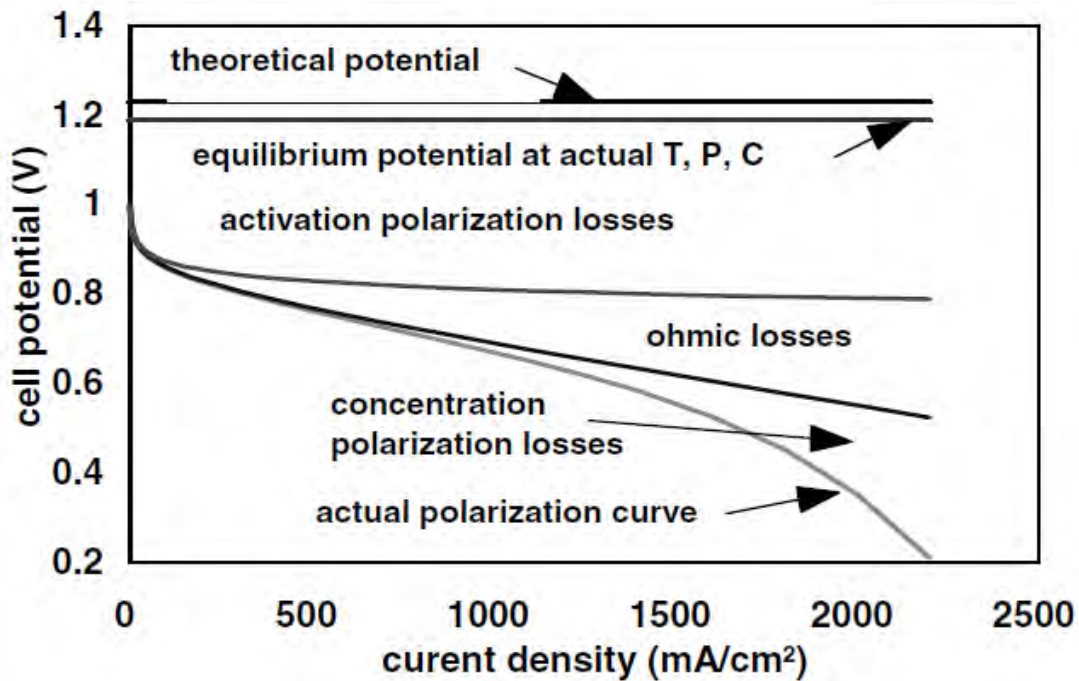


Figure 4 The various losses and resulting polarisation curves.(Barbir)

PEM fuel cells require a complex management system in order to work properly. For this reason, other components are added to the basic components in order to make sure the fuel cell operates continuously. A complete PEM Fuel Cell contains the following components outlined below in detail:

#### 1.4. Membrane Electrode Assembly (MEA)

The membrane electrode assembly (MEA) is a multiple layer structure composed of 5 layers as shown in Figure 1. The inner structure consists of a membrane with both the sides covered by a catalyst layer and this layer is known as a catalyst-coated membrane, the membrane is Nafion® perfluorosulfonic acid, and the membrane thickness ranges from 25 to 50 micrometers. The catalyst-coated membrane (CCM) is essentially a thin film sandwich that requires thin film manufacturing treating such as roll-to-roll processing and deposition such as ink jet printing. The catalyst layers next to each face of the membrane are platinum braced on carbon (~50 wt %) with loading equaling to or less than  $0.4 \text{ mg Pt/cm}^2$ , the thickness of the catalyst layer can be as high as 25 micrometers but is typically thinner. The outer two layers of 5-layered assembly are known as the gas diffusion layers (GDLs), both are next to the catalyst layer. The GDLs are significantly thicker porous carbon layers with thickness of around 300 micrometers per layer. Woven carbon/graphite cloths and carbon felts are the technologies used for manufacturing GDLs. The carbon felts are made using paper processing. For many fuel cells according to their needs, the GDL is chemically treated in order to control its hydrophobic/hydrophilic properties. Thin film processes like vapor and physical deposition are used to apply the hydrophobic/hydrophilic properties. (Leblanc 2010)

#### 1.5. Function Of The Nafion® Membrane In MEA

Nafion® was developed in the 1960s by DuPont. To this day Nafion® is one of the most extensively studied and commercially available proton conducting material. The Nafion® membrane is an expensive component of the PEMFC; the proton exchange membrane is the heart of the PEM system. It conducts protons but not electrons and separates reactants; the Nafion® membrane is an ionically conductive polymer. Due to their high electrochemical stability, low permeability to reactant species, high ionic conductivity and ability to provide electronic insulation Nafion® finds many uses in the industry. Many attempts have been made in order to replace Nafion® due to the cost issues however it is still the most preferred polymer electrolyte for fuel cell operation. Nafion® membrane consists of polytetrafluoroethylene (PTFE) backbone and side chains with acidic functionality. The synthesis of Nafion® is based on the copolymerization of tetrafluoroethylene (TFE) and a

functional fluorinated monomer (vinyl ether). The sulphonic acid group functionality is introduced through the functional sulphonyl fluoride groups (SO<sub>2</sub>F). The length of the side chain, the composition of the polymer backbone and the processing of a film determine the final properties of the polymer electrolyte membrane. The perfluorinated backbone provides chemical and mechanical stability, the ether groups provides flexibility, while the sulphonic acid groups yields high ionic conductivity. The acid groups are fixed to the polymer and cannot leach out, while the counterions (H<sup>+</sup>) are free to migrate and can be readily exchanged with other ions. (Leblanc 2010)

## **2. CHAPTER 2 ULTRASOUND AND SONOCHEMISTRY**

### **2.1. What Is Ultrasound**

Ultrasound is defined as a sound wave with a frequency above 16 kHz with the upper limit usually taken to be 5 MHz for gases and 500 MHz for liquids and solids. The application of ultrasound in physical and biological sciences can be divided into two main groups: (i) low frequency or power ultrasound (20-100 kHz) and (ii) high frequency or diagnostic ultrasound (2-10 MHz).

### **2.2. Sonochemistry and Applications**

The past few years has seen an increase in the use of power ultrasound, Ultrasound has found widespread applications in the chemical and processing industries where it is used to enhance both synthetic and catalytic processes and to generate new products. This area of research has been named sonochemistry, which mainly concerns reactions involving a liquid leading to an increase in reaction rates, product yields and erosion of surfaces. These effects are due to phenomenon known as cavitation. Cavitation is the formation of little bubbles when a very low pressure is applied to a solution. When a liquid is sonicated the distance between rarefaction area which is region of low pressure and low amplitude can surpass the critical molecular distance and produce the breakdown of the liquid and formation of tiny bubbles. These bubbles continue to grow until they reach a stable size during each cycle. The bubbles finally collapse violently and generate energy for chemical and mechanical effects. The cavitation bubbles are considered to be high energy micro reactors. During collapsing, temperatures can reach upto 5000°C and 200 atm.

Bubble formation is a three-step process consisting of nucleation; bubble growth and collapse of gas vapour filled bubbles in a liquid phase. Cavitation phenomenon is known to cause erosion, emulsification, molecular degradation, sonoluminescence and sonochemical enhancements of reactivity solely attributed to the collapse of cavitation bubbles. (Pollet 2010)

## Applications

- Ultrasound is used in sonography- looking at human babies in the mother's womb. Ultrasound is used to work out the baby's age, determine its location, find the location of the placenta, determine the sex of the baby, check for heartbeat, and look for any abnormalities.
- In industry, ultrasound is used to determine the thickness of objects such as metals and plastic.
- Ultrasonic waves are used to weld plastics together. The waves make heat energy between the objects that are joined.

Power ultrasound is regarded as the effect of the sound wave on the medium and has been used in ultrasonic cleaning, drilling, soldering, chemical processes and emulsification.

The past few years has seen power ultrasound find widespread applications in the chemical and processing industries. For the last 20 years, there have been reports on the use of ultrasound for fabricating noble metals and catalysts, preparing fuel cell materials or enhancing mass transport of electro active species from the bulk solution to the fuel cell electrode surface. This review highlights the main uses of ultrasound in Fuel Cell technologies.

In addition one of the beneficial applications of ultrasound is for the polymer degradation. Sonochemical degradation of polymers has proved to be an attractive process because there are no changes in the chemical nature of the polymer and the reduction in molecular weight (also the intrinsic viscosity) is simply by splitting the most susceptible chemical bonds. Application of ultrasonic energy for polymer degradation dates back to the 1930s when natural polymers were subjected to sonication, which resulted in a reduction in viscosity. Ultrasound has been used for degradation of a range of polymers. The ultrasonic degradation of polymers is of great interest and is also the focus of this thesis. The degradation can be used in polymer processing and therefore it is desired. Its main use is as an alternative method for controlling the rate of polymerization and thus determines the properties of the resulting polymer. It can also be used in reducing the high molecular weight of the polymer.



### 2.3. Effect of Sonication on Polymers

Ultrasound has been regarded as a very advantageous method for depolymerising macromolecules because it reduces their molecular weight simply by splitting the most vulnerable chemical bonds without causing any changes in the chemical nature of the polymer. The effects involved in controlling molecular weight are mainly attributed to the large shear gradients and shock waves generated around collapsing cavitation bubbles (see later). Shear forces generated by the rapid motion of the solvent following cavitation collapse result in the breakage of the chemical bonds within the polymer. Long-time exposure of solutions of macromolecules to high-energy ultrasonic waves produces a permanent reduction in viscosity. Even when the irradiated polymers are isolated and re-dissolved their viscosity remains low in comparison with that of non-irradiated solutions. Majority of the effects in Sonochemistry arise from cavitation (see later), the effects involved in controlling molecular weight can be attributed to the large shear gradients and shock waves generated around collapsing cavitation bubbles discussed earlier. Degradation is caused by:

- The hydrodynamic forces of cavitation, i.e the shock wave energy released on bubble implosion.
  - The shear stresses at the interface of the pulsating bubbles;
  - The associated thermal and pressure increase within the bubbles themselves.
- (Grönroos 2001)

### 2.4. Sonochemical Degradation of Nafion®

The use of ultrasound in the preparation of fuel cell material is a new emerging field and has shown potential of promising results in the near futures, sonochemistry itself is not a new field itself and has been used for several decades. Sonochemistry is the application of ultrasound to chemical reactions and processes.(Leblanc 2010)

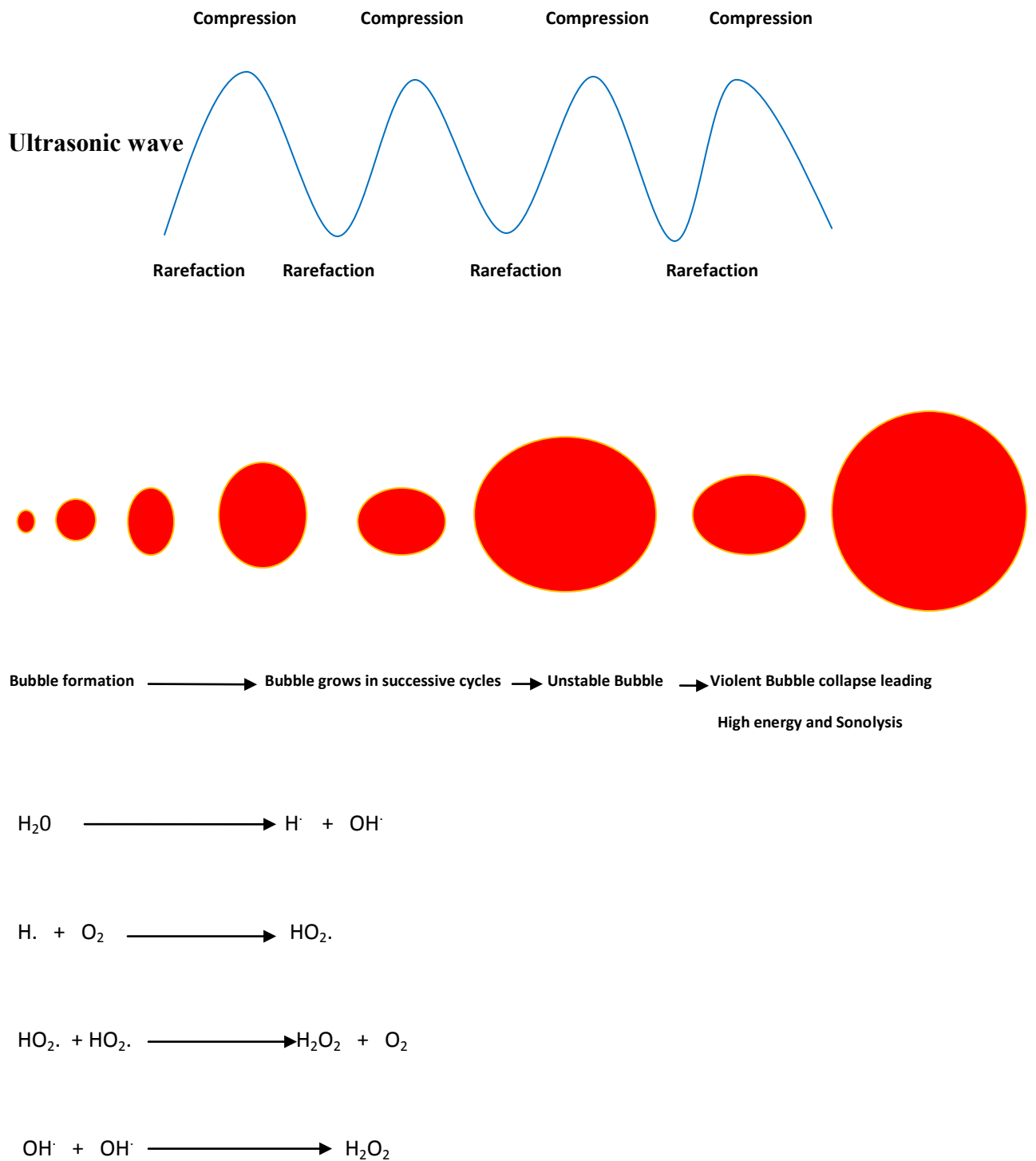


**Figure 5 Cavitation bubble formation at various stages during alternating compression and rarefaction cycles of the ultrasonic wave and asymmetric bubble collapse on a surface leading to (i) high energy with temperature up to 5000 K and pressure of up to 200 atms and (ii) the sonolysis of water caused by the high energy where OH· are hydroxyl radicals, HO<sub>2</sub>· are perhydroxyl radicals and H<sub>2</sub>O<sub>2</sub> is hydrogen peroxide.**

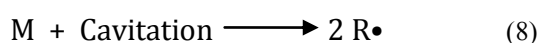
Cavitation is a phenomenon where micro bubbles are formed which tend to implode and collapse violently in the liquid leading to the formation of high velocity jets of liquid. Cavitation phenomenon is known to cause erosion, emulsification, molecular degradation,

sonoluminescence and sonochemical enhancements of reactivity purely attributed to the collapse of cavitation bubbles, cavitation bubble collapse leads to near adiabatic heating of the vapour that is inside the bubble, creating the so-called “hot-spot” in the fluid, where High temperatures (ca. 5000 K) and high pressures (ca. 200 atms) are generated with cooling rates of  $10^9$ - $10^{10}$  K s<sup>-1</sup> during the collapsing of cavitation bubbles are observed. Water vapour is ‘pyrolyzed’ into hydrogen radicals (H) and hydroxyl radicals (OH), known as water sonolysis. Temperature is lower in the interior of the bubbles than the exterior but high enough for thermal decomposition of the solutes and greater local hydroxyl radical concentrations in this region. The reactions of solute molecules with hydrogen atoms and hydroxyl radicals occur in the bulk solution at ambient temperature. (Pollet 2010)

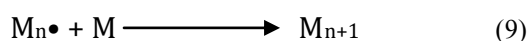
## 2.5. Polymerization Due To Ultrasound Induced Cavitation

Generally, free-radical polymerization consists of four elementary steps; initiation, propagation, chain-transfer and termination. When ultrasound is used to initiate polymerization, radicals can be formed both from monomer and from polymer molecules. This implies that due to radical formation by polymer scission, an additional elementary step is introduced in ultrasound-induced polymerization as indicated in the mechanism show below in fig 6:

### Initiation

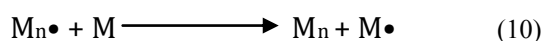


### Propagation

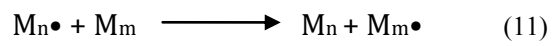


### Chain Transfer

To monomer

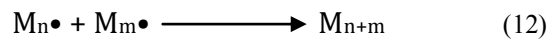


**To polymer**

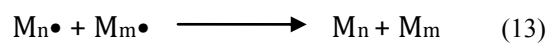


## **Termination**

**By combination**



**By disproportionation**



## **Polymer Scission**

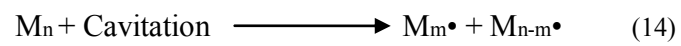


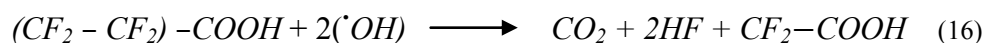
**Figure 6 Reaction mechanism of ultrasound-induced radical polymerization, assuming intrinsic polymerization and avoiding thermal initiation.**

## 2.6. Degradation Mechanism of Nafion®

PEMFC's degradation mechanisms have been the focus of many experimental and theoretical studies. Thermal, mechanical, and chemical degradation have all been recognised as contributors to membrane damage. The degree to which each plays a part in membrane failure depends on cell operating conditions and membrane composition. Degradation processes are polymer dependent. Fuel cell membranes have been made of polymers with different chemical compositions. Nafion® is important among these because of its durability and high power density. Secondly, it has been studied to a greater extent than other membranes and is therefore an excellent system to study and simulate membrane degradation. From Research on the degradation mechanisms of PEMFC's shows that the main damage to the polymers is the result of attack by the reactive oxygen species of free radicals such as hydroxyl radicals. These reactive oxygen species are generated by reduction of H<sub>2</sub>O<sub>2</sub> with iron ions (Fe<sup>2+</sup>), as part of the Fenton reaction, H<sub>2</sub>O<sub>2</sub> is formed on the anode side catalyst by reaction of hydrogen with oxygen from either cathode side or leaked through the gasket (which is a teflon sealant that seals the system and it stops the leaks). The hydrogen peroxide decomposes into a hydroxyl radical in the presence of trace metal contaminants such as iron. The Fe<sup>2+</sup> released from the steel electrode or other metal ion contaminants also react with by products of H<sub>2</sub>O<sub>2</sub> at the anode.



The hydroxyl radical produced attacks the membrane fluorinated end groups according to the following equation:(Fernandes and Ticianelli 2009)



This unzipping slowly dissociates the proton conducting sulfuric acid side chains of the polymer, resulting in reduced conductivity and mechanical stability. Hydrogen fluoride is given off in this reaction and the fluoride emission rate (FER) is one way of measuring chemical deterioration. The hydroxyl radical mechanism of membrane deterioration has been

confirmed in the literature. But, a model that simulates the useful lifetime of a fuel cell membrane based on hydrogen peroxide and contaminant iron concentrations has not yet been developed. A basic model could provide important and informative insight into the features of membrane degradation and allow for the contrast of alternative methods to improve membrane durability. It has been stated that membrane failure occurs after 10% of the sulfonic acid cation exchange sites have been lost. From this, the useful lifetime of the membrane can be predicted. The useful life estimate together with industry standards of life expectancy were used to conclude the upper limit for the hydrogen peroxide concentration at a fixed iron concentration. (King 2009)

A review of the available literature on PEMFC's degradation can be found in literature. Nafion® perfluorosulfonic acid (PFSA) membrane is a copolymer of Tetrafluoroethylene (TFE) and Vinyl Ether. The molecular formula can be written (C<sub>20</sub>F<sub>39</sub>O<sub>5</sub>S) with a structure given in Figure 7 below.

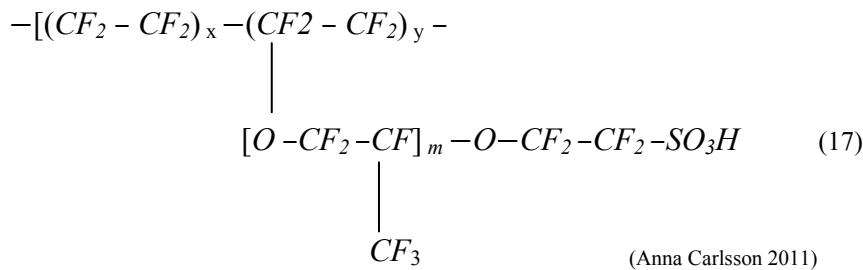


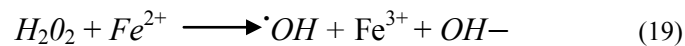
**Figure 7 The molecular formula of Nafion®**

Hydrogen cation exchange occurs via the pendent sulfonyl groups. The mode of chemical degradation in the PEMFC's occurs due to peroxy and hydroperoxy free-radical attack. In fuel cells, H<sub>2</sub>O<sub>2</sub> forms at the platinum catalyst on the anode side via the following mechanism. (King 2009). (Wu 2008)



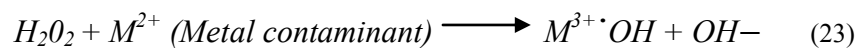
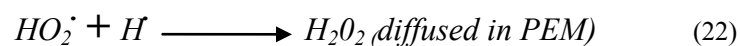
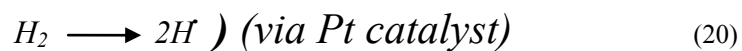
The presence of oxygen results from cross-over from the cathode, air bleed on the Anode side, or cell reversal caused by fuel starvation. The concentration and subsequent transport of hydrogen peroxide within the membrane is a function of hydration. Dry operation leads to more H<sub>2</sub>O<sub>2</sub> in the membrane pore space. It has been noted that the presence of H<sub>2</sub>O<sub>2</sub>

in an working fuel cell using cyclic voltometry and were additionally able to characterize the H<sub>2</sub>O<sub>2</sub> concentration gradient from high to low at the anode. It was also noted that peroxide concentration is a function of the membrane thickness. It was seen that a concentration of 23 ppm in a membrane with a thickness of 50 μm (Nafion® -112) after an undisclosed period of operation. Additional studies report that degradation is proportional to the logarithm of hydrogen peroxide concentration with approximately 0.3% needed to initiate fluoride ion release. The H<sub>2</sub>O decomposes to form radicals in the presence of trace metal impurities. (King 2009)



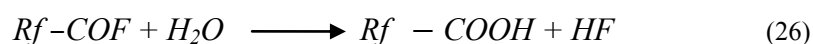
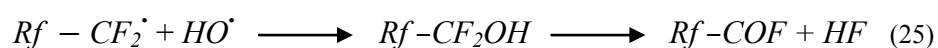
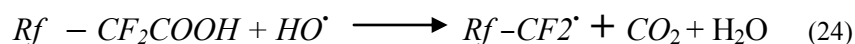
These metal ion contaminants come from the surfaces of materials such as: humidifiers, diffusion media, flow field substrates and water recovery/humidification systems. The presence of Fe<sup>2+</sup> in as-received Nafion® -112 was reported to be 1 ppm using electron probe microanalysis. Immobilization of Fe<sup>2+</sup> ions on Nafion® has also been investigated for use as a preliminary step in biological wastewater treatment and the photo-Fenton method.

It has been believed that cumulative deterioration of the membrane is caused by trace radicals attacking the ionomer chain. The generation of hydrogen radical, hydroxyl radical and degradation products by scission of the ionomer chain is summarized as follows: (Kurniawan 2013)



Hydroxy or peroxy radicals resulting from the decomposition of hydrogen peroxide in the fuel cell attack the polymer at the end group sites and initiate decomposition.

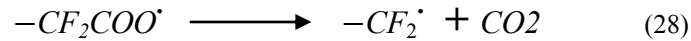
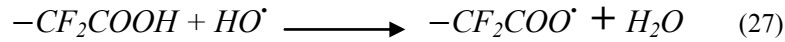
The reactive end groups can be formed during the polymer manufacturing process and may be present in the polymer in small quantities. An example of attack on an end group such as CF<sub>2</sub>X, where X = COOH, is shown below:



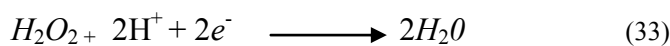
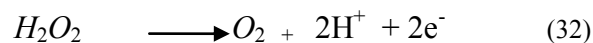
Several proposed mechanisms include the following sequential reactions: abstraction of hydrogen from an acid end group to give a perfluorocarbon radical, carbon dioxide and water (step 1). The perfluorocarbon radical can react with hydroxy radical to form an intermediate that rearranges to an acid fluoride and one equivalent of hydrogen fluoride (step 2). Hydrolysis of the acid fluoride generates a second equivalent of HF and another acid end group (step 3). The presence of the degradation product of the above mechanism, with a structure of  $HOOC - CF(CF_3) - O - CF_2 - CF_2 - SO_3H$ , has been observed by mass spectrometry and F19 NMR spectroscopy. From the degradation mechanism reported, it can be seen that HF emission from the membrane exhaust water is proportional to membrane deterioration. It was seen that by re treating the membrane elemental fluoride the concentration of weak end groups were reduced by 61% with a reduction in fluoride ion generation of 56%. The rate constants were proposed for two possible mechanisms of Nafion® degradation. The first is based on an ‘unzipping’ of the backbone polymer chain described by peroxy radical attack of the carboxylic acid end groups as shown in the following reaction steps. Once the carboxylic acid end groups are formed, the degradation proceeds via an unzipping reaction that involves a series of steps demonstrated below. The attacking species may also involve other radical species besides the hydroxyl radical. For ease of demonstration, however, we use the



hydroxyl radical OH to represent all possible attacking species, assuming that the other species react in a similar fashion as OH. Overall, each carboxylic acid end group reacts with two hydroxyl radicals to lose one CF<sub>2</sub> unit in the form of one carbon dioxide and two hydrogen fluoride molecules, as summarized below. (Xie and Hayden 2007), (Curtin 2004)



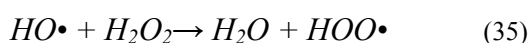
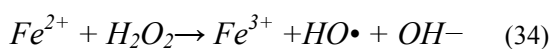
The second is based on attack of the polymer side chain through currently undetermined reacting agent and site. From various assumptions made about the mechanisms of degradation it was possible to develop a kinetic model of Nafion® degradation. Linking the Fluorine fractional loss and carboxylic acid end groups to the ratio of apparent rate constants between the side chain and main chain reactions. Several preventative measures for minimizing PEM degradation have been proposed. Some of these include: avoiding metal contamination, decreasing gas permeation through the membrane by optimizing water content, applying radical inhibitors to membrane surface, and depositing peroxide-decomposition catalysts within the membrane. The later of these methods has found to be most promising. Their idea involves depositing nanoparticles of catalytic material to decompose H<sub>2</sub>O<sub>2</sub> based on the reactions.(King 2009)



Because the reaction occurs as the sum of both reduction and oxidation, therefore it can occur in acidic media. Moreover, if sufficient particles could be optimally spread through the membrane, the net reaction would be the decomposition of H<sub>2</sub>O<sub>2</sub> to oxygen and water. The measured FER for a variety of membranes that were ion-exchanged with Pt and/or Fe<sup>2+</sup>. It was seen that there was a significant reduction in FER for the as-received H<sup>+</sup> membrane over the Fe<sup>2+</sup> membrane and also a major reduction for the Pt exchange membrane over the H<sup>+</sup> membrane. Detected bubbling at the surface of the catalyst is attributed to oxygen production via hydrogen peroxide decomposition. The proposed five step decomposition mechanism for Nafion® is as follows. In the first step H<sub>2</sub> reacts with O<sub>2</sub> crossed over from the cathode on the platinum catalyst surface between the membranes and catalyst layers where H<sub>2</sub>O<sub>2</sub> is formed as a bi-product. Some of the H<sub>2</sub>O<sub>2</sub> is evaporated while the rest is diffused into the membrane and catalyst layers. This is where OH<sup>-</sup> Radicals form in the presence of Fe<sup>2+</sup> and degrade the polymer, releasing F<sup>-</sup>. It is further hypothesized that some H<sub>2</sub>O<sub>2</sub> is scavenged by Pt particles distributed in membrane or catalyst. (King 2009)

The above mechanism of degradation has been confirmed by using Fenton's test and then further backed by solid state and solution NMR spectroscopy and FTIR spectroscopy and will be discussed below. Inside the fuel cell, radicals can originate from electrochemical and chemical reactions on both the anode and the cathode side. Two sources for radical formation are discussed for fuel cells. One is the presence of transition metal cations or heat which can split hydrogen peroxide produced from a two electron oxygen reduction. The second is the direct reaction of H<sub>2</sub> or O<sub>2</sub> on the surface of the Pt catalyst. Oxygen crossover from the cathode (at low currents) or hydrogen crossover from the anode (at high currents) may provide the basis for such reactions. (Ghassemzadeh 2011)

In ex situ degradation tests, the Fenton's solution is the most common method for radical formation, and the Fenton reaction is commonly used for evaluation of the chemical stability of polymer electrolyte membranes. In 1894, Fenton reported that the combination of H<sub>2</sub>O<sub>2</sub> and a ferrous salt, "Fenton's reagent", is an effective oxidant for a wide variety of organic substrates. The produced HO• and HOO• radicals in the Fenton reaction can be therefore used for attacking different sites in PFSA ionomer. (Ghassemzadeh 2011)



Although the situation in a Fenton test does not simulate neither the cathode nor the anode side of the fuel cell, the stability of the polymers against the Fenton's reagent is nonetheless taken as one of the basic tests to assess the durability of such electrolyte membranes. The presence of a metallic catalyst and a high concentration of hydrogen peroxide provide very harsh conditions. Which differ from an operating fuel cell, and the membranes becomes very rigid in a short time at much higher degradation rate. Therefore, the Fenton test is considered as a fast and easy evaluation test that is applicable to any kind of membrane. It provides radicals that can attack the polymer in a similar way as expected in an operating fuel cell. As a primary test prior to real fuel cell tests, the Fenton ex situ test is very useful, and the membranes that can survive the Fenton test with less degradation, usually also shows better strength during in situ fuel cell tests. However, it should be stressed that the results from the ex situ Fenton test not necessarily reflect the behaviour of a fuel cell membrane under operation conditions. For example, hydrocarbon membranes with narrow water channels exhibit reduced gas cross-over in a fuel cell test, and therefore less degradation is expected which, however, is opposite to the experimental observation. Current spectroscopic studies have showed new insights into the structural changes during various degradation tests. These studies addressed both in situ degradation and a newly designed ex situ setup which can avoid the use of the traditional Fenton test in order to simulate a situation that is closer to the operating fuel cell condition. In depth information was gained by solid-state NMR spectroscopy which gave a clear picture about the structural features and dynamic behaviour prior and after degradation. In this context, high resolution  $^{19}\text{F}$  MAS NMR spectroscopy is a site-selective technique and is able to differentiate between the segments in the polymer main and side chains. These studies mainly addressed the polymer side chain segments which exhibited substantial degradation during the various tests. The derived results were in qualitative agreement with independent electron spin resonance (ESR) spectroscopic and mass spectrometric (MS) studies. (Ghassemzadeh 2011)

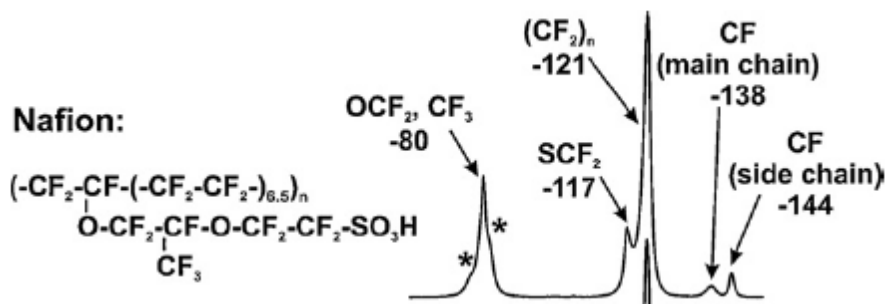


**Figure 8** Chemical structures and solid-state <sup>19</sup>F NMR spectra of Nafion® 117. Asterisks indicate spinning side bands. The given spectra are normalized to the dominant peak of the backbone CF<sub>2</sub> groups.

<sup>19</sup>F MAS NMR spectra of Nafion® is shown in [fig 8](#). The given <sup>19</sup>F signal assignment is based on former solution and solid-state NMR investigations. The <sup>19</sup>F NMR spectra show separate signals for the side and the main chain segments of the Nafion® Ion membranes. The CF<sub>2</sub> groups of the backbone give rise to a peak at -121ppm similar to a signal of <sup>19</sup>F NMR in Teflon, while the <sup>19</sup>F peak at -138ppm represents the backbone CF group at which the side chain is attached. The signal of the CF group in the side chain appears at -144ppm. The <sup>19</sup>F peak at -117ppm reflects the SCF<sub>2</sub> groups, while two peaks referring to the two OCF<sub>2</sub> groups and the CF<sub>3</sub> group of the side chain appear at about -80 ppm. (Ghassemzadeh 2011)

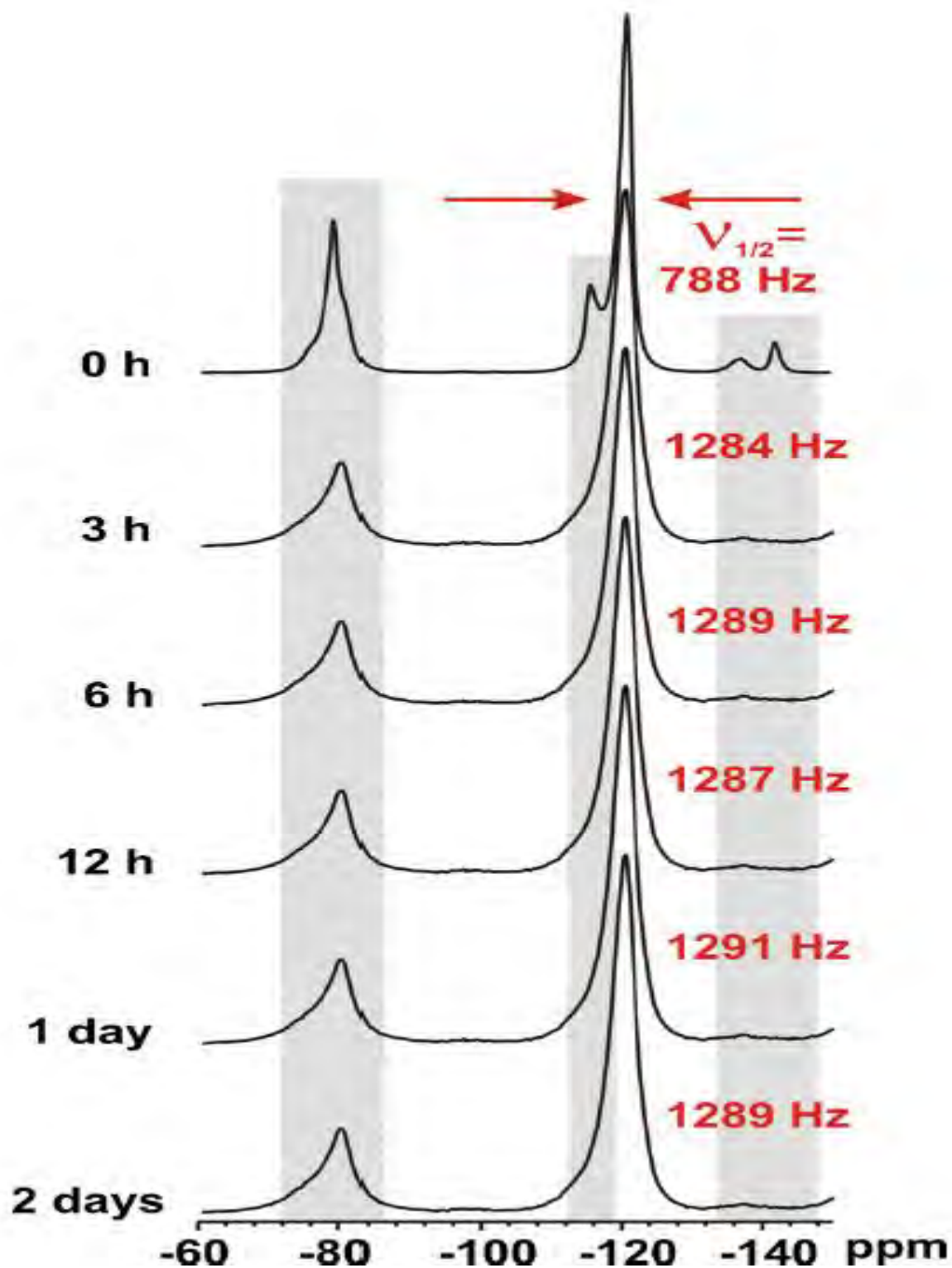


Figure 9 Solid-state  $^{19}\text{F}$  NMR spectra of Nafion® 117 samples after treatment with 0.1M  $\text{Fe}^{2+}$  in 30 v/v%  $\text{H}_2\text{O}_2$ . The line widths,  $V_{1/2}$ , of the peak at -121 ppm, referring to the backbone  $\text{CF}_2$  groups, are shown. Exposure times are given to the left of the figure.

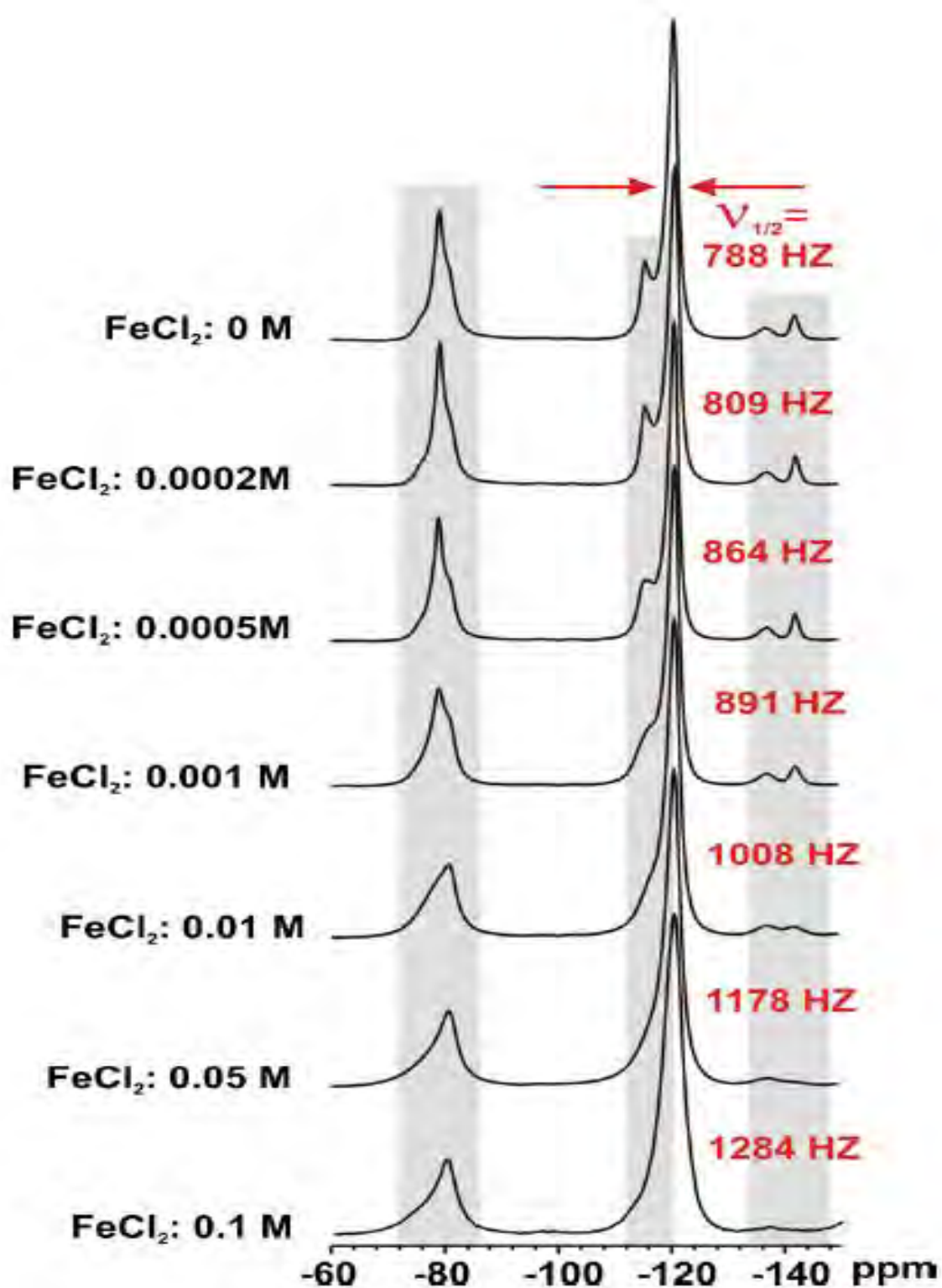


Figure 10 Solid-state  $^{19}\text{F}$  NMR spectra of Nafion® 117 samples after 3 h of with different  $\text{Fe}^{2+}$  concentrations, as indicated, in 30 v/v%  $\text{H}_2\text{O}_2$  solutions. The line widths,  $V_{1/2}$ , of the peak due to the backbone  $\text{CF}_2$  groups are shown.

To examine the degradation of the present membranes during the Fenton test, in a first attempt Nafion® 117 was treated with a 0.1M  $\text{Fe}^{2+}$  solution, as also done in the above-mentioned ex situ Fenton study. Fig. 9 shows the respective solid-state  $^{19}\text{F}$  NMR spectra of these samples after exposure to the Fenton test reagent for the periods given in the figure. A general line broadening was seen for all samples after treatment with the Fenton's solution. In agreement with the former work, the spectra of the treated samples are virtually identical, and show a substantial line broadening by nearly a factor of two as compared to the untreated sample (see top spectrum). Therefore, it is very likely that the line broadening obscures all other spectral alterations which might occur during the ex situ test.

In order to further clarify these findings, the test was repeated with different concentrations of the Fenton's reagent. Fig. 10 displays  $^{19}\text{F}$  NMR spectra of Nafion® 117 samples which were exposed for 3 hour to the Fenton's reagent with different  $\text{Fe}^{2+}$  concentrations. As given in the figure. It is observed that the line widths strongly vary with the actual concentration. As an example, the line widths,  $\Delta\nu_{1/2}$ , of the main chain  $\text{CF}_2$  group are reported in the figure. The difference in spectral line width for the samples treated with 0.0002M and 0.1M  $\text{Fe}^{2+}$  solution is almost 500 Hz. Therefore, for  $\text{Fe}^{2+}$  concentrations  $>0.0005\text{M}$  the  $\text{SCF}_2$  group signal only appears as a shoulder next to the dominant  $\text{CF}_2$  peak, and at the highest concentrations it is completely disguised. A similar line broadening effect is seen for all other peaks. Nonetheless, independent of the spectral broadening, a decrease of the relative intensity for the side chain  $\text{SCF}_2$  group can be identified for the solutions with lower  $\text{Fe}^{2+}$  concentration. In order to follow the time evolution of the spectra during the ex situ Fenton test, a  $\text{Fe}^{2+}$  concentration of 0.0002M has been chosen. The respective  $^{19}\text{F}$  NMR spectra are given in Fig. 11. It is seen that line width of the main chain  $\text{CF}_2$  peak, as denoted in the figure, marginally increases by about 50 Hz, if the non-treated membrane is compared to the membrane being in the Fenton's solution for 2 days. At the same time, in comparison to situation shown in Fig. 9, a Continuous decrease (with exposure time) of the  $\text{SCF}_2$  group intensity can be noticeably identified. These changes in the relative signal intensities will be quantified by spectral deconvolution, and will be further defined below. (Ghassemzadeh 2011)

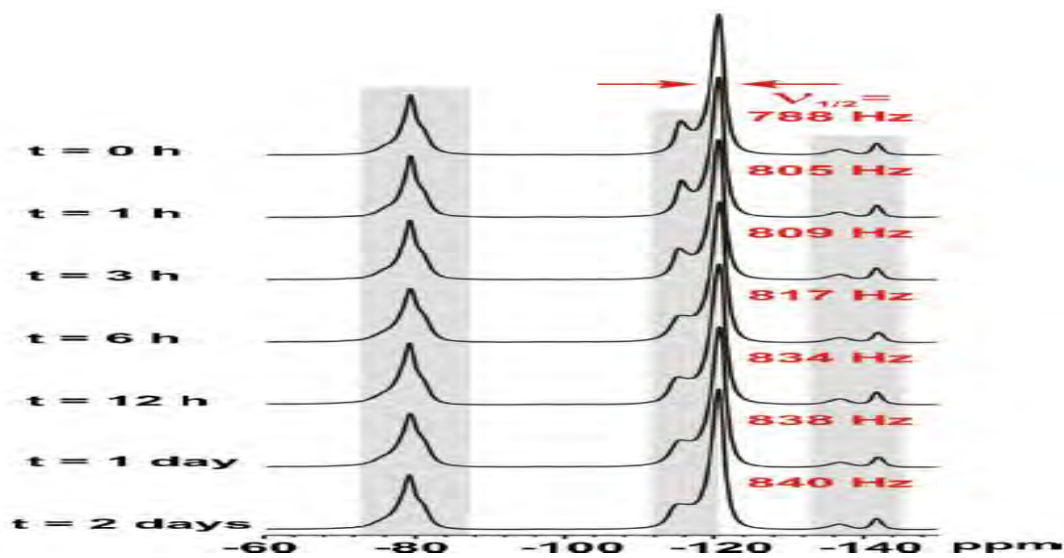


Figure 11 . Solid-state  $^{19}\text{F}$  NMR spectra of Nafion® 117 samples after Fenton tests with  $0.0002\text{M}$   $\text{Fe}^{2+}$  in  $30\text{ v/v\%}$   $\text{H}_2\text{O}_2$ . Exposure times are given to the left of the figure.

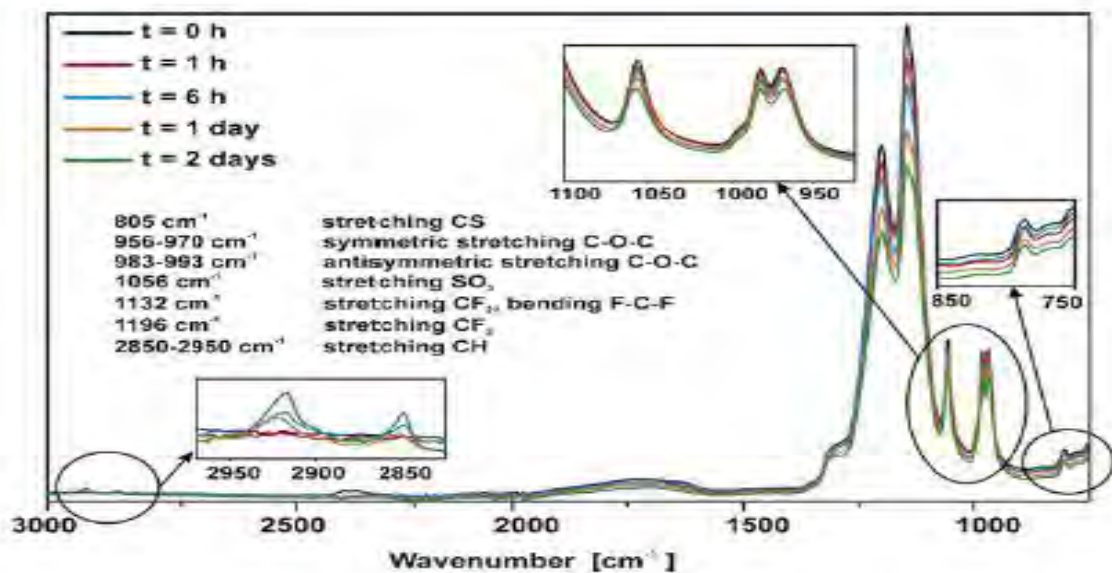


Figure 12 ATR-IR spectra of Nafion® 117 samples after Fenton tests with  $0.0002\text{M}$   $\text{Fe}^{2+}$  in  $30\text{ v/v\%}$   $\text{H}_2\text{O}_2$ .



The structural evolution of the Nafion® 117 sample during the Fenton test was also studied by ATR-FTIR spectroscopy. The respective IR spectra of the same Nafion® samples are shown in Fig. 12. The major peaks in these ATR-FTIR spectra and their assignment are also listed. The comparison of the spectra before and after the Fenton degradation test displays a decrease in intensity of the C–O–C (at 960 and 980 $\text{cm}^{-1}$ ), S–C (805 $\text{cm}^{-1}$ ) and S–O (1056 $\text{cm}^{-1}$ ) stretching modes. At the same time, an intensity decrease is detected for the peaks at 1132 and 1196 $\text{cm}^{-1}$  which are related to the stretching modes of the  $\text{CF}_2$  groups.

Furthermore there is also the appearance of two new peaks at around 2850 and 2920 $\text{cm}^{-1}$  which are due to symmetric and asymmetric CH stretching modes, and their intensities slowly increase with longer exposure times. It should be noted that solid-state  $^1\text{H}$  NMR measurements were done as well. However, no  $^1\text{H}$ NMR signals of aliphatic protons were detected and unequivocal and independent proof for the presence of such CH groups could not be given, most likely due to their low concentration. From these results it is concluded that despite the major of degradation studies which emphasised the presence of main chain degradation, these solid-state NMR studies noticeably proved substantial degradation in the polymer side chains. The results from the present ex situ Fenton test studies confirm these former results. They show that structural changes and bond cleavages also take place in the polymer side chains, and therefore represent an important contribution for chemical degradation of such ionomer membranes. In the present work it is found that the membranes, after treatment with Fenton's solution at  $\text{Fe}^{2+}$  concentrations larger than 0.0005 M, show substantial line broadening in the solid-state  $^{19}\text{F}$  NMR spectra. The spectral broadening is visible for all  $^{19}\text{F}$  NMR signals, but is slightly more pronounced for the signals of the side chain region. A similar line broadening effect was also seen after soaking the membrane in a  $\text{FeCl}_2$ /water solution which suggests that the spectral changes are not related to membrane degradation, but due to existence of the paramagnetic iron ions. Iron ions not only affect the solid-state NMR data, but are also observable during other experimental studies. Therefore, they can easily exchange with the acidic proton in the membrane, and—without any chemical degradation—decrease the ion exchange capacity and electric conductivity of the polymer. These changes are reversible after treating the membrane with an acidic solution. Performing the Fenton test with the lowest manageable concentration of  $\text{FeCl}_2$  (0.0002M=10ppm) gives experimental  $^{19}\text{F}$  NMR spectra with good resolution. Their analysis shows constant degradation in the side chain region upon increasing reaction time. This is also confirmed by the ATR-FTIR spectra which—together with the detection of the strong F- peak in the liquid

NMR spectra—also point to main chain degradation, not directly observable in the solid-state  $^{19}\text{F}$  NMR spectra. Based on these results and in agreement with other works, the sites for radical attack in PFSA membranes are clearly both the main and the side chain regions. Therefore in general, the polymer side chains can be attacked via the C–S bond or via the tertiary carbons in the side and main chains. The comparison of the CF peak integral for the side chain and main chain in Nafion® after the degradation shows that the changes for the main chain CF group is very slight, while for the side chain CF group signal a much bigger reduction can be found. Consequently, for Nafion® the intensity decrease of the peak at  $-80\text{ppm}$  (referring to the  $\text{OCF}_2$  and  $\text{CF}_3$  groups) is predominantly caused by the  $\text{OCF}_2$  peak closer to the end of the side chain and to the  $\text{CF}_3$  group, and not by the  $\text{OCF}_2$  group next to the polymer main chain. (Ghassemzadeh 2011)

## 2.7. Sonochemical Degradation of Polymers Quantified by GC/MS

The sonochemical degradation of aqueous solutions containing low concentrations of six phthalate esters at an ultrasonic frequency of 80 kHz was investigated. Ultrasonic treatment was found capable of removing the four higher molecular mass phthalates (di-n-butyl phthalate, butylbenzyl phthalate, di-(2-ethylhexyl) phthalate and di-noctyl phthalate) within 30–60 min of irradiation. The rest (dimethyl phthalate and diethyl phthalate) were more recalcitrant and nearly complete removal could be achieved only after prolonged irradiation times. GC–MS proved to be a powerful analytical tool to monitor the sonochemical degradation of phthalate esters at low concentration levels.

An aqueous solution containing  $40\ \mu\text{g l}^{-1}$  of each phthalate (i.e. an initial overall concentration of  $240\ \mu\text{g l}^{-1}$ ) was subject to continuous ultrasonic irradiation for 240 min at a constant electric power output of 150 W and a constant water bath temperature  $21\ ^\circ\text{C}$ . Direct comparison between the total ion chromatograms (Fig.13) obtained by means of GC–MS at the beginning (time zero) and at the end (after 240 min of sonication) of the experiment, reveals that all peaks corresponding to the six phthalates are essentially gone by the end of the experiment. (Psillakis 2004)

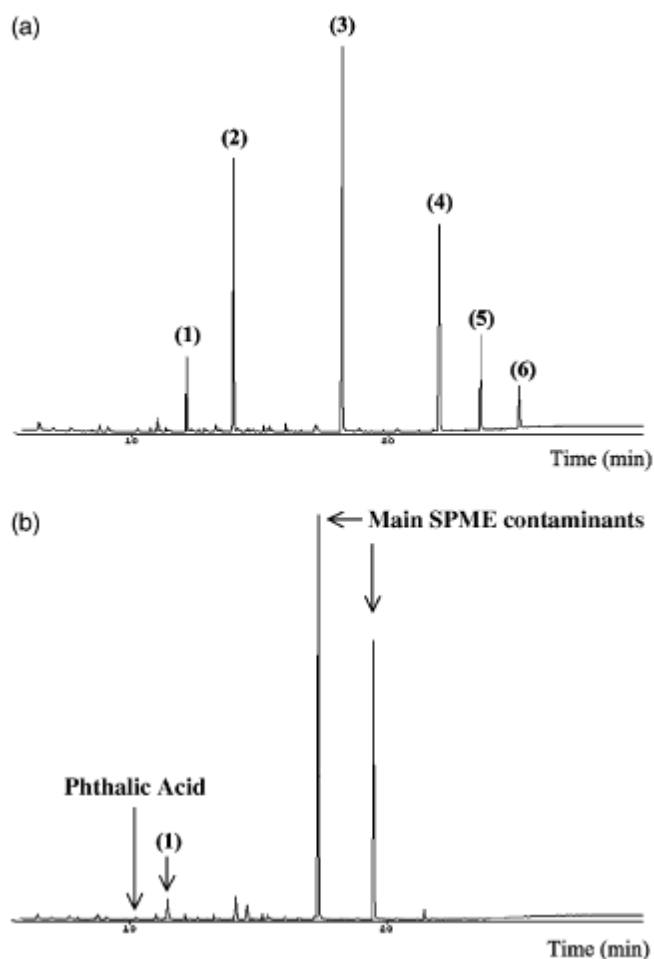


**Figure 13** Total ion chromatograms obtained with SPME/GC–MS of (a) the reaction mixture at time zero containing  $40 \mu\text{g l}^{-1}$  of each phthalate (i.e. initial overall phthalates concentration of  $240 \mu\text{g l}^{-1}$ ) where (1) DMP, (2) DEP, (3) DBP, (4) BBP, (5) DEHP and (6) DOP; and (b) after 240 min of sonication. The two extra peaks assigned as SPME contaminants originate from the partial loss of the SPME coating due to increased usage. The extra eluting peak assigned as phthalic acid is the only degradation product which could be detected with a certain degree of confidence. Other experimental conditions: 80 kHz of ultrasound frequency, 150 W of electric power output, 21 °C water bath temperature. (Psillakis 2004)

It appears that the more hydrophobic DBP, BBP, DEHP and DOP are all readily susceptible to sonochemical degradation and nearly complete removal is achieved within 30–60 min of irradiation at the conditions under consideration. Conversely, the less hydrophobic DMP and DEP are more recalcitrant and complete degradation can be achieved only after prolonged ultrasonic irradiation. (Psillakis 2004)

## 2.8. Degardation of Polymers Quantified by GC/MS

From literature the degradation mechanisms or degradation products for various polymers have been elucidated using GC/MS. For example photochemical degradation of commercial polyvinyl acetate (PVAc) homopolymer and PVAc paints mixed with burnt umber, cobalt blue, cadmium red dark, nickel azo yellow and titanium white commonly used for artworks were studied using GC/MS. The GC/MS analysis was used to study the differences in the specimens before and after UV ageing, including the changes of detectable amounts of deacetylation product – acetic acid and plasticizers such as diethyl phthalate (DEP).

Thermal degradation of unaged PVAc was studied at different pyrolysis temperatures by Py–GC/MS. The pyrograms obtained are depicted in Fig 14. (Wei 2012)

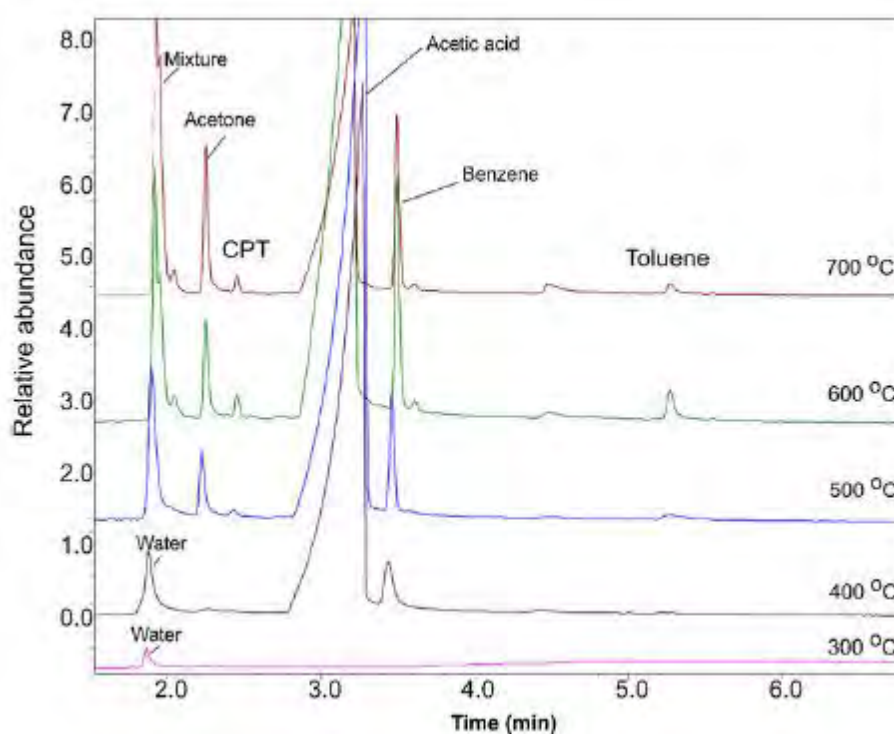


**Figure 14** Chromatograms of Mowilith® 50 obtained by Py–GC/MS analysis: (a) 300 °C; (b) 400 °C; (c) 500 °C; (d) 600 °C; (e) 700 °C; mixture: CO, CO<sub>2</sub> and H<sub>2</sub>O; CPT, 1-3- cyclopentadiene. (Wei 2012)

From the comparison between the chromatograms obtained at different temperatures by GC/MS, it can be seen that at 300 °C, only water at retention time (RT) 2.0 min was detected, which was probably absorbed by the sample from the environment. No acetic acid was detected, which means that deacetylation reaction did not occur at this temperature. In

contrast to that result, in the pyrogram obtained at 400°C the most dominant peak is that of acetic acid at RT of 3.2 min ( $m/z = 60$ ), with a smaller amount of water at RT 2.0 min ( $m/z = 18$ ) and benzene at RT 3.5 min ( $m/z = 78$ ), indicating deacetylation reaction occurs at 400 °C. At temperatures above 500°C, the main pyrolysis products are carbon dioxide, carbon monoxide and water at RT 2.0 min based on the ions ( $m/z = 18, 28, 42, 44$ ), acetone at RT 2.2 min ( $m/z = 15, 43, 58$ ), 1-3-cyclopentadiene at RT 2.4 min ( $m/z = 39, 66$ ), acetic acid, benzene and toluene at RT 5.3 min ( $m/z = 91$ ). It can be seen the pyrolyses at temperature above 500°C allowed the formation of more products such as 1-3-cyclopentadiene, benzene and toluene, showing the decomposition of PVAc during deacetylation reaction into a highly regular unsaturated material or polyene. The results are in agreement with the thermal degradation mechanism of PVAc by non-isothermal and dynamic thermal gravimetry including the formation of acetone, and solid-state NMR, thermogravimetry coupled with mass spectrometry and differential thermal analysis. In the literature, it was reported the first and most intense degradation step-deacetylation occurs between 300°C and 400°C with temperature rate at 20°C/min. The chain scission reaction occurs at the end of the polymer main chain during deacetylation. (Wei 2012)

This technique is a useful way of elucidating the degradation products and it will be applied to our results to find out the sonochemical degradation mechanism of Nafion.

### 3. CHAPTER 3 EXPERIMENTAL METHODS AND MATERIALS

#### 3.1. Experimental Plan

The aim of the thesis was to find out the effect of ultrasound on Nafion® therefore in order to see these effects control experiments on Nafion® were performed without ultrasound. The effect of temperature on Nafion® in the absence of ultrasound was investigated. High shear mixing experiments were performed on Nafion® at different shearing rates of 5000 rpm and 10000 rpm without ultrasound to see the change in viscosity and glass transition temperature (T<sub>g</sub>) using high shear mixing. This was done in order to see what effect this has on the Nafion® properties in terms of (T<sub>g</sub>) and viscosity. These control experiments were then compared to Nafion® subjected to different ultrasonic conditions. 4 different concentrations of Nafion® were used in the experiments, 2.5, 5, 7.5 and 10% and the different concentrations were then subjected to ultrasound using ultrasonic probe and ultrasonic bath at various powers, amplitudes and time ranges of 0 to 120 minutes.

The ultrasound probe experiments were performed with 20 kHz ultrasonic probe system and the ultrasound bath experiments were carried out using sonomatic 40 kHz ultrasound bath. The power ranges used for ultrasonic ultrasonic probe runs were 1.86, 3.84, 6.42 and 11.28 W at 20%, 40%, 60% and 80% amplitude. The power used for ultrasound bath was 0.32 W.

The different ultrasound treated samples at various ultrasound intensities and times were then used to measure the viscosity using Rheometer and the T<sub>g</sub> was obtained using Differential Scanning Calorimetry. These results were then compared to silent conditions in order to see the ultrasound induced effects on Nafion®.

### 3.2. Experimental Setup

(a)

(b)

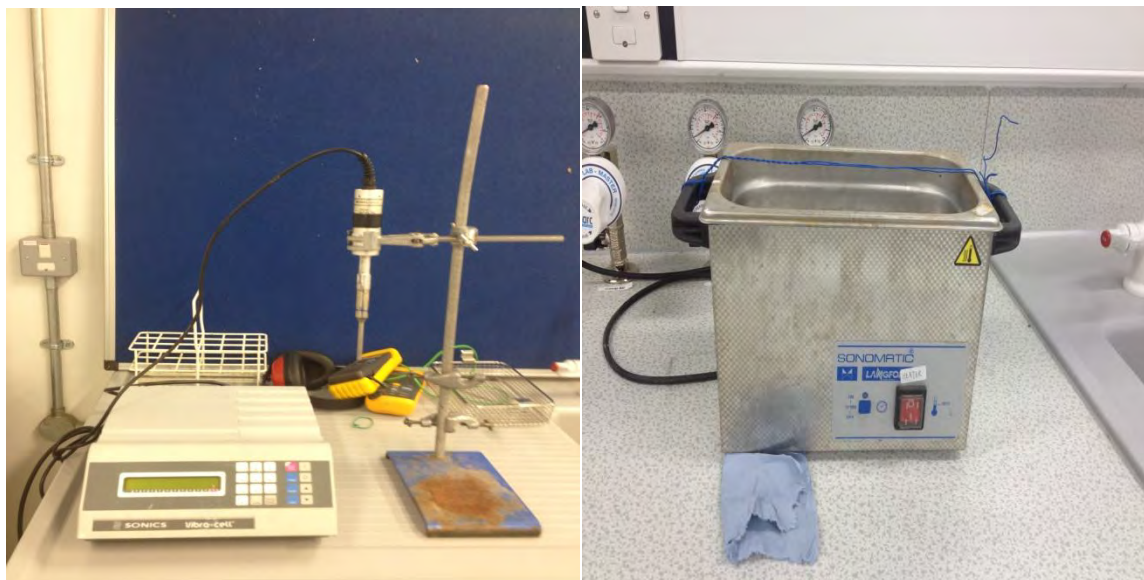


Figure 15 Sonochemical [(a) Sonics 20KHz ultrasonic probe system; (b) Sonomatic 40KHz ultrasonic bath system used for Sonication studies on Nafion® . (Pollet 2010)

### 3.3. Experimental Procedures

#### 3.3.1. Ultrasound bath 40kHz

1. Samples consisting of 2.5% Nafion® solution in water were treated in an ultrasonic bath (40kHz) for 120 minutes.
2. Immediately upon completion, the samples were separated into 2 parts.
3. The first part was tested on the rheometer. (see above for specific procedure)
4. The 2nd part was vacuum dried until crystals were formed before being tested with the DSC apparatus. (See above for specific procedure). 2 to 3 drops of Isopropyl Alcohol was used as solvent.
5. A fresh sample of 2.5% Nafion® solution was next used for each time increment of 60, 40, 30, 15, 10 and 5 minutes.
6. Steps (1) to (5) were repeated for the remaining 3 concentrations of Nafion® solution.

### 3.3.2. Ultrasound probe 20kHz

1. One sample of 2.5% Nafion® solution was treated with an ultrasound probe (20kHz) at power level P1 for 5 minutes.
2. Immediately upon completion the sample was separated into 2 parts.
3. The first part was tested on the rheometer.
4. The 2nd part was vacuum dried until crystals were formed before being tested with the DSC apparatus. (See above for specific procedure). 2 to 3 drops of Isopropyl Alcohol was used as solvent.
5. Steps (1) to (4) were repeated for power levels P2 and P3.
6. Steps (1) to (5) were repeated with fresh samples of 2.5% Nafion® solution for each time increment of 60, 40, 30, 15, 10 and 5 minutes.
7. Steps (1) to (6) were repeated for the remaining 3 concentrations of Nafion® solution.

### 3.4. Experimental Apparatus

1. Standard lab apparatus (beakers, pipettes, weighing machine etc.)
2. Ultrasound bath (40kHz)
3. Ultrasound probes (20kHz)
4. Storage bottles (30ml)
5. Stopwatch
6. Rheometer
7. High Shear Mixer (5krpm and 10krpm)
8. Differential scanning calorimetry (DSC) apparatus
9. GC/MS

### 3.5. Materials List

1. Deionised (DI) water
2. Nafion® solution 10% wt.
3. IPA



### 3.6. Nafion® Sample Preparation

The available Nafion® solution of 10% wt. is diluted with IPA and DI water to form concentrations of 2.5%, 5%, 7.5%. The ratio of IPA to DI water is based on literature values of 19ml DI water and 6ml IPA for every 100µl of 5% Nafion® solution (Takahashi and Kocha 2010). It is reproduced in the interest of bench-marking.

### 3.7. Experimental Parameters and Variables

#### Parameters/Variables

**Table 1 Showing the parameters and variables used during the experiments**

Fixed	Temperature	25°C
	Pressure	1atm
Manipulated	Ultrasound frequency	20, 40kHz
	Power	P1, P2, P3 (20kHz) and P4 (40kHz)
	Nafion® concentration	2.5, 5.0, 7.5, 10.0%
	Exposure time to ultrasound	1,2.5, 5, 10, 15, 30, 40, 60, 120min
Measured	RMM (GPC, DSC)	-
	Viscosity (Rheometer)	-

### 3.8. Power Measurements

Two ultrasonic equipment were used in this study for the effect of ultrasound on Nafion®. Ultrasonic probe was sonomatic 20 KHz and ultrasound bath was sonomatic 40 KHz. Before sonicating the different Nafion® samples, the power measurements were worked out by performing experiments. The energy input was controlled by varying the amplitude of the sonicator probe (sonotrode) that transmits the ultrasound into the samples. The sonotrode was immersed into the samples

at a depth of approximately 2cm within a sample vial. The volume of the sample used was 0.02 litres. The ultrasonic sample temperature was taken from 0 to 60 minutes and plotted against time. Ultrasonic power is considered to be mechanical energy and it is partly lost in the form of heat when ultrasound travels through the medium. Heat is produced by the ultrasonic irradiation of a liquid; therefore acoustic power can be estimated by recording the temperature as a function of time using the following equation.

$$P = mC_p \frac{dT}{dt} \quad (36)$$

where  $dT/dt$  is the change in temperature along with the whole time range ( $^{\circ}\text{Cs}^{-1}$ ) and determined by polynomial curve fitting,  $C_p$ . (Karaman 2012)

### 3.9. Depth of the Horn

The depth of ultrasonic horn was always kept at the same level because it could affect the extent of degradation therefore the ultrasonic probe was immersed at the same level. This was done by making marking on the clamp and boss that held the ultrasound probe. This meant each time a sample was sonicated the ultrasound probe was immersed at the same level.

### 3.10. Equipment setup

#### A. Ultrasonic bath

1. The water level is checked.
2. The fixtures are checked to ensure the sample bottle remains stationary during ultrasound treatment.

#### B. Ultrasonic Probe

1. The Ultrasonic probe is fixed at the same level for each run using clamps and bosses.
2. The fixtures are checked to ensure the sample bottle remains stationary during ultrasound treatment.

### C. Rheometer

A Rheometer is a laboratory equipment used to measure the way in which a liquid, suspension or slurry flows when a force is applied. It is used for particular fluids which cannot be defined by a single value of viscosity and thus need more parameters to be set and measured than in the case for a viscometer. Rheometer measures the rheology of the fluid. Parallel plates with a diameter of 25 mm were chosen. Temperature control was attained by electrically heated plates, which had an accuracy of  $\pm 0.1$  C. All measurements were done under Argon atmosphere to prevent any degradation and take-up of moisture. The following small amplitude oscillatory shear measurements were carried out for each blend at a fixed composition: (1) dynamic time sweeps (DTS) at a given temperature and frequency (from 0.1 to 1 rad/s), in order to gain steady state and therefore ensure that measurements were performed under “dynamic equilibrium” conditions; (2) dynamic stress sweeps (DSS) at specified temperature and frequency (0.1 – 100 rad/s), to determine the limits of linear viscoelasticity; (3) dynamic frequency sweeps (DFS) from 0.1 to 150 rad/s at a given stress, in order to determine the behaviour of the storage ( $G'$ ) and loss ( $G''$ ) moduli in the homogeneous, transitional, and two-phase regions. The measurement accuracy of dynamic shear rheology measurement was  $\pm 0.001$  Pa. The complete AR 2000 Rheometer setup is given in figure 16.



Figure 16 Showing complete setup of AR 2000 Rheometer.

#### **D. Sample Preparation for DSC Analysis**

The different samples of Nafion® were prepared for (DSC) analysis using a suitable solvent in order to ensure that the solvent did not have any effect on the results obtained and thus only the sonication was the result of any change observed. The suitable solvent chosen from the literature was THF (Tetrahydrofuran). The sonicated samples at various times and ultrasound power were transferred to sample vial and dried in a oven overnight at 40° C for 24 hours. After the sonicated Nafion® sample was dried than a small amount of the sample was dissolved into THF and stirred until the sample dissolved into the solvent. The sample was then dried in a vacuum oven at 0.25 atm and 55°C because THF has a boiling point of 66°C for 20 hours to remove the residual solvent. 5mg of the sample was then taken for DSC analysis. All the other samples were prepared in the same way. The unsonicated Nafion® sample was also prepared in the same way so it could be compared to the sonicated Nafion® samples. The samples were then put into Differential Scanning Calorimetry in order to measure the heating effects of the samples. The procedure for using (DSC) is given below.

#### **E. Differential Scanning Calorimetry Apparatus**

A Perkin Elmer Pyris 1 Differential scanning calorimeter (DSC) was used to see the heating effects of Nafion® after sonication, and to do this we had to use special equipment called Differential scanning Calorimetry. Before beginning the measurements, the calorimeter was calibrated for temperature and sensitivity using the melting curves of pure In, Zn, Al, Ag, and Au. To avoid sample oxidation, the experiments were done under a He flow (30 mL/min) after evacuating the working chamber three times to a vacuum level of 10<sup>-2</sup> bar. The purity of the He used was higher than 99.999 pct. There are two pans used. In one pan, the sample pan, you put your polymer sample. The other pan is the reference pan. You leave it empty. The samples used for analyzing were 3µg to 8 µg. DSC was furnished with an ethylene glycol cooling system maintained at 5°C. The measurements on cooling were done at different rates from 10 to 2 K/min. All experiments were performed under Argon atmosphere.

The fast cooling runs at 10 K/min were performed from 185°C to 60°C to ensure that the instrumental cooling rate was well controlled at  $T_g$ . The standard deviation of calorimetric  $T_g$  values was  $\pm 0.3^\circ\text{C}$  based on two or three measurements performed at each cooling rate. The complete DSC setup is shown below in Figure 17.



**Figure 17 Complete Perkin Elmer Pyris 1 Differential Scanning Calorimeter Setup**

## F. GC/MS Analysis

The GCMS instrument is made up of two parts. The gas chromatography (GC) portion separates the chemical mixture into pulses of pure chemicals and the mass spectrometer (MS) identifies and quantifies the chemicals. For the analysis of the samples we used Fissions MD-800 chromatograph/ Mass Spectrometer.

The different Nafion® samples were analyzed with GC/MS by following the procedure given below.

### Gas chromatography (GC)

One microliter (1  $\mu\text{l}$ , or 0.000001 L) of solvent containing the mixture of molecules is injected into the injection port of the GC. The sample is carried by inert (non-reactive) gas through the instrument, usually helium. The inject port is heated to 300°C to cause the chemicals to become gases. The outer part of the GC is a very specialized oven. The column is heated to move the molecules through the column. Typical oven temperatures range from 40°C to 320°C. Inside the oven is the column which is a 30 meter thin tube with a special polymer coating on the inside. Chemical mixtures are separated based on their volatility and are carried through the column by helium. Chemicals with high volatility travel through the column more quickly than chemicals with low volatility.

### Mass Spectrometer (MS)

After passing through the GC, the chemical pulses continue to the MS. The molecules are blasted with electrons, which cause them to break into pieces and turn into positively charged particles called ions. This is important because the particles must be charged to pass through the filter. As the ions continue through the MS, they travel through an electromagnetic field that filters the ions based on mass. Adjustment was made to allow appropriate range of masses through the filter. The filter continuously scans through the range of masses as the stream of ions come from the ion source. A detector counts the number of ions with a specific mass. This information is sent to a computer and a mass spectrum is created. The mass

spectrum is a graph of the number of ions with different masses that travelled through the filter.

## Computer

The data from the mass spectrometer is sent to a computer and plotted on a graph called a mass spectrum. The computer on the GC-MS has a library of spectra that can be used to identify an unknown chemical in the sample mixture. The library compares the mass spectrum from a sample component and compares it to mass spectra in the library. It reports a list of likely identifications along with the statistical probability of the match.

The same procedure was followed for the other samples to be analysed with GC/MS and the results are given in the results section.

### G. High shear mixer

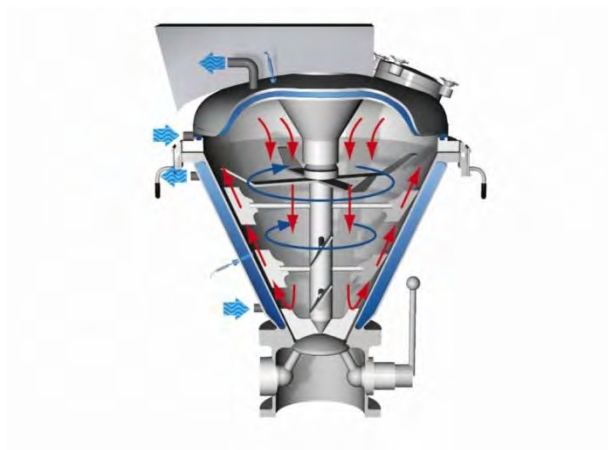


Figure 18 Schematic representation of High Shear Mixer

1. One sample of 2.5% Nafion® solution was subjected to high shear mixing (speed of 5krpm and 10krpm) for 5 minutes.
2. Immediately upon completion, the sample was separated into 2 parts.
3. The first part was tested on the rheometer.
4. The 2nd part was vacuum dried until crystals were formed before being tested with the DSC apparatus. (See above for specific procedure). 2 to 3 drops of THF (tetrahydrofuran) was used as solvent.
5. A fresh sample of 2.5% Nafion® solution was next used for each time of 60, 40, 30, 15, 10 and 5 minutes.
6. Steps (1) to (5) were repeated for the remaining 3 concentrations of Nafion® solution.

### 3.11. Temperature Control

The temperature of the Nafion® samples was monitored because it was important to control all the parameters that could degrade Nafion®. Because our main objective was to see ultrasound effect on Nafion®. The temperature of the polymer solution was maintained constant within  $\pm 2$  °C by circulating cold water through the jacketed reactor.



Figure 19 showing jacketed reactor

### 3.12. Volume Used

The volume used to prepare the samples was always kept constant because this can manipulate the ultrasound effect on Nafion®.



## **4. CHAPTER 4 RESULTS AND DISCUSSION**

### **4.1. Silent Conditions**

The experiments focused on the effect of temperature and high shear mixing (i.e under silent conditions) on Nafion® in order to separate the thermal, cavitation and high agitation induced by ultrasound under silent conditions. The samples for control experiments were made by keeping a constant volume; the procedures for making the samples are given in the experimental procedure. The samples were then analysed using Rheometer and a Differential Scanning Calorimetry to measure changes in viscosity and glass transition temperatures, and then were compared with samples subjected to ultrasonic treatments at various ultrasonic powers and high shear mixing at different rotation speeds. The control experiments are given below. The temperature was also kept at 298 k for all the experiments performed.

The choice of comparing ultrasound experiments to temperature and shear-mixer experiments was to see if shear- mixer and temperature gives the same results. As explained earlier the motivation for this thesis was the result of ultrasonic applications being used more frequently in fabrication of fuel cell materials. Because ultrasound and high Shear mixing are both mechanical processes in origin comparing the two is a good way of distinguishing which technique could be better suitable for fabrication of Nafion® for fuel cell use.

#### **4.1.1. The Effect of Ultrasound on Nafion® At Various temperatures**

Sonication of Nafion® at various temperatures has an effect on the degree of degradation therefore all the experiments were performed at the same temperature of 298 k. Most of the chemical processes are accelerated by increase in temperature however the opposite effect is noticed in mechanical processing such as ultrasound. This negative temperature coefficient therefore suggests that the process is mechanical in origin. Sonochemical processes show faster rates at lower temperature than higher temperatures. Furthermore the primary sonochemical step is more efficient at low temperatures. At higher temperatures, the solvent vapour pressure is more therefore the vapour enters the cavitation bubble. This effectively cushions the collapse and thus the movement of solvent molecules is slowed down and therefore the shock waves are reduced. Therefore the experiments were carefully performed

at the same temperature using jacketed reactor in order to separate the ultrasound effect on Nafion® from temperature driven effects.(Price and Smith 1993, Vijayalakshmi and Madras 2004).

#### 4.1.2. Effect of Nafion® Concentration

Preliminary studies focused on the effect of Nafion® concentration on viscosity at fixed temperature and in the absence of ultrasound. The results are given in table 2.

**Table 2 Showing the viscosity of different Nafion® solution's under controlled conditions**

Concentration (wt %)	Viscosity( $\eta$ ) pa.s (x10 <sup>-3</sup> )	Temperature (oC)	Sonication Time (MIN)
2.5	1.709	25	0
5.0	2.762	25	0
7.5	6.252	25	0
10	11.390	25	0

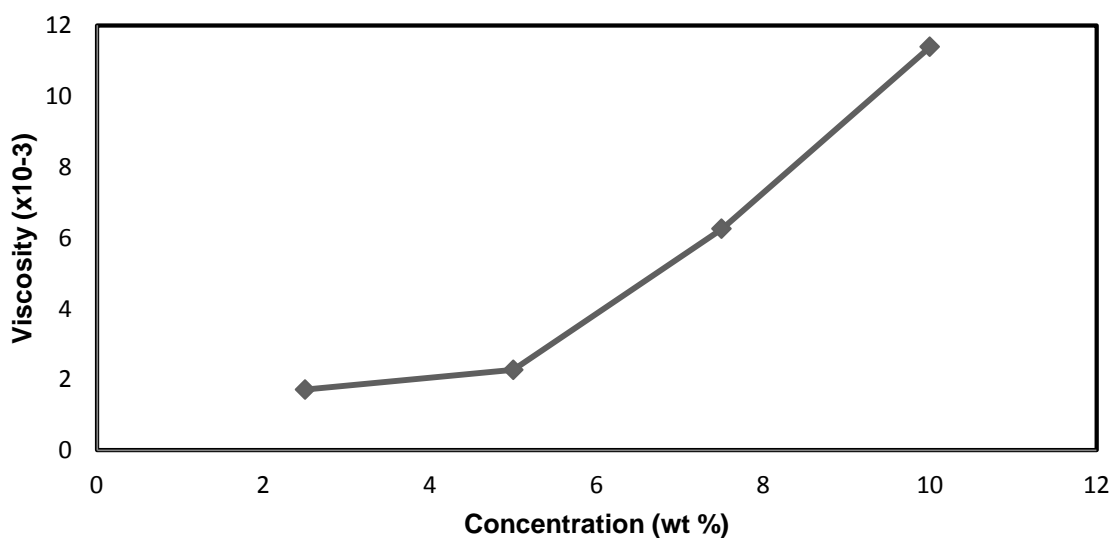


**Figure 20 Graph showing viscosities ( $\eta$ ) of different concentration Nafion® solutions at no ultrasound and constant temperature of 25°C**

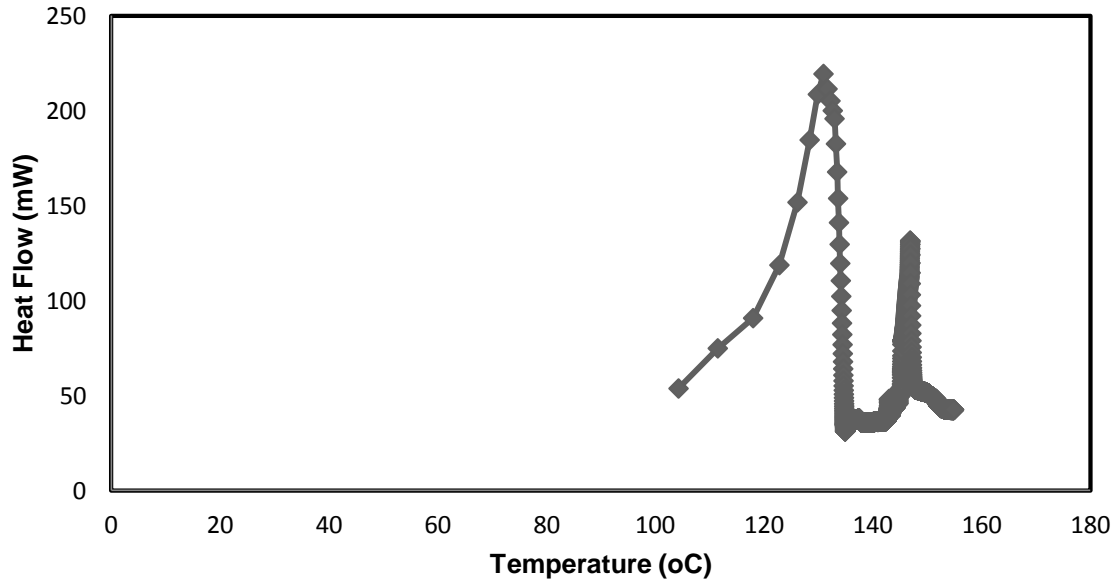


**Figure 21 Graph showing Tg of Nafion® of control experiment with no ultrasound and no high shear mixer.**

From the preliminary experiments the initial viscosity and Glass transition temperature of Nafion® were deduced prior to ultrasound and high shear mixing treatment. The purpose of these preliminary experiments was to establish what effect ultrasound and high shear mixing has on Nafion® degradation. The glass transition temperature of Nafion® from the preliminary experiments is 148°C which agrees with the literature value of 148°C. The following results and discussion show our findings.

#### **4.1.3. The Effect of Temperature on Nafion®**

Increasing the operating temperature of fuel cells is desirable because it reduces CO poisoning of the catalyst. CO and H<sub>2</sub> compete to absorb on the platinum based catalyst. Below 100°C, if the concentration of CO is higher than 1-10 ppm, CO will win this competition, which results in a drop in performance. As the temperature of the fuel cell increases, more and more CO can be tolerated. Higher operating temperatures also make the rejection of waste heat easier. Conversely, common fuel cell membranes including Nafion® perform poorly at higher temperature and degrade more quickly. (Satterfield 2007)

The mechanical properties of Nafion® are strongly dependent on temperature; this is because as the temperature increases the bonding strength between the polymer chains reduces. As temperature increases, the thermal energy of Nafion®'s molecules eventually becomes greater than that of the polymer's secondary bonds, and chains are able to move past one another freely when force is applied. Secondary bonds in Nafion® contain hydrogen bond cross-linking between the sulfonic acid groups and Van der Waals interactions between main chains. Numerous studies have addressed the issue of thermal stability and thermal degradation of PFSA membranes. The polytetrafluoroethylene (PTFE)-like molecular backbone gives Nafion® membranes their relative stability until beyond 150°C due to the strength of the C–F bond and the shielding effect of the electronegative fluorine atoms. At higher temperatures, Nafion begins to decompose via its side sulfonate acid groups. PFSA membranes are subject to critical breakdown at high temperatures due to the glass transition temperatures of PFSA polymers. (Majsztrik 2008)

Thermal degradation of polymers is molecular deterioration as a result of overheating. At high temperatures the functional groups of the long chain backbone of the polymer can begin to separate (molecular scission) and react with one another to change the properties of the polymer. Thermal degradation usually involves changes to the molecular weight (and molecular weight distribution) of the polymer and characteristic changes include reduction in ductility, embrittlement, chalking, colour changes, cracking, overall reduction in most other desirable physical properties.(Alwai 2009)

The 2.5% Nafion® solutions were made by keeping a constant volume and then the different solutions were tested to see the effect of temperature increase on the polymer, the temperature range used was from 20 to 80°C and 4 samples were tested at 25, 40, 60 and 80°C for 1 hour. The results are given in table 6 and fig 16. The degradation was measured in the same way by measuring the change from initial viscosity. The initial viscosity of 2.5% Nafion® solution at room temperature was  $1.709 \times 10^{-3}$  pa.s. From the results it can be concluded that there is no significant change in viscosity from the initial viscosity at room temperature. At 80 °C reduced to only  $1.69 \times 10^{-3}$  pa.s although there is a slight decrease in viscosity, it is not significant enough to conclude that polymer has fully degraded. This can be the result of thermal energy of Nafion® being sufficient enough to cause the breakage of secondary bonds within the polymer, and thus the chains are able to move past one another easily hence the slight reduction in viscosity. It can be concluded that there are no breakages

of the primary covalent and ionic bonds within the polymer at 80°C because there is no significant reduction in viscosity. Secondly the primary bonding within Nafion® is considerably strong and gives Nafion® stability until beyond 150°C due to the strength of the C–F bond and the shielding effect of the electronegative fluorine atoms as explained earlier.

**Table 3 Showing The Effect of Temperature On 2.5% Nafion® at 60 Minutes at various temperatures**

Nafion® Concentration (% wt)	Temperature exposing Time (mins)	Temperature (oC)	Viscosity $\eta$ ( $\times 10^{-3}$ pa.s)
2.5	60	25	1.709
2.5	60	20	1.709
2.5	60	40	1.709
2.5	60	60	1.706
2.5	60	80	1.690

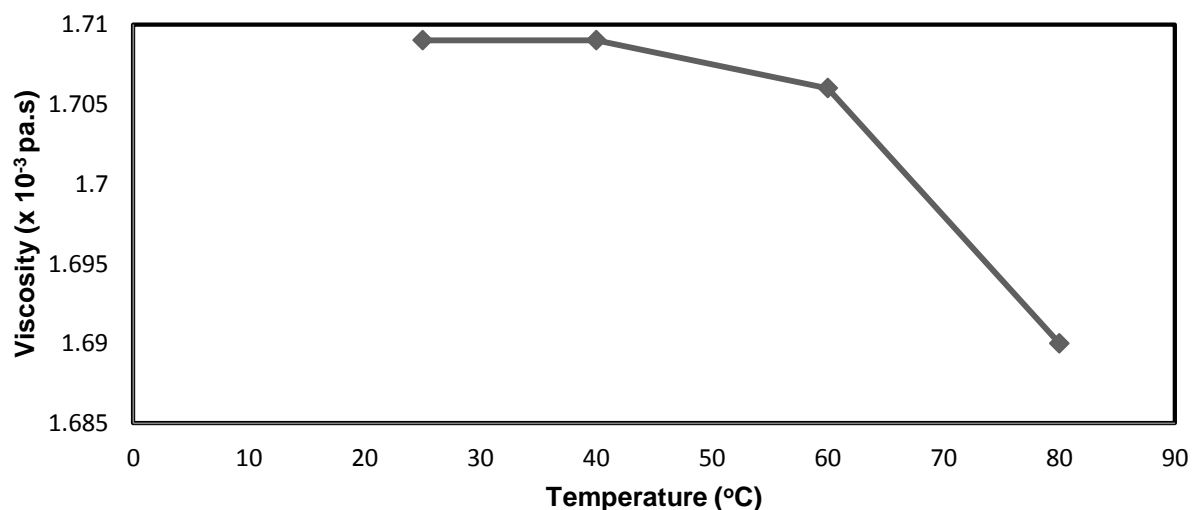


**Figure 22 Showing The Effect of Temperature On 2.5% Nafion® at 60 Minutes at Various Temperature**

#### 4.1.4. Effect of High Shear Mixing on Nafion® in the Absence of Ultrasound

The effect of high shear mixer on Nafion® was also investigated. The samples for the experiment were made in the same way by keeping a constant volume the experimental procedure is given in chapter 3. The different 5% concentration samples were mixed for time periods of 1, 5, 10, 20, 30, 60, and 120 minutes at rates of 5krpm and 10krpm.

From the results in fig 23 and 24 and table 4 and 5 it can be concluded that there is a steady decrease in the viscosity of the Nafion® solution from 1 minute shear mixing to 120 minutes. The initial viscosity of the 5% solution is  $2.762 \times 10^{-3}$  pa.s and after 120 minutes it decreased to  $2.53 \times 10^{-3}$  pa.s for the 5krpm rate and  $2.33 \times 10^{-3}$  pa.s for the 10krpm however it is important to point out that the decrease in viscosity is not as significant when compared to sonication where the viscosity reduced to  $1.798 \times 10^{-3}$  pa.s. This proves that although high shear mixer degrades the polymer it does not degrade it as much as ultrasound does and this can be attributed to the fact that mechanical degradation breaks the bonds within the polymer near the end of the molecule whereas the ultrasound irradiation causes breakage at the centre of the molecule each time therefore resulting in more severe degradation. There is also no sudden increases in viscosity of the polymer therefore we can assume that the shear mixer does not contribute to polymerization as was noticed for the ultrasound irradiated samples.(C), (Redl 2003)

**Table 4 The effect of high shear mixer on 5% Nafion® At Shear Rates of 5000 rpm**

Shear Mixer Rate : 5000 rpm	
Nafion® Concentration: 5%	
Shear Mixing Time (Mins)	Change in Viscosity $\eta$ ( $\times 10^{-3}$ pa.s)
0	2.762
1	2.76
2.5	2.75
5	2.75
10	2.69
30	2.62
60	2.59
120	2.53

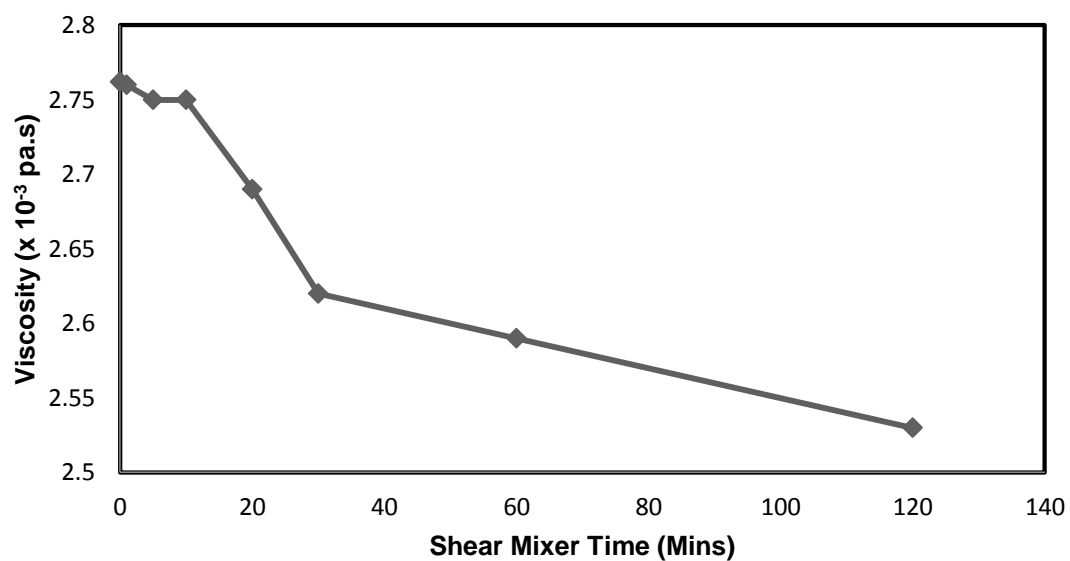


Figure 23 Graph Showing change in Viscosity for 5% Nafion® At Shear Rates of 5000 rpm

Table 5 The effect of high shear mixer on 5% Nafion® At Shear Rates of 10,000 rpm

Shear Mixer Rate : 10,000rpm	
Nafion® Concentration: 5%	
Shear Mixing Time (Mins)	Change in Viscosity $\eta$ (x10-3 pa.s)
0	2.762
1	2.7
2.5	2.68
5	2.6
10	2.52
30	2.48
60	2.41
120	2.33

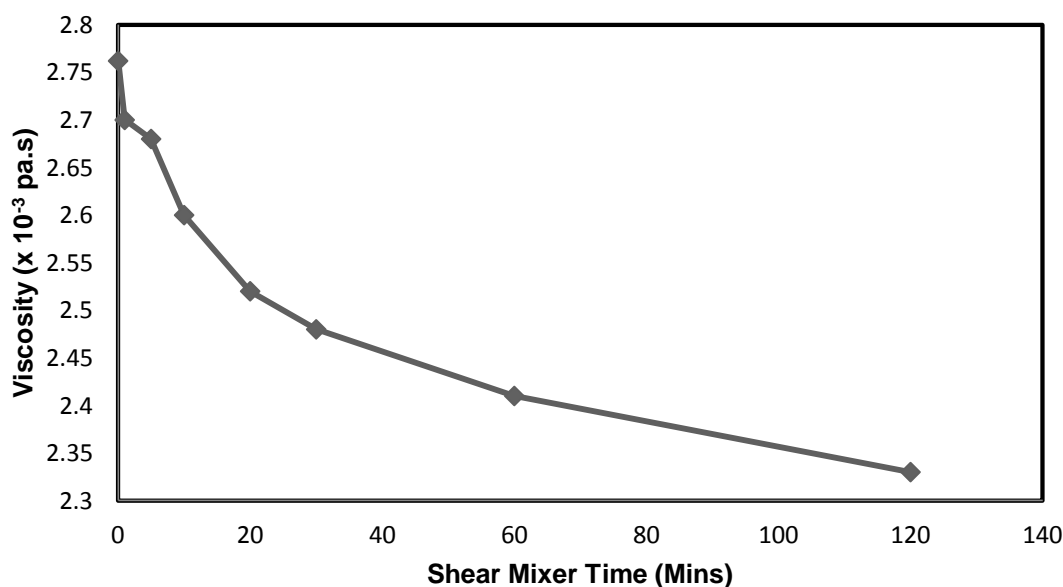


Figure 24 Graph Showing change in Viscosity ( $\eta$ ) for 5% Nafion® At Shear Rates of 10,000 rpm

#### 4.1.5. DSC measurement Of High Shear mixed Nafion samples

Different samples of Nafion® were analysed by Differential Scanning Calorimetry in order to see the effect of high Shear mixing on the physical properties of the polymer in question. The results are given in (fig 25 to fig 28). The DSC analysis of high shear mixer experiments show that there is no increase in the Tg for the shear mixing done at 5krpm for time periods of 5 and 30 minutes fig 25 and fig 26, however for the high shear mixing done at 10krpm for time periods of 10 minutes and 5 minutes (fig 27 and fig 28) there is a decrease in the Tg. this can be attributed to the damage by generation of heat, at high shear mixing rate of 10krpm, There may be separate particles but generation of heat may cause scission of chains thereby reducing Tg (Nguyen 1995)



## DSC Analysis of High Shear Mixer

- **Nafion® 10% In THF 5 Minutes High Shear Mixer (HSM) 5000 rpm**

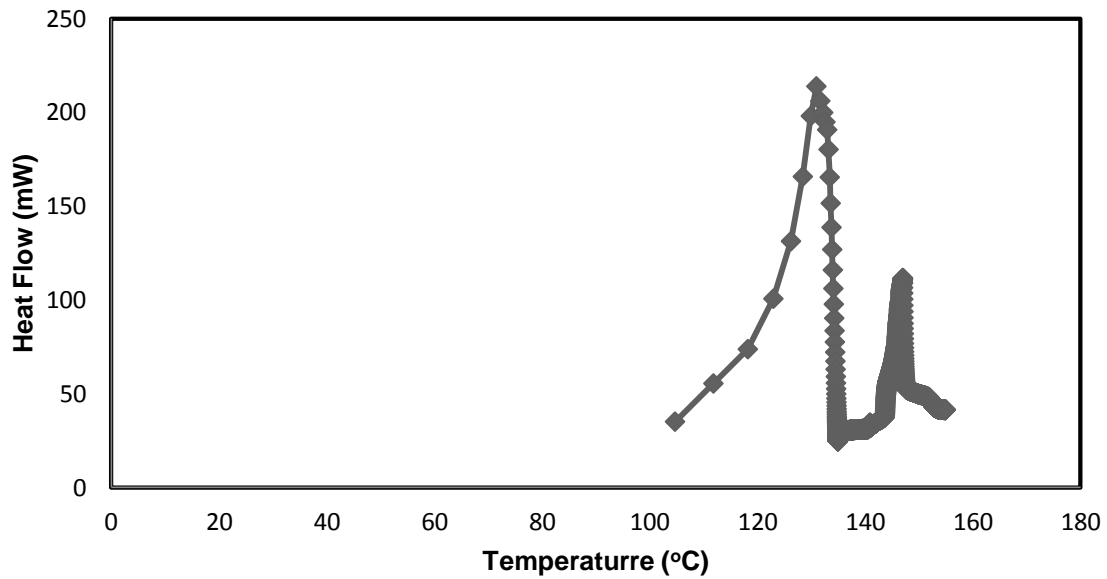


Figure 25 Graph showing No change of Tg for Nafion® 10% In THF 5 Minutes High Shear Mixer (HSM) 5000 rpm

- **Nafion® 10% In THF 30 Minutes High Shear Mixer (HSM) 5000 rpm**

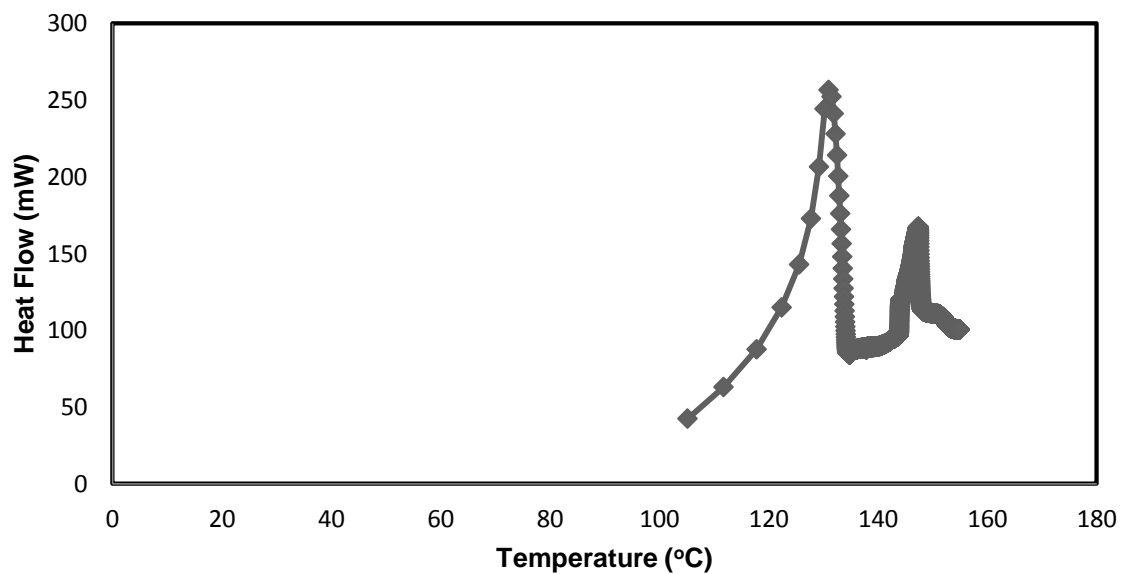
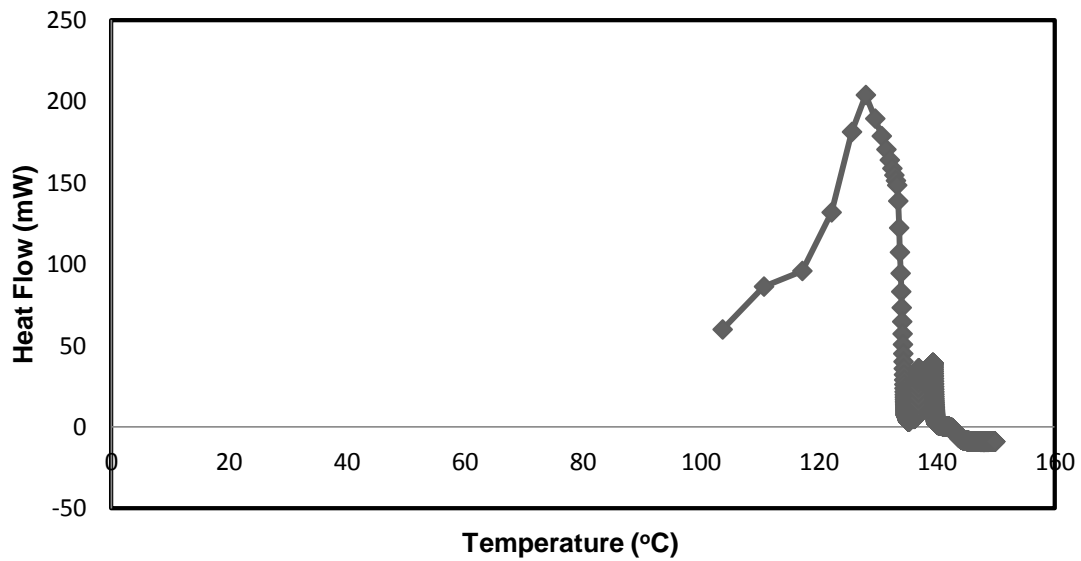


Figure 26 Graph showing No change of Tg for Nafion® 10% In THF 30 Minutes High Shear Mixer (HSM) 5000 rpm

- **Nafion® 10% In THF 10 Minutes High Shear Mixer (HSM) 10,000 rpm**



**Figure 27 Graph showing Decrease in Tg for Nafion® 10% In THF 10 Minutes High Shear Mixer (HSM) 10,000 rpm**

- **Nafion® 10% In THF 5 Minutes High Shear Mixer (HSM) 10,000 rpm**

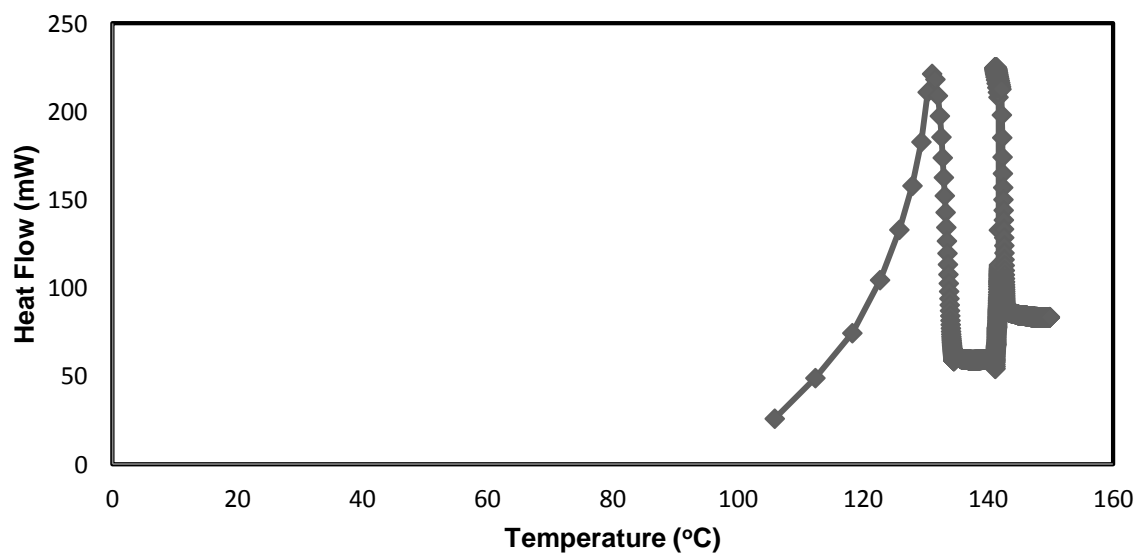


**Figure 28 Graph Showing Decrease in Tg for Nafion® 10% In THF 5 Minutes High Shear Mixer (HSM) 10,000 rpm**

## 4.2. Ultrasonic Conditions

### 4.2.1. Effect of Nafion® Concentration

The effect of Nafion® concentration at constant volume and same ultrasound power was investigated. The results from table 6 and fig 29 shows that higher concentration of Nafion® shows the extent of viscosity reduction decreases with an increase in the solution concentration at the same supplied ultrasonic power. In other words the degradation is lower at higher concentration of Nafion® solution compared to lower concentration of Nafion® where the degradation is higher. The increase of polymer concentration increases the viscosity of the polymer solution and intensity of cavitation falls down with an increase in the viscosity of the medium. As the formation of cavitation in the liquid requires that the negative pressure in the rarefaction region of wave function must overcome the natural cohesive forces acting within the liquid. Cavitation is more difficult to produce in viscous liquids, where the cohesive forces are stronger. It should be noted here that independent bubble dynamics studies have clearly indicated that an increase in the viscosity results in a decrease in the collapse pressure generated due to cavitation. So an increase in viscosity with concentration results in the molecules to become less mobile in solution and the velocity gradients around the collapsing bubbles to therefore become smaller, resulting in lower extents of viscosity reduction in the case of polymer systems. Therefore in terms of the degradation of Nafion® the extent of degradation is therefore expected to be lower at higher concentration of the Nafion® solution.

This coincides well with similar results published by Desai et al who studied the ultrasonic degradation at different concentrations. For example from the results it is clearly seen that after 30 minutes of sonication the higher viscosity is seen for the 10 percent Nafion® solution  $15.320 \times 10^{-3}$  Pa.s compared to Nafion® concentration of 2.5% after 30 minutes of sonication where the viscosity reduced to as little as  $1.709 \times 10^{-3}$  Pa.s, and since in polymer chemistry degradation is quantified by either molecular weight distribution or by change in intrinsic viscosity therefore we can safely assume that the greater degradation will occur at lower concentration of the Nafion® solution. Another explanation for this phenomenon is because at high Concentrations, entanglements influence the energy transfer processes between solvent and polymer and appears to reduce the probability of degradation. Also at

higher concentrations the intensity of cavitation phenomenon is depressed and therefore the extent of polymer chain breaking decreases.(Mohod 2011). The results indicate that the percentage degradation reduced with increasing concentration which affects the cavitation intensity in the system. (Desai 2008)

**Table 6 Showing effect of ultrasound on Different Nafion® Concentrations at 30 minutes using ultrasound Probe %20AMP at 25°C**

		Power : 1.86 W
		Ultrasound Probe
Nafion® Concentration (% wt)	Sonication Time (Mins)	Viscosity (x10 <sup>-3</sup> pa.s)
2.5	30	1.709
5	30	2.762
7.5	30	6.252
10	30	15.320

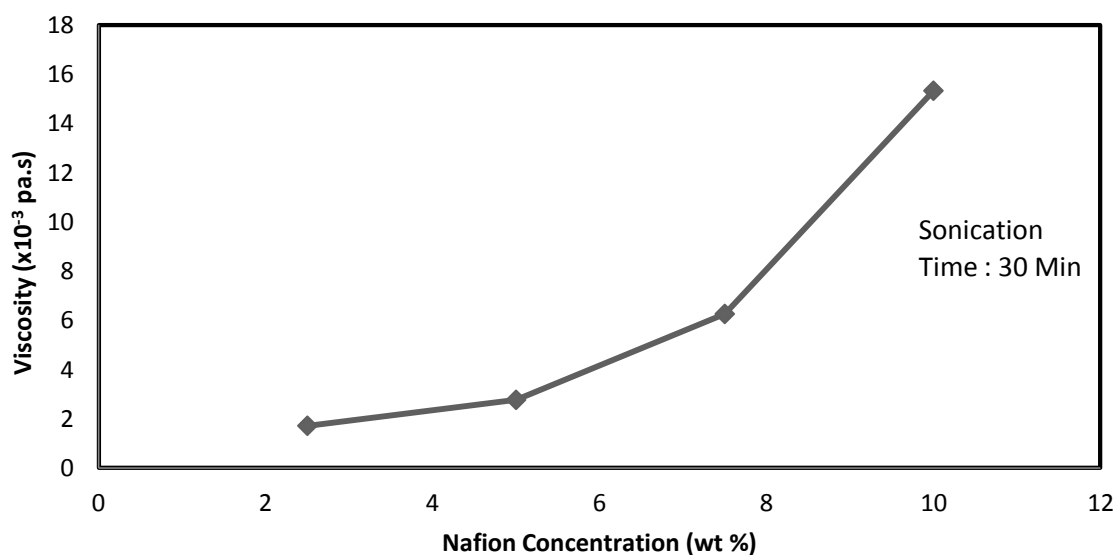


**Figure 29 Showing effect of ultrasound on Different Nafion® Concentrations at 30 minutes using ultrasound Probe %20amp at 25°C**

#### 4.2.2. 5% Nafion® Solutions Sonicated at 0.32 W (Bath)

The experiments were conducted by making different solutions of Nafion® (the experimental procedure is given in Chapter 3) were made by diluting it with ultrapure water, the solutions made were of the concentration of 2.5%, 5%, 7.5% and 10% respectively, these solutions were then subjected to ultrasound using ultrasound probes and ultrasound bath for time periods of 1, 2.5, 5, 10, 30, 60 and 120 minutes. The power measurements for the ultrasound probe and the ultrasound bath were worked out and the results along with power measurements are given in the Appendix 1A. (Mohod 2011)

The results show that the most extensive degradation of the Nafion® polymer occurred at the lowest ultrasonic frequency when the input ultrasonic power was above the cavitation threshold indicating that the shear forces generated by the rapid motion of the solvent were responsible for the breakage of chemical bonds within the polymer. For the ultrasonic bath experiments it was observed that in the range of sonication period of 0 minute to 120 minutes the Nafion® solution viscosity decreased from  $2.762 \times 10^{-3}$  to  $1.845 \times 10^{-3}$  Pa.s at an ultrasonic power of 0.48W. The ultrasonic probe experiments showed the viscosity of Nafion® reduced from  $2.762 \times 10^{-3}$  Pa.s at 0 mins down to  $1.949 \times 10^{-3}$  Pa.s at 120 minutes at a power of 1.86W;-this obvious decrease in viscosity could be attributed to the fact that covalent bonds within the Nafion® polymers broke when the input ultrasonic power exceeded the cavitation threshold. Furthermore from the results it can be seen that after 120 minutes of sonication the degradation reached a point where the Nafion® viscosity reduced permanently. Because from the ultrasonic bath results it can be seen that after 120 minutes of sonication the viscosity obtained from the rheometer was  $1.845 \times 10^{-3}$  Pa.s compared to the viscosity of 120 minute ultrasonic bath sonicated samples left overnight, for which the measured viscosity was  $1.820 \times 10^{-3}$  Pa.s. This proves that there is a very small difference between the viscosities of the fresh sample compared to viscosity of overnight samples. This further backs the argument that at 120 minutes there is permanent reduction in viscosity of the Nafion®, the results show that depolymerised Nafion® does not repolymerise. This observed trend in our results is in good agreement with similar work performed on the ultrasonic depolymerisation of aqueous polyvinyl alcohol.(Grönroos 2001). However before we can be certain that permanent reduction in viscosity is reached at 120 minutes of

sonication at the power used in our experiments further experiments need to be performed to observe whether the viscosity reduces further than  $1.845 \times 10^{-3}$  Pa.s. (Mohod 2011)

Different models have been used to explain the degradation mechanisms of the polymers, in the first model; the degradation is interpreted in terms of the high temperature and pressure generated during the bubble collapse. jetlink model attributes chain scission of the polymer chain as the increased frictional force generated on cavitation collapse. The other model describes degradation as the interaction between the formation of eddies due to shock waves are responsible for interaction with the macromolecule in solution. From the literature it is generally agreed and accepted that hydrodynamic forces have the primary importance in degradation of polymers. Due to these forces which are the result of increased frictional forces between the ultrasonically accelerated faster moving solvent molecules and the much slower and less mobile polymer;- these hydrodynamic forces may also be the result of cavitation bubble collapse. It is important to emphasise that degradation due to ultrasound is different than chemical and thermal decomposition and the cleavage takes place almost in the centre of the polymer and therefore resulting in more degradation of the larger macromolecules. (Mohod 2011)

Ultrasonic irradiation has an important effect on polymers in terms of their mechanical, mechano-chemical and morphological properties. Understanding the effect of different operating parameters on the extent of degradation of polymers thus becomes very important. From our results it can be observed that the viscosity attained after 120 minutes of sonication at ultrasonic bath is the limiting intrinsic viscosity. This viscosity could well be the point at which the polymer chain is so short that it follows ultrasonic vibrations flexibly, and cleavage at the centre of the molecule does not take place further.(Mohod 2011)

**Table 7 Showing change in viscosity for 5% Nafion® solution using ultrasonic bath and Probe over 120 minutes at 25°C**

Viscosity $\eta$ ( $\times 10^{-3}$ Pa.s)		
Power: 0.32 W		
Power: 1.86 W		
Sonication Time (Mins)	Bath	Probe

0	2.762	2.762
1	2.71	2.74
2.5	2.69	2.71
5	2.62	2.66
10	2.54	2.6
30	2.7	2.72
60	2.58	2.35
120	1.845	1.949

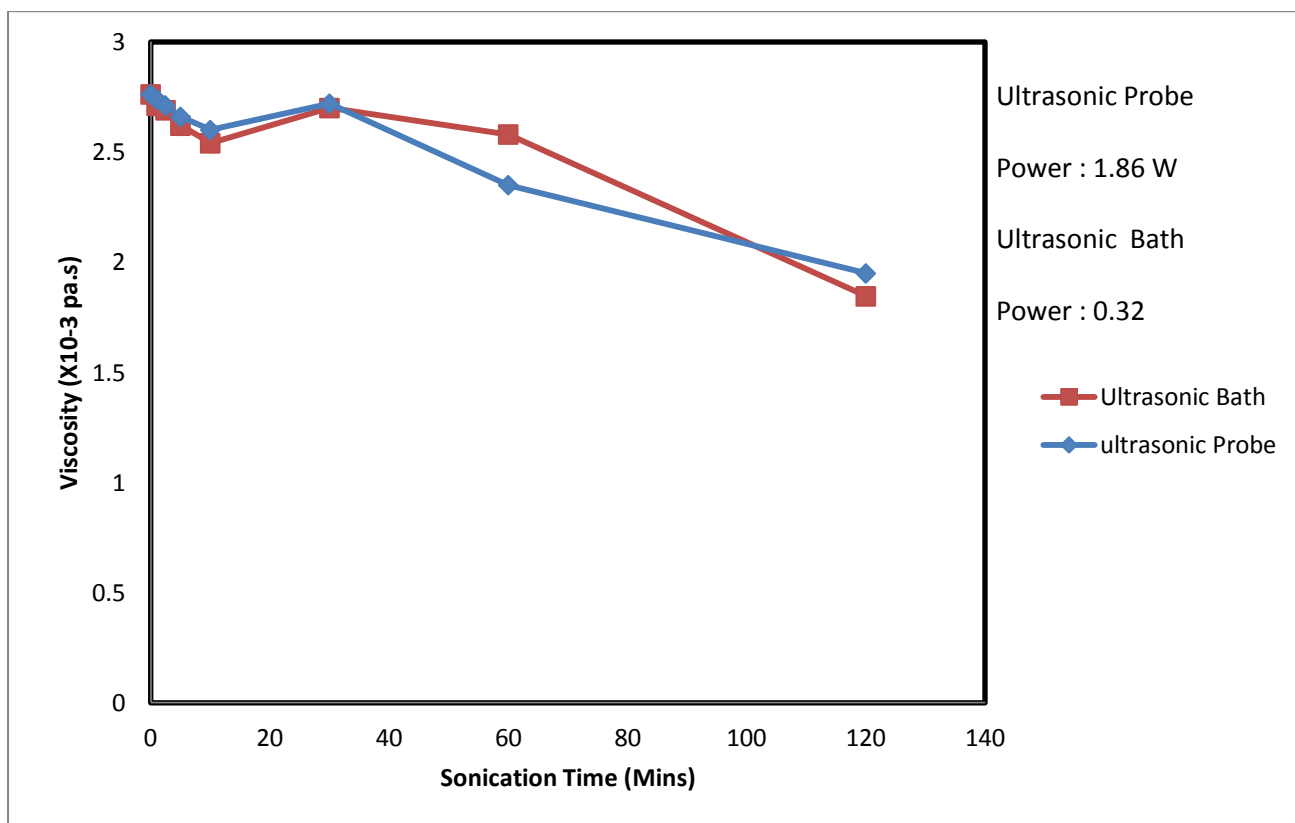
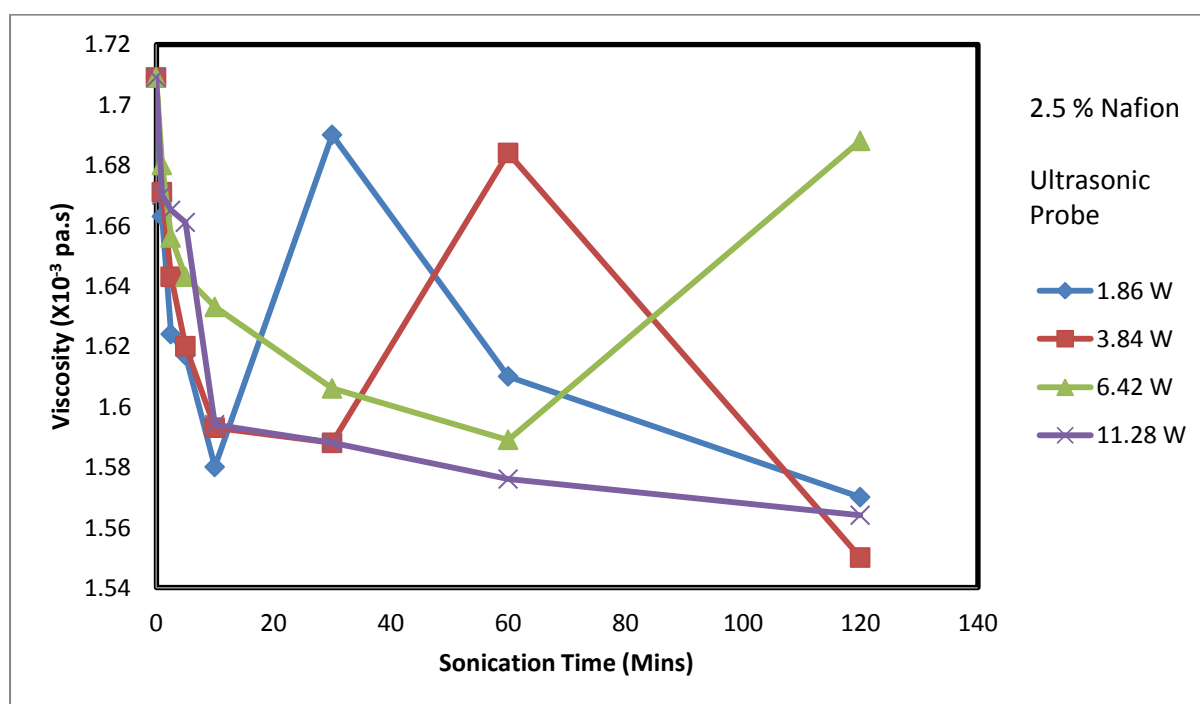


Figure 30 Showing Change in Viscosity  $\eta$  of 5% Nafion® solution Using Ultrasonic bath and Probe Over 120 minutes at 25°C

### 4.2.3. 2.5 Nafion® Solution Sonicated at Different Powers With US (Probe)

**Table 8 Showing Change in Viscosity ( $\eta$ ) of 2.5% Nafion® Solution Using Ultrasonic Probe at 20%, 40 %, 60% and 80 % AMP Over 120 minutes at 25°C**

	Power : 1.86 W	Power : 3.84 W	Power : 6.42 W	Power : 11.28 W
	Ultrasound probe	Ultrasound probe	Ultrasound probe	Ultrasound probe
Sonication Time (Mins)	Change in Viscosity $\eta$ (x10-3 Pa.s)	Change in Viscosity $\eta$ (x10-3 Pa.s)	Change in Viscosity $\eta$ (x10-3 Pa.s)	Change in Viscosity $\eta$ (x10-3 Pa.s)
0	1.709	1.709	1.709	1.709
1	1.663	1.671	1.68	1.67
2.5	1.624	1.643	1.656	1.665
5	1.617	1.62	1.643	1.661
10	1.58	1.593	1.633	1.594
30	1.69	1.588	1.606	1.588
60	1.61	1.684	1.589	1.576
120	1.57	1.55	1.688	1.564



**Figure 31 Showing Change in Viscosity ( $\eta$ ) of 2.5% Nafion® Solution Using Ultrasonic Probe at 20%, 40 %, 60% and 80 % AMP Over 120 minutes at 25°C**



The 2.5% Nafion® samples were sonicated using ultrasonic probes and bath for irradiation time periods of 1, 2.5, 5, 10, 30, 60 and 120 minutes, the power measurements were determined for both the ultrasound probe and the ultrasound bath from experiments and are given in appendix 1a. From the results in figure 31 and table 8 it is apparent that there is a gradual decrease in the viscosity of Nafion® for all the samples sonicated at different ultrasound power. For example the viscosity for the ultrasound probe runs show at 0 minute the starting viscosity was  $1.709 \times 10^{-3}$  Pa.s and reduced to  $1.570 \times 10^{-3}$  Pa.s after 120 minutes. The reasoning for this observed trend is the same as discussed above for the 5% Nafion® solution. When the input power exceeds the cavitation threshold, it results in the increase of shear forces generated by the rapid motion of the solvent. These shear forces are responsible for the breakage of chemical bonds within the polymer. However the viscosity measured after 30 minutes of sonication at ultrasound power of 1.86 W shows an increase from viscosity at 10 minutes of sonication, the viscosity measured at 30 minutes ultrasound probe run is  $1.69 \times 10^{-3}$  Pa.s compared with 10 minute sonication of  $1.58 \times 10^{-3}$  Pa.s. The reason for this is that several polymerization studies using ultrasound have been carried out starting with a solution of polymer. The scission of polymer bonds due to ultrasound (depolymerisation) supplies new chain carriers for polymerization. Under carefully chosen conditions, it is possible to initiate polymerization reactions using ultrasound. The products obtained vary depending on the functional groups present or absent. After 10 minute sonication the percentage degradation was 7.5% for 2.5% Nafion® sample and because 30 minutes sonication showed an increase in viscosity we can therefore conclude 7.5% degradation is required to produce sufficient chain carriers for polymerisation as stated above. Further study is needed to see how the nature of the product and the polymerization rate changes with conditions, for example temperature, adducts, impurities, solvents, gases, pulsing of ultrasound, intensity, frequency, etc. It is, however, possible that ultrasonically-initiated polymerization will prove to be advantageous for some applications.

Some surprising experimental results show that for low molecular weight polyamide PA6 (LPA6), the viscosity-average molecular weight of LPA6 increases in the presence of ultrasonic oscillations due to extension reaction of end groups (-COOH and -NH<sub>2</sub>). The rupture of molecular chains of HPA6 occurs due to the initial molecular weight being higher than the critical molecular weight ( $M_n$ ): The degradation of HPA6 melt was divided into three stages, The viscosity-average molecular weight  $M_n$  decreases greatly with irradiation time before 60 s. It increases slowly with irradiation time between 60 and 120 s, and tends to a limiting

molecular weight ( $4.6 \times 10^4$ ) after 120 s. The ultrasonic degradation rate of HPA6 melt is higher than that of polymer solution, and the degradation kinetics obey the following equations: (Li 2004)

$$\overline{M}_n = 2.1 \times 10^4 + 6.4 \times 10^4 e^{-0.0269t} \quad 0 < t \leq 60 \text{ s} \quad (37)$$

$$\overline{M}_n = 4.6 \times 10^4 - 1.2 \times 10^4 e^{-0.0304(t-60)} \quad 60 \text{ s} < t \quad (38)$$

(Li 2004)

The ultrasonic rupture of C-N bond of HPA6 melt causes the formation of new end groups (-COOH and-NH<sub>2</sub>). Between 60 and 120 s, the rate of chain extension via end group coupling is higher than the rupture rate, resulting in an increase of  $M_n$ ; these results are analogous to our result for 60 minutes of sonication where the viscosity is increased.(Li 2004), (Berlin 1962)

For the Nafion® solution sonicated at 40% amplitude at a power of 3.84 W there is the same general trend of a steady decrease in the viscosity of 2.5% Nafion® solution. The sonication was carried out using the same time periods as given in fig. However the rise in viscosity occurs at 60 Min instead of 30 minute sonication. Furthermore the extent of viscosity reduction and hence the extent of degradation is lower than the 2.5% samples sonicated at 20%AMP and this is because above a certain intensity the increase number of bubbles means that the ultrasound field does not pass through the solution as efficiently reducing cavitation. There is also insufficient time between consecutive rarefaction cycles for complete bubble collapse to take place. Therefore the efficiency of the process falls at high intensity. The percentage degradation after 30 minute ultrasound exposure was 7.1% and the viscosity increase was seen at 60 percent due to the same reasons mentioned above. This behaviour was similar to the 2.5% solution sonicated at 20% amplitude and 1.86W.

The 2.5% Nafion® solution sonicated at 60% amplitude at power of 6.42 W shows a steady decrease in viscosity. The viscosity reduction is apparent from 1 minute sonication upto 60 minute sonication. However at 120 minutes there is a rise in viscosity which means that at 120 minutes there is sufficient scission of the bonds which provides enough chain carriers for polymerization and thus the viscosity is seen to increase. It is important to note that in this case the sudden jump in viscosity occurred at 120 minutes compared to 60 minutes for the 2.5 % sample at 40% Amplitude. This further backs the argument that above certain intensity ultrasound efficiency is hindered in the medium for reasons discussed above. Most effects in sonochemistry arise from cavitation. After 60 minute ultrasound the percentage degradation is 7.02% and the rise in viscosity was therefore seen after 120 minutes of ultrasound exposure because in order for polymerization to occur in the presence of ultrasound sufficient chain carriers need to be present for polymerization to occur. From this we can conclude that for the 2.5% Nafion® solution subjected to ultrasound when degradation reaches certain percentage at certain ultrasound frequency only can than polymerization occur and is evident by viscosity rise.

While some consequences of this, such as radical production, are used in making polymers, the exact origin of the effects, whether from thermal 'hot spots' or electrical or corona discharges is relatively unimportant to the polymer chemist. Most of the effects involved in controlling molecular weight can be attributed to the large shear gradients and shock waves generated around collapsing cavitation bubbles. (Price 1994)

The 2.5% Nafion® solution sonicated at 80% amplitude at power of 11.28 W also shows viscosity reduction however the extent of viscosity reduction and hence degradation is the lowest for sonication at 80AMP and power of 11.28 W. Secondly there is no sudden rise in viscosity even after 120 minutes of sonication which means that there are insufficient chain carriers present for polymerization and therefore sonication needs to be carried out for a longer period of time to see polymerization effect. This proves two things. Firstly that above certain intensity ultrasound is ineffective for degradation of Nafion® and secondly the extent of degradation reduces as the ultrasound power increases.

#### 4.2.4. 5% Nafion® Solution Sonicated at Different Powers With US (Probe)

**Table 9 Showing Change in Viscosity ( $\eta$ ) of 5% Nafion® Solution Using Ultrasonic Probe at 20%, 40 %, 60% and 80 % AMP Over 120 minutes at 25°C**

	Power : 1.86 W	Power : 3.84 W	Power : 6.42 W	Power : 11.28 W
	Ultrasound probe	Ultrasound probe	Ultrasound probe	Ultrasound probe
Sonication Time (Mins)	Change in Viscosity $\eta$ (x10 <sup>-3</sup> Pa.s)	Change in Viscosity $\eta$ (x10 <sup>-3</sup> Pa.s)	Change in Viscosity $\eta$ (x10 <sup>-3</sup> Pa.s)	Change in Viscosity $\eta$ (x10 <sup>-3</sup> Pa.s)
0	2.762	2.762	2.762	2.762
1	2.692	2.512	2.53	2.613
2.5	2.106	2.399	2.405	2.568
5	1.943	2.31	2.345	2.456
10	1.765	1.989	2.011	2.12
30	2.543	1.965	1.98	2.132
60	1.696	2.561	1.873	1.983
120	1.687	1.893	2.671	1.887

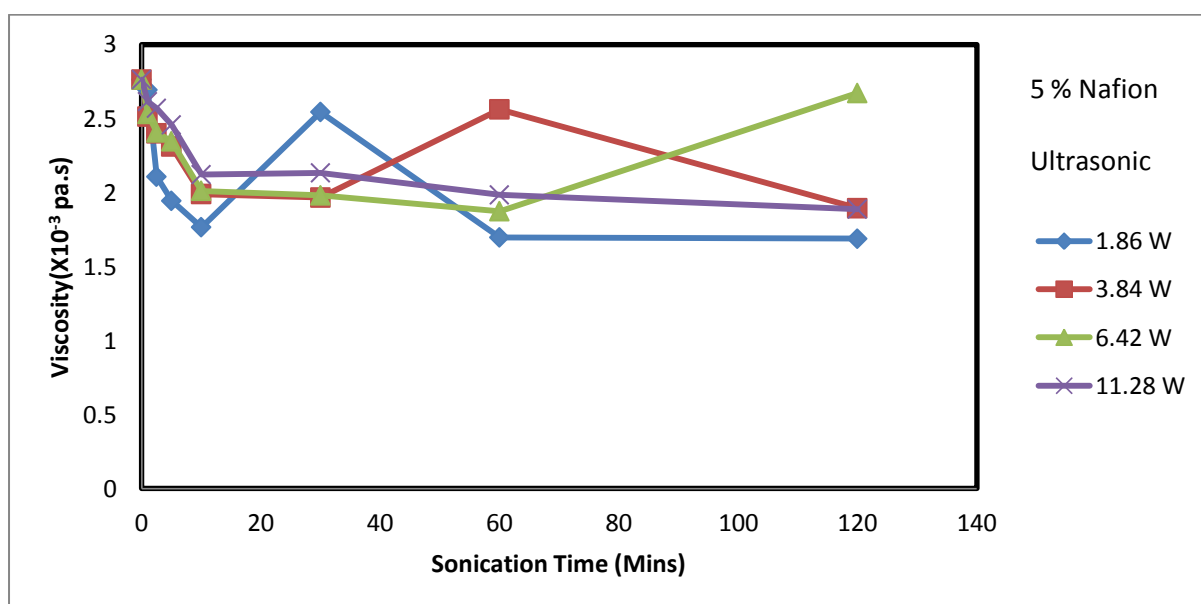


**Figure 32 Showing Change in Viscosity ( $\eta$ ) of 5% Nafion® Solution Using Ultrasonic Probe at 20%, 40 %, 60% and 80 % AMP Over 120 minutes at 25°C**

From Table 9 and Fig 32 it can be seen that there is a steady decrease in the viscosity of 5% Nafion® solution sonicated at 20% AMP at power of 1.86 W with ultrasound probe. The sonication was carried out using the same time periods. The initial viscosity of the 5% solution without sonication is  $2.762 \times 10^{-3}$  Pa.s and it gradually reduces with increase in sonication length at the above given frequency. From the results it can be seen that after 30 minutes of sonication there is a rise in the viscosity and this is the result of sufficient scissions of the bonds to produce enough chain carriers for polymerisation and hence the rise in viscosity. When the molecules are exposed to alternating compression and rarefaction cycles it results in rapid strike to the molecules resulting in friction which causes bond rupture in the macromolecules and it believed that this results in the production of copolymers and these copolymers acts to stabilize the morphological structure. Later on in the thesis the DSC analysis further backs this fact because the Tg for 5% Nafion® solution at 30 minute sonication at 1.86W showed an increase in Tg which means that the morphology was improved due to ultrasound. (Chen 2005). After 10 minutes of ultrasound exposure the percentage degradation is 36% and from 10 minutes onwards sonication time the polymerization occurs which can be seen due to the rise in viscosity. Therefore the viscosity of the 30 minute ultrasound sample was higher.

At 120 minutes of sonication the limiting intrinsic viscosity is reached and there is no further reduction in viscosity. Below the limiting viscosity, the polymer chain was so short that it followed ultrasonic vibrations flexibly and cleavage at the centre of the molecule did not take place anymore.

The 5% samples sonicated using ultrasound probe at 40% amplitude show that the initial viscosity of the 5% sample without sonication is  $2.267 \times 10^{-3}$  Pa.s and there is a steady decrease in the viscosity of the polymer due to degradation following hydrodynamic forces following cavitation collapse as mentioned earlier. However at 60 minutes sonication there is an unexpected rise in the viscosity of the Nafion® solution and this can be attributed to the same reasons discussed above. The percentage degradation after 30 minutes ultrasound exposure is 28.9% and thus from this point onwards polymerization starts to occur which is why the rise in viscosity is seen at 60 minutes ultrasound exposure and not 30 minutes. Many such studies are concerned with production of block copolymer. Because Nafion® is a copolymer these effects of increase in viscosity due to polymerization under the influence of

ultrasound are often seen. Furthermore the Tg for the 5% Nafion® sample showed that there was an increase in Tg for Nafion® sonicated at 3.84W at 40% amplitude which suggests that there is a link between the increase in viscosity attained at specific time and ultrasound power and improvement in polymer morphology backed by DSC results. (Chen 2005)

The 5% Nafion® solution sonicated at 60% AMP at power of 6.42 W with ultrasound probe was carried out using the same time periods. The extent of viscosity reduction is lower compared to samples sonicated at 1.86 W and 3.84 W. There is insufficient time between consecutive rarefaction cycles for complete bubble collapse to take place. Therefore the efficiency of the process falls at very high intensity. The sudden jump in viscosity occurs only at 120 minutes and therefore we can conclude that ultrasonic efficiency is hindered due to the reasons discussed above. The percentage degradation at 60 minutes ultrasound exposure is 32.2% and therefore the rise in viscosity was only seen at 120 minutes. The 5% Nafion® solutions followed similar trend to the 2.5% Nafion® solutions and proves that viscosity increase can only occur after certain level of degradation is achieved to provide enough chain carriers in order to initiate polymerization. The intrinsic viscosity has not reached at 120 minutes. Ultrasonic irradiation could be used as a source of free radicals generation. Acoustic cavitation generates small cavities which grow and collapse in microsecond. This collapse is an adiabatic process and generates very high local temperatures (>10,000 K) and pressures (>1000 atm). Because of this extreme environment, decomposition of water, surfactant, monomers and oligomers take place causing radical generation which helps in initiating and propagating polymerization.

The 5% Nafion® solution sonicated at 80% amplitude at power of 11.28 W shows that the extent of viscosity reduction and hence degradation is the lowest for sonication at 80AMP and power of 11.28 W compared to the other 3 powers. Furthermore there is no jump in viscosity even after 120 minutes of sonication which suggests that ultrasonic efficiency has decreased for reasons mentioned before. This trend in change in viscosity is also seen for 2.5% samples sonicated at the same frequency. Therefore the arguments given for the behaviour of viscosity change seems reliable and it is further backed by similar work done in the literature.

#### 4.2.5. 7.5% Nafion® Solution Sonicated at Different Powers With US (Probe)

**Table 10 Showing Change in Viscosity ( $\eta$ ) of 7.5% Nafion® Solution Using Ultrasonic Probe at 20%, 40 %, 60% and 80 % AMP Over 120 minutes at 25°C**

	Power : 1.86 W	Power : 3.84 W	Power : 6.42 W	Power : 11.28 W
	Ultrasound probe	Ultrasound probe	Ultrasound probe	Ultrasound probe
Sonication Time (Mins)	Change in Viscosity $\eta$ (x10 <sup>-3</sup> Pa.s)	Change in Viscosity $\eta$ (x10 <sup>-3</sup> Pa.s)	Change in Viscosity $\eta$ (x10 <sup>-3</sup> Pa.s)	Change in Viscosity $\eta$ (x10 <sup>-3</sup> Pa.s)
0	6.252	6.252	6.252	6.252
1	6.105	6.108	6.15	6.222
2.5	5.94	6.102	6.139	6.212
5	5.81	5.962	6.124	6.198
10	5.69	5.763	6.052	6.189
30	6.22	5.61	5.986	6.11
60	5.576	6.19	5.892	6.05
120	5.489	5.49	5.451	5.98

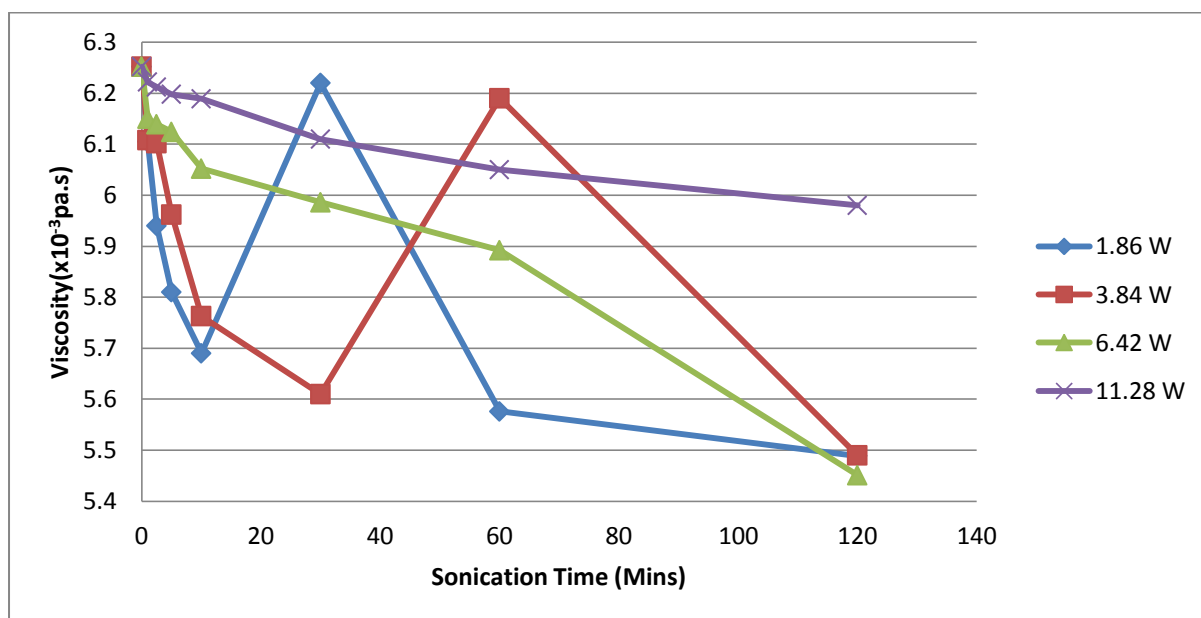


**Figure 33 Showing Change in Viscosity ( $\eta$ ) of 7.5% Nafion® Solution Using Ultrasonic Probe at 20%, 40 %, 60% and 80 % AMP Over 120 minutes at 25°C**

The 7.5% solution was made in the same way by keeping a constant volume, the different samples were sonicated with ultrasound probe and the power measurement for which is given in appendix 1a. The experimental procedure for mixing the required Nafion® concentration is given in chapter 3. From the results in table 10 and fig 33 there is a steady decrease in Viscosity but at 30 minutes there is a sudden rise in viscosity which can be attributed to the fact that scission of polymer bonds due to ultrasound (depolymerisation) supplies new chain carriers for polymerization. This effect is seen for other Nafion® concentrations where unexpected jump in viscosity is seen and therefore we can conclude that polymerization due to new chain carries results in increase in viscosity of the Nafion® solution.

The 7.5% Nafion® solution sonicated at 40% amplitude and 3.84 W shows a steady decrease in the viscosity of Nafion®. This is the result of degradation of the polymer which arises because the growth and explosive collapse of microscopic bubbles. The sound wave propagates through the fluid result in extreme conditions of temperature (>2000 K) and pressure (>500 bar) on a microsecond timescale leading to the formation of reactive intermediates such as radicals. The motion of fluid around the bubbles is rapid resulting in very efficient mixing and the formation of liquid jets. The rapid motion can result in effective shear degradation of polymer chains in the vicinity of cavitation bubbles. The initial viscosity of the 7.5% Nafion® solution is  $6.252 \times 10^{-3}$  Pa.s and reduced to  $5.490 \times 10^{-3}$  Pa.s. The extent of degradation is lower compared to Nafion® sonicated for same time intervals at 1.86 W. The sample sonicated for 60 minutes shows a sudden rise in viscosity and this is attributed to , the fact that it has convincingly been shown that the use of high intensity ultrasound can significantly enhance reactivity in these polymerisations. A number of factors associated with sonication of polymer systems could account for these results. Sonication can promote very efficient mass transfer and mixing. In other polymerizations, it has been demonstrated that this can lead to good distribution of catalysts through reactants leading to efficient initiation

Of polymerisation.(Gareth J 2003). There is similarity between the trend in viscosity reduction and thus degradation for 7.5% and 5% Nafion® solution, for example both concentrations follow the same trend for 1.86W and 3.84W. The sonicated sample at 1.86W shows rise in viscosity at 30 minutes ultrasound exposure and the sample sonicated at 3.84 shows increase in viscosity after 60 minutes exposure similar to the 5% trend. This suggests that desirable morphological changes do take place due to ultrasound initiating formation of



copolymers for stable morphology. It is expected that DSC analysis would therefore show an increase in T<sub>g</sub> similar to the 5% solution.

The 7.5% Nafion® solution sonicated at 60% amplitude at power of 6.42 W again showed a similar trend of viscosity reduction, the reasons for viscosity reduction and hence degradation is the same as discussed previously. The extent of viscosity reduction and hence degradation is lower compared to sonicating at 1.86 and 3.84 W. there are no sudden viscosity increase firstly because ultrasonic efficiency decreases at higher intensity, and secondly the solution concentration has increased which means the strength of the solution is strong.

The 7.5% solution sonicated at 80% amplitude and 11.28 W it shows a steady decrease in the viscosity. The extent of viscosity reduction and hence degradation is the lowest for sonication at 80AMP and power of 11.28 W compared to sonication at 20, 40 and 60% AMP. Furthermore there is only reduction in viscosity and no sudden increases in viscosity for reasons mentioned before. In general, it has been found that polymer chains cleave preferentially near their centres. Higher molecular weight fractions degrade faster than ones of lower molecular weight, and a lower molecular weight limit exists below which no further degradation occurs. no depolymerisation occurred at intensities below the threshold of cavitation and in solutions that had been degassed to prevent cavitation. However, in some cases frictional forces between polymers and solvent molecules may be sufficient for chain scission, and both mechanisms may occur simultaneously. Shear stresses during stable cavitation arise from the movement of solvent molecules around resonating bubbles. Transient cavitation generates intense shock waves during bubble collapse. The flow of solvent in the vicinity of resonating bubbles places the polymer chains under stress, and the shock waves due to bubble collapse lead to polymer breakage.(Riesz and Kondo 1992). Lastly the 7.5% Nafion® solutions showed similar trend to the 2.5% and 5% Nafion® solutions subjected to ultrasound and it was shown again that after the percentage degradation reaches a certain value only can than viscosity increase due to polymerization be seen.

#### 4.2.6. 10% Nafion® Solutions Comparison between Bath and Probe

The 10% solution was made in the same way by keeping a constant volume, the different samples were sonicated with ultrasound probe and bath and the power measurement for which is given in appendix 1a. From the results in table 11 and fig 34 it can be seen that the viscosity of the 10% Nafion® solution is higher than 2.5%, 5 % and 7.5% as expected because the increase of polymer concentration increases the viscosity of the polymer solution. It can also be seen that the extent of degradation is reduced because increase of polymer concentration increases the viscosity of the polymer solution. The intensity of cavitation falls down with an increase in the viscosity of the medium. As the formation of cavitation in the liquid requires that the negative pressure in the rarefaction region of wave function must overcome the natural cohesive forces acting within the liquid. Cavitation is more difficult to produce in viscous liquids, where the cohesive forces are stronger. The initial viscosity for 10% solution without sonication is  $11.390 \times 10^{-3}$  Pa.s and reduces to  $3.308 \times 10^{-3}$  Pa.s after 2 hour of sonication and if this is compared to the 2.5% solution the viscosity reduces to  $1.538 \times 10^{-3}$  pa.s therefore it confirms the above explanation. Another thing to point out is that in the 10% Nafion® solution there is no sudden increases in viscosity, like it was seen for the 2.5% Nafion® solution, where the viscosity measured after 60 minutes of sonication showed an increase from viscosity at 30 minutes of sonication. The viscosity measured at 60 minutes ultrasound probe run is  $1.909 \times 10^{-3}$  Pa.s compared with 30 minute sonication of  $1.709 \times 10^{-3}$ . Under carefully chosen conditions, it is possible to initiate polymerization reactions using ultrasound. The reason why we do not get increases in viscosity is because at high concentrations, entanglements influence the energy transfer processes between solvent and polymer and appears to reduce the probability of degradation and therefore the extent of degradation reduces which is why there are not significant amount of new chain carriers for polymerization. Therefore the viscosity only reduces but does not increase in the 10% Nafion® solution. From the results it can be seen that ultrasound probe degrades the polymer more compared to ultrasound bath because the ultrasound bath power is considerably less.

**Table 11 Showing Comparison between Changes in Viscosity ( $\eta$ ) of 10% Nafion® Using Ultrasonic Probe vs Ultrasound Bath Over 120 minutes at 25°C**

Sonication Time	Viscosity $\eta$ (x10-3 Pa.s)	
	Power: 0.32 W	Power: 1.86 W
	Bath	Probe
0	11.390	11.39
1	4.203	11.01
2.5	4.206	10.43
5	3.814	9.87
10	3.623	7.65
30	4.333	4.57
60	4.078	4.03
120	3.374	3.308

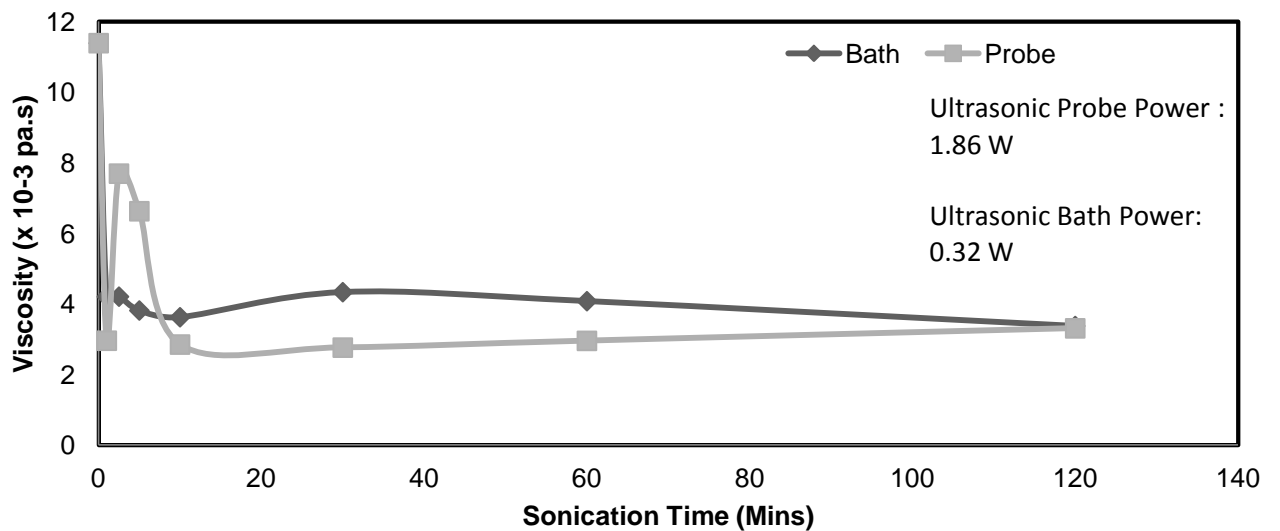


**Figure 34 Showing Comparison between Changes in Viscosity ( $\eta$ ) of 10% Nafion® Using Ultrasonic Probe vs Ultrasound Bath Over 120 minutes at 25°C**

#### 4.2.7. 10% Nafion® Solution Sonicated at Different Powers With US (Probe)

**Table 12 Showing Change in Viscosity ( $\eta$ ) of 10% Nafion® Solution Using Ultrasonic Probe at 20%, 40 %, 60% and 80 % AMP Over 120 minutes at 25°C**

	Power : 1.86 W Ultrasound probe	Power : 3.84 W Ultrasound probe	Power : 6.42 W Ultrasound probe	Power : 11.28 W Ultrasound probe
Sonication Time (Mins)	Change in Viscosity $\eta$ (x10 <sup>-3</sup> Pa.s)	Change in Viscosity $\eta$ (x10 <sup>-3</sup> Pa.s)	Change in Viscosity $\eta$ (x10 <sup>-3</sup> Pa.s)	Change in Viscosity $\eta$ (x10 <sup>-3</sup> Pa.s)
0	11.39	11.39	11.39	11.39
1	11.01	11.289	11.35	11.386
2.5	10.43	11.196	11.322	11.38
5	9.87	11.186	11.222	11.371
10	7.65	11.09	11.21	11.295
30	4.57	11.05	11.197	11.279
60	4.03	10.998	11.105	11.253
120	3.308	10.99	11.999	11.249

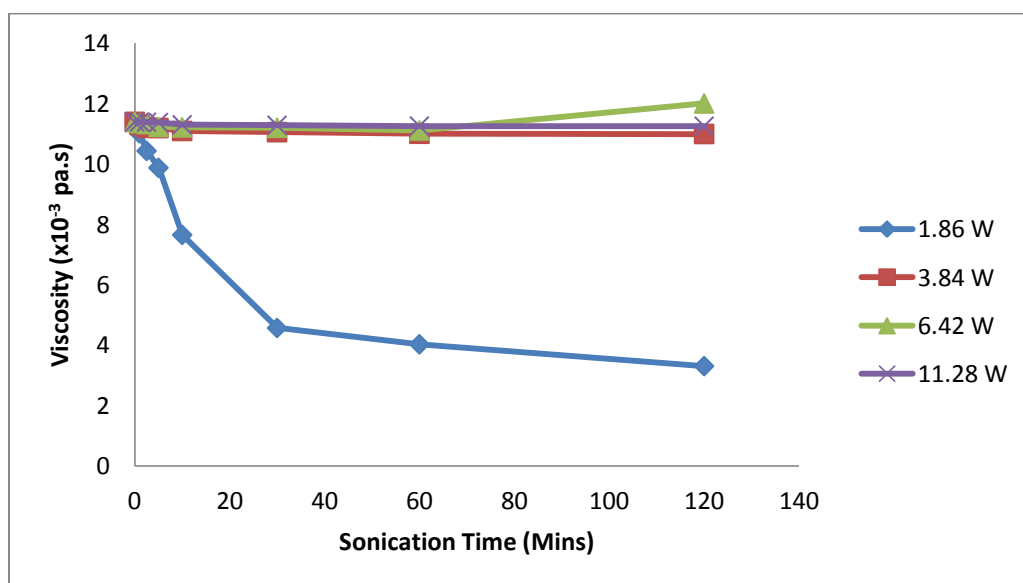


**Figure 35 Showing Change in Viscosity ( $\eta$ ) of 10% Nafion® Solution Using Ultrasonic Probe at 20%, 40 %, 60% and 80 % AMP Over 120 minutes at 25°C**

From the results in table 12 and fig 35 it can be seen that the viscosity of the 10% Nafion® solution is higher than 2.5%, 5 % and 7.5% as expected because the increase of polymer concentration increases the viscosity of the polymer solution. It can also be seen that the extent of degradation for 10% solution sonicated at 1.86W at 20% amplitude is reduced because the increase of polymer concentration. The initial viscosity for 10% solution without sonication is  $11.390 \times 10^{-3}$  Pa.s and reduces to  $3.308 \times 10^{-3}$  Pa.s after 2 hour of sonication. The reason why there is sudden increases in viscosity is because at high concentrations, entanglements influence the energy transfer processes between solvent and polymer and appears to reduce the probability of degradation and therefore the extent of degradation reduces which is why there are not significant amount of new chain carriers for polymerization. Therefore the viscosity only reduces but does not increase in the 10% Nafion® solution. The ultrasonic power of 1.86 W at 20% amplitude was the most effective in reducing the polymer viscosity because higher intensities of ultrasound are not always effective due to reasons mentioned earlier. Furthermore the 10% Nafion® solution sonicated at 1.86 W at 20% Amplitude showed that the Tg was reduced from 148°C to 141°C at 120 minute sonication time and from 148°C to 144°C at 60 minutes sonication time. This further backs the fact that there is a link between the degradation and Tg. As the 10% Nafion® solution at 20% Amplitude and 1.86W only showed degradation due to reduction in viscosity therefore the glass transition temperature was also reduced. If there were any sudden increases in viscosity during different sonication times than most likely this would also have shown an increase in Tg as seen for the 2.5% Nafion® solution. The DSC graphs later on in the thesis shows this decrease in Tg and are given in figure 50 and figure 51.

The viscosity of the other 10% Nafion® solutions sonicated at powers of 3.84 W, 6.42W and 11.42W at amplitudes of 40, 60 and 80% showed the general trend of steady viscosity reduction due to degradation and there were no sudden jumps in viscosity.

The extent of viscosity reduction for these 10% solutions was not as high as the 10% Nafion® solution sonicated at 20% amplitude at power of 1.86 W due to ultrasound field being ineffective due to increased bubble formation. The Tg of the 10% Nafion® solutions at all the different ultrasound powers and time ranges did not show any change in the Tg. Because from the viscosity experiments using Rheometer the trend was only a decrease in viscosity attributed to degradation and because there was no increase in viscosity it can be

concluded that there were no copolymers formed in the 10% solution at other ultrasonic powers used in the experiments.

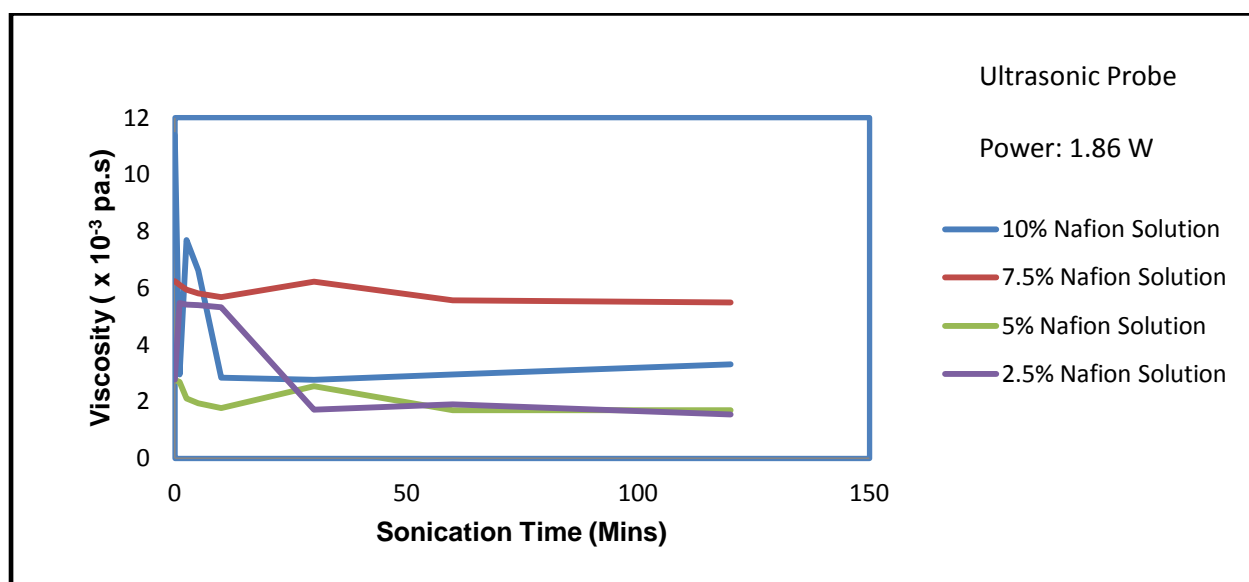


Figure 36 Graph showing comparison between change in viscosity ( $\eta$ ) for different concentration Nafion® solutions sonicated with 20%AMP ultrasound probe over 120 minutes at 25°C

#### 4.2.8. Viscosity Variations between Overnight and Fresh samples

The 5% ultrasound bath samples were analysed to see repolymerisation of the Nafion® polymer. The fresh sonicated samples were compared to the ones left overnight to see repolymerization by measuring the change in viscosity of the different samples. From the results in table 13 and fig 37 it can be seen that after 2 hours of sonication the viscosity measured was  $1.845 \times 10^{-3}$  Pa.s for the fresh sample and the viscosity of 2 hour sonicated sample which was left overnight is  $1.820 \times 10^{-3}$  Pa.s and therefore we can conclude that the Nafion® polymer if left overnight does not repolymerise. This is because the difference in viscosity is not significant. The same trend is seen for different time intervals of fresh and overnight samples where the difference in viscosity is not very significant and the explanation for this can be that prolonged exposure of solutions of macromolecules to high-energy ultrasonic waves produces a permanent reduction in viscosity. Even when the

irradiated polymers are isolated and redissolved their viscosity remains low in comparison with that of non-irradiated solutions. This effect is seen in these results because the polymer viscosity remains low in comparison to the fresh sonicated samples and the original Nafion® viscosity. Another thing to point out is that during the ultrasound exposure the polymer degrades initially however at specific intensity and time frame of exposure the rise in viscosity is seen due to repolymerisation, but this can only occur during sonication where ultrasound causes the breakage of macromolecules that results in the formation of copolymers which can be seen as a rise in viscosity. However in the absence of ultrasound this cannot be achieved. This is backed by work done by Chen et al.(Chen 2005)

**5% US bath 0.32 W**

**Table 13 Showing variations in Viscosity ( $\eta$ ) of 5% Nafion® Using Ultrasonic Bath Over 120 minutes vs Overnight Sample at 25°C**

Time (min)	Viscosity $\eta$ ( $\times 10^{-3}$ Pa.s)	Overnight
0	2.267	
1	2.170	1.878
2.5	1.943	
5	1.808	1.943
10	1.967	
30	1.949	1.809
60	1.847	
120	1.845	1.820

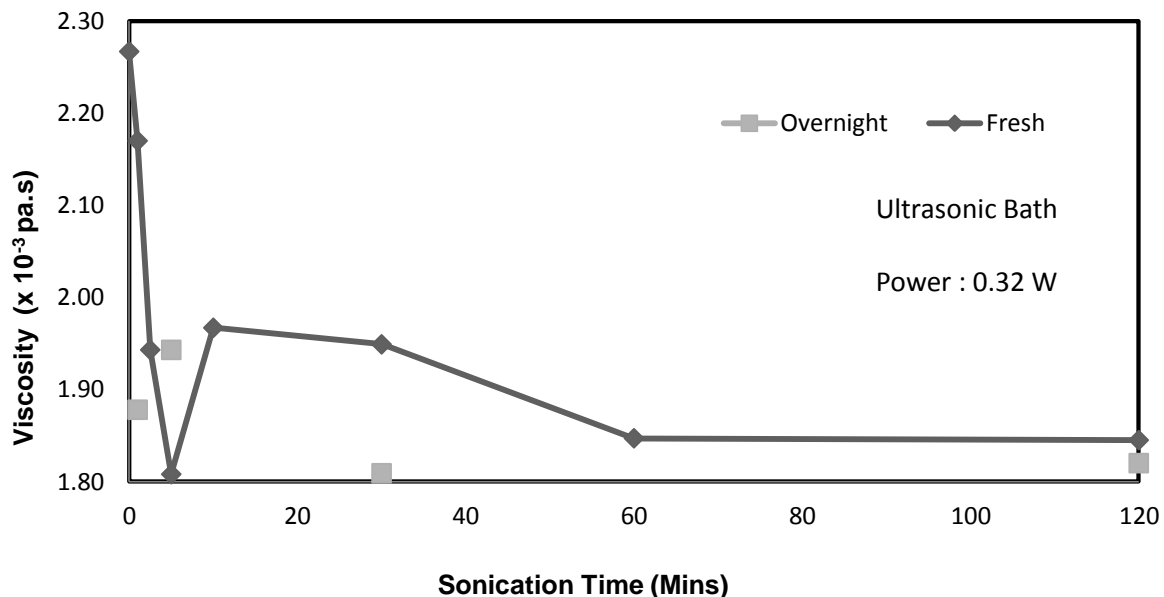


Figure 37 Showing Difference in Viscosity ( $\eta$ ) of 5% Nafion® Using Ultrasonic Bath Over 120 minutes vs Overnight Sample at 25°C

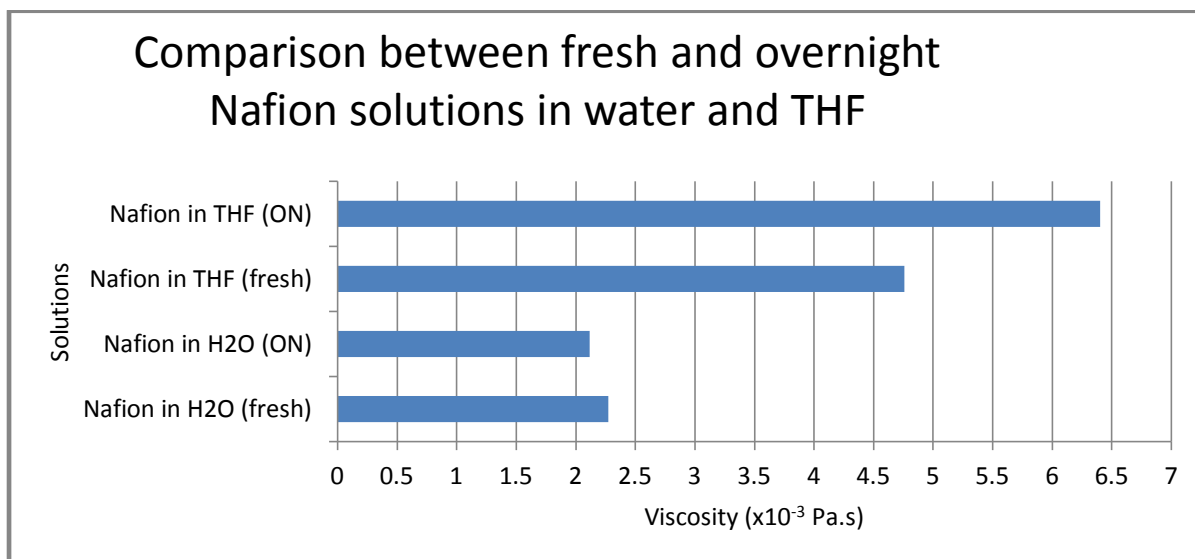


Figure 38 Bar Chart showing comparison between fresh and overnight Nafion® Solution in water and THF



#### 4.2.9. DSC ANALYSIS

The physical properties of polymer materials depend highly on their glass transition temperature ( $T_g$ ). When the temperature is lower than  $T_g$ , the polymer is in its glassy state and when the temperature is higher than  $T_g$ , it is in its rubber or viscous liquid state. A sudden change of the physical properties takes place in the glass transition region. (Balakrishnan and Guria 2007),  $T_g$  of polymers is determined by measuring the heat capacity (differential scanning calorimetric analysis) or the thermal expansion (thermomechanical analysis). More techniques have also been proposed, such as thermodielectric or thermogravimetric analysis. The glass transition phenomena happens in a fairly large temperature range and the different characterization methods do not all give the same values of  $T_g$ . Some allow determination of the beginning of the transition; others detect the middle or the final temperature. (Balakrishnan 2007). (Weir 2004)

An understanding of the degree of crystallinity for a polymer is vital because crystallinity affects physical properties such as storage modulus, permeability, density and melting temperature. Whereas most of these manifestations of crystallinity can be determined, a direct measure of degree of crystallinity provides a fundamental property from which these other physical properties can be predicted. (Price 1994). (Weir 2004)

In the experiments several different sample of Nafion® were analysed by differential scanning calorimetry in order to investigate the effect of ultrasonic irradiation on the physical properties of the polymer in question. The results in fig 39 to fig 49 shows that upon sonicating the Nafion® polymer there is a shift in the glass transition temperature by  $8^\circ\text{C}$  for some of the polymer samples. While for some samples there is no change in the  $T_g$ . The different samples were prepared in the same way and the only difference between the different samples were ultrasonic irradiation time and power. This study therefore confirms that ultrasound can shift the glass transition temperature of polymers and this is backed by similar work on other polymers in the literature. For example the glass transition temperature of the Nafion® polymer in the literature is around  $148^\circ\text{C}$  and from the results the sample analysed without sonication agrees with this result. The highest change in the glass transition occurs for the 5% Nafion® sample sonicated for 30 minutes US probe 20% amplitude where the glass transition temperature changed from the literature value of  $148^\circ\text{C}$  to  $156^\circ\text{C}$  figure 41, and the explanation for this could possibly be that mechanochemical methods such as

ultrasound can modify homopolymers by production of blocks and grafts by using mechanochemical decomposition.

Ultrasound can significantly improve the toughness of polymer blends, and this effect is due to structural changes of the Nafion® chains. Ultrasound makes the molecular chains of Nafion® disentangled and orientated; Ultrasound increases the degree of order in the melt, and thus increases the crystallinity of the two phases when the blend cools down. This increase in the T<sub>g</sub> is seen for some other sonicated samples where the ultrasound irradiation causes a shift in T<sub>g</sub> in exactly the same manner. These results mean that ultrasound improves the durability of Nafion® upto certain extent. Because unsonicated Nafion® has a glass transition temperature of 148°C which means at this temperature it phase changes and the increase from 148 to 155 means that the phase change occurs at 155 rather than 148°C .The fact that high temperatures are desirable for a better efficiency and CO tolerance ultrasound can thus prove to be advantageous in fuel cells. In general the higher the T<sub>g</sub> of a material the longer its thermal stability.(Chen 2005) , (Berlin 1962).

From the results explained above where ultrasound treatment of Nafon has increased the glass transition temperature for some samples at specific irradiation power and time, however the opposite is seen for some other different sample where ultrasonic power and time change results in decrease in the glass transition temperature. For example the most significant decrease in the glass transition temperature is seen for 10% Nafion® solution at 60% amplitude where the T<sub>g</sub> is changed from 148 of the original Nafion® T<sub>g</sub> to 143°C after sonication and this can be attributed to the damage by generation of heat, at 60% amplitude there may be separate particles but generation of heat may cause scission of chains thereby reducing T<sub>g</sub>. This coincides well with literature where at 70% amplitude there was a decrease in T<sub>g</sub> observed. From these results we can confirm that under certain conditions of irradiation and time T<sub>g</sub> will increase and by changing the irradiation power the T<sub>g</sub> will decrease for reasons mentioned above. However as we know increase in T<sub>g</sub> results in better thermal stability, therefore the irradiation power and time of interest to us is where the glass transition temperature increases.(Goyat 2011).From fig 46 to fig 49 we can see that there is no shift in the glass transition temperature from the literature value of 148°C. Fig 50 and fig 51 shows the decrease in glass transition temperature from 148°C to 141°C for 10% Nafion® sonicated at 1.86W at 20% Amplitude at 120 minutes, and from 148°C literature value to 144°C at 1.86W at 20% Amplitude sonicated for 60 minutes Us probe.

Differential Scanning Calorimetry (fig 39 to fig 45 shows increase in Tg)

Note the Tg peak has been inverted due to software issue with the machine which is why the peak dips upwards rather than downwards.

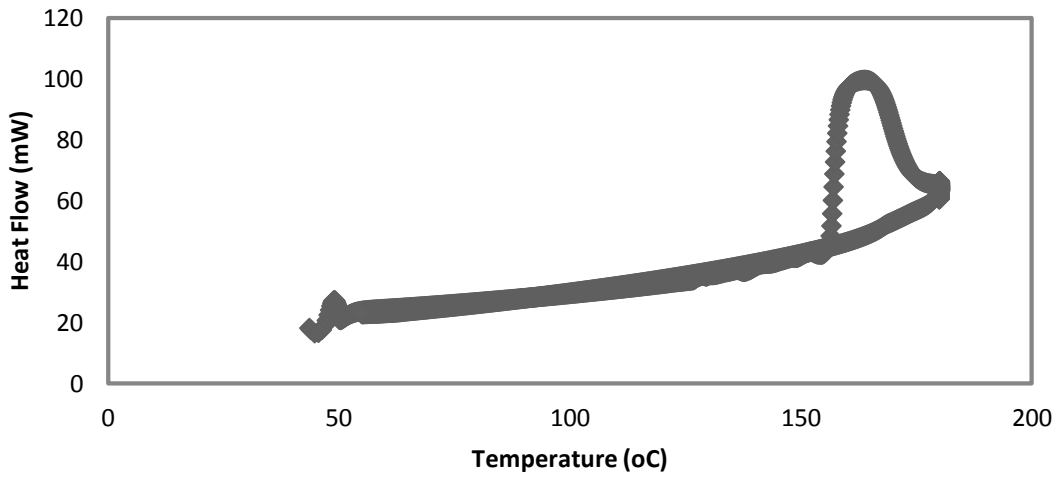


Figure 39 Graph Showing Increase in Tg for 5wt% Nafion® Sonicated for 30min with US Probe 20AMP% Fast Scan sample

- Nafion® 5% wt 30min US Probe 20% Fast Scan

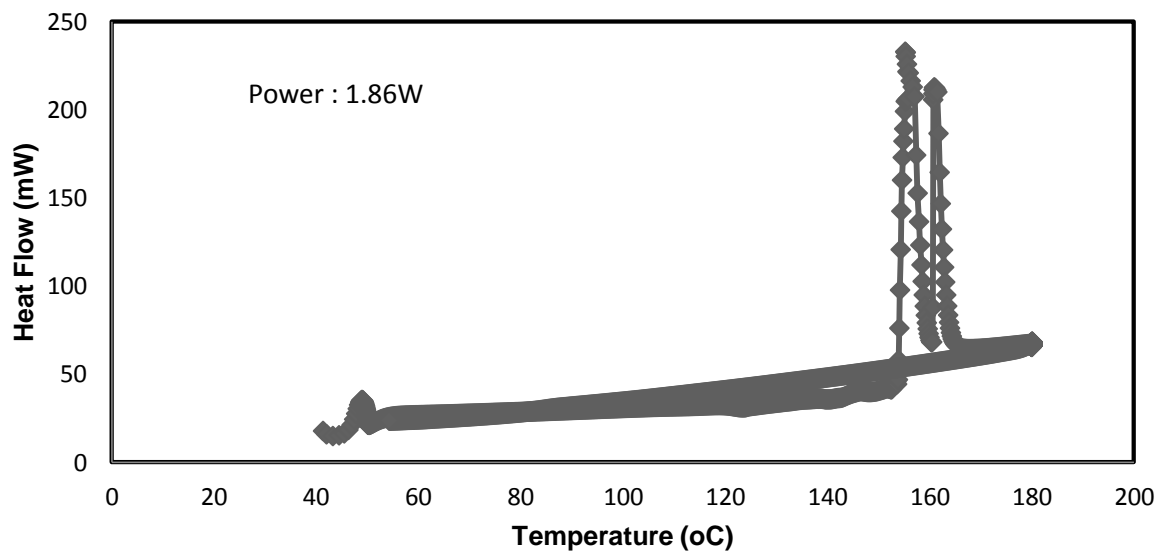


Figure 40 Graph Showing Increase in Tg for 5wt% Nafion® Sonicated for 30min with US Probe 20AMP% Fast Scan

- Nafion® 5%wt 30min US Probe 20% Fast Scan 2<sup>nd</sup> sample

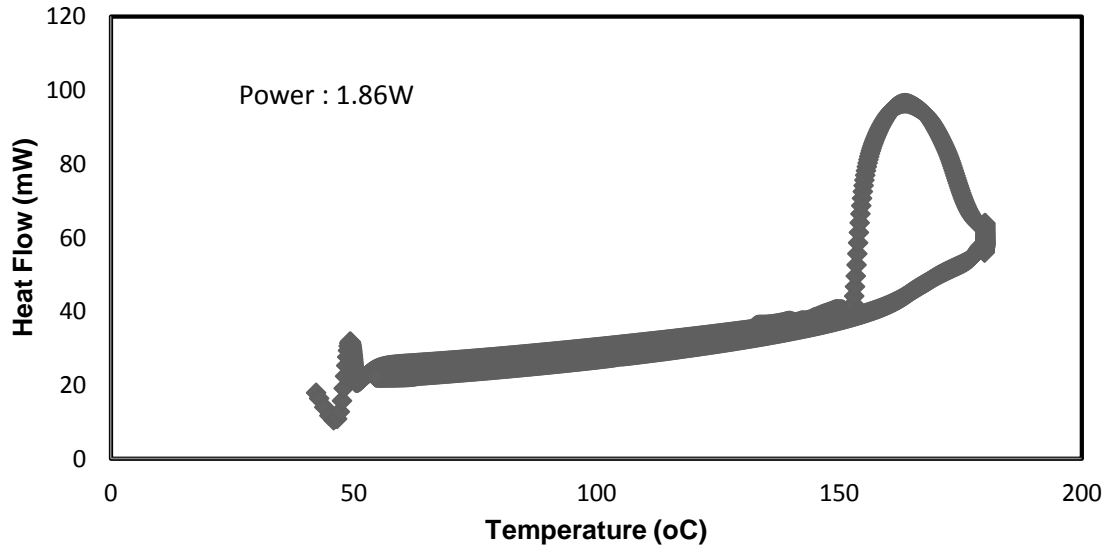


Figure 41 Graph Showing Increase in Tg of Nafion® 5% wt Sonicated for 30min with US Probe 20% Fast Scan 2<sup>nd</sup> sample

- Nafion® 5% wt 30min US Probe 20% Fast Scan 3<sup>rd</sup> sample

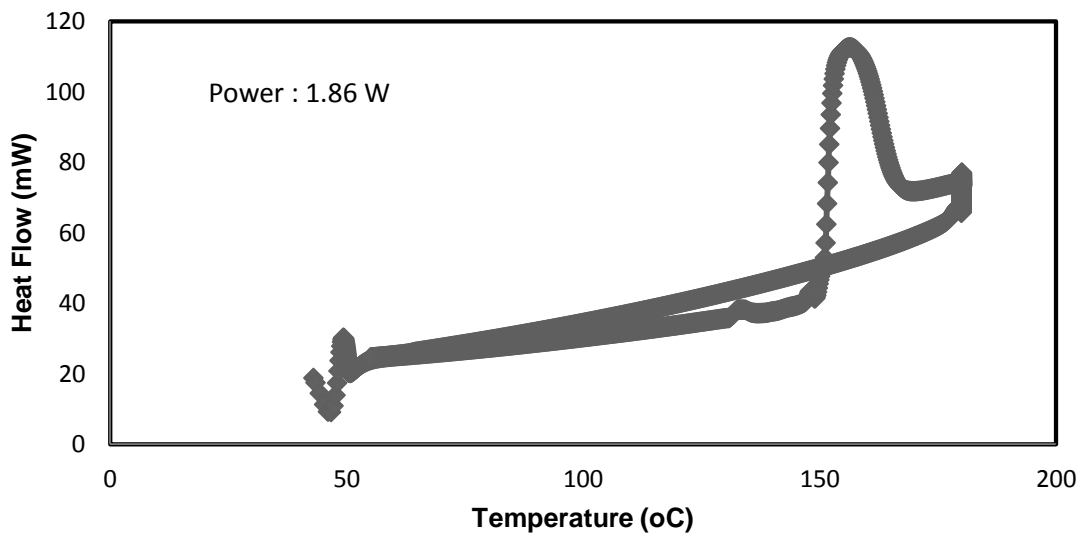
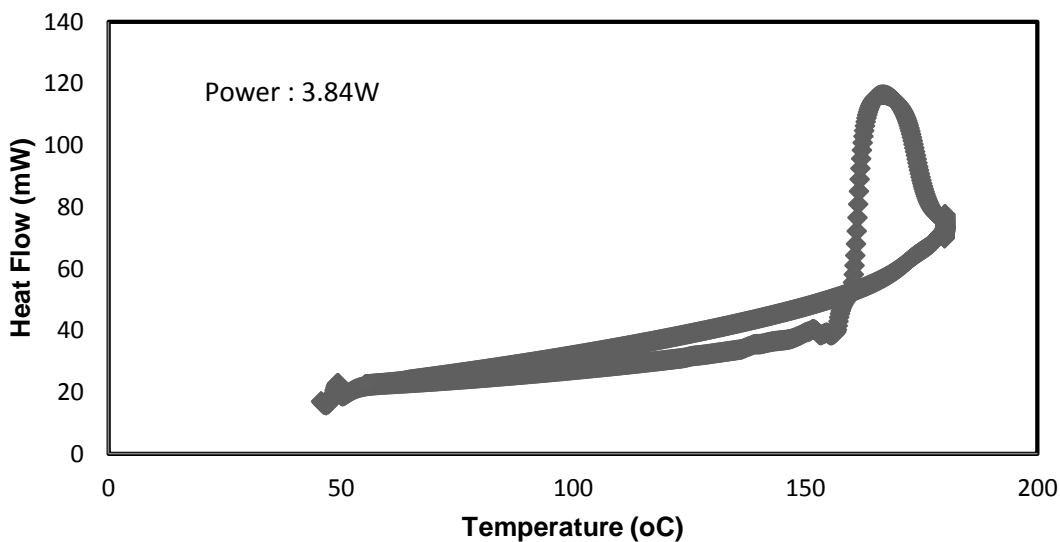


Figure 42 Graph Showing Increase in Tg for Nafion® 5% wt Sonicated for 30min with US Probe 20%AMP Fast Scan 3<sup>rd</sup> sample

- **Nafion® 5% wt 60min US Probe 40% Fast Scan sample 1**



**Figure 43 Graph Showing Increase in Tg for Nafion® 5% wt sonicated for 60min using US Probe 40 AMP% Fast Scan sample 1**

- **Nafion® 5% wt 60min US Probe 40% Slow Scan sample 2**

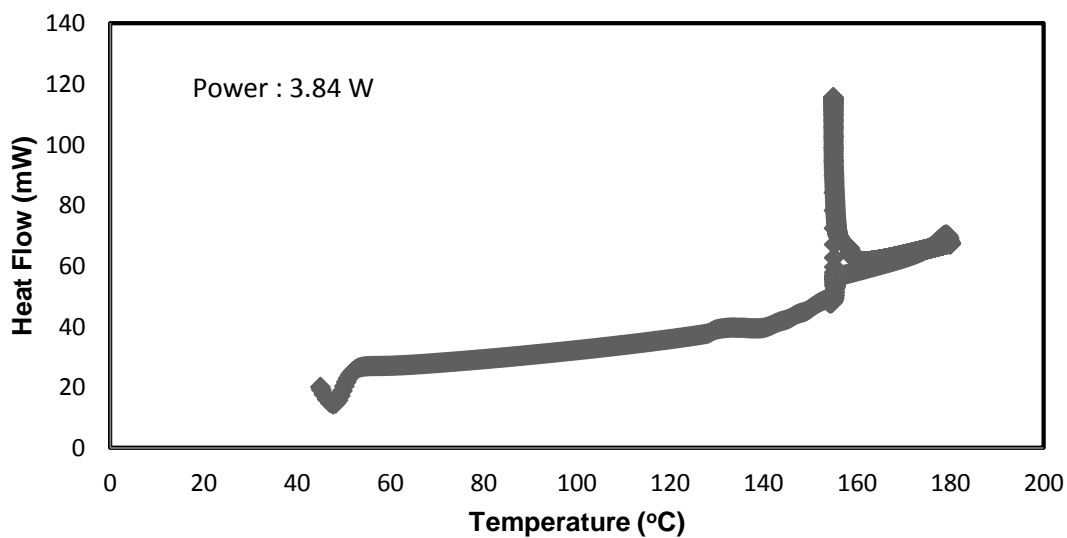


**Figure 44 Graph showing Increase in Tg for Nafion® 5% wt Sonicated for 60min using US Probe 40%AMP Slow Scan sample 2**

- **Nafion® 5% wt 60min US Probe 40% Slow Scan sample 3**

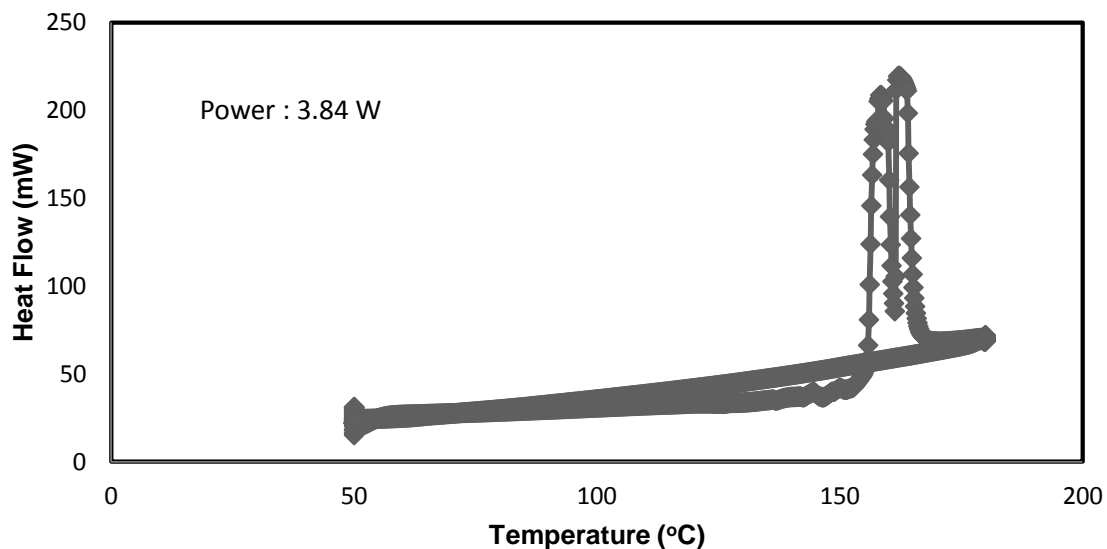


**Figure 45 Graph Showing Increase in Tg for Nafion® 5% wt Sonicated for 60min using US Probe 40%AMP Slow Scan sample 3**

**Nafion® 10% in THF 20 Min Us Probe 40% (Fig 46 to Fig 49 no change in Tg)**

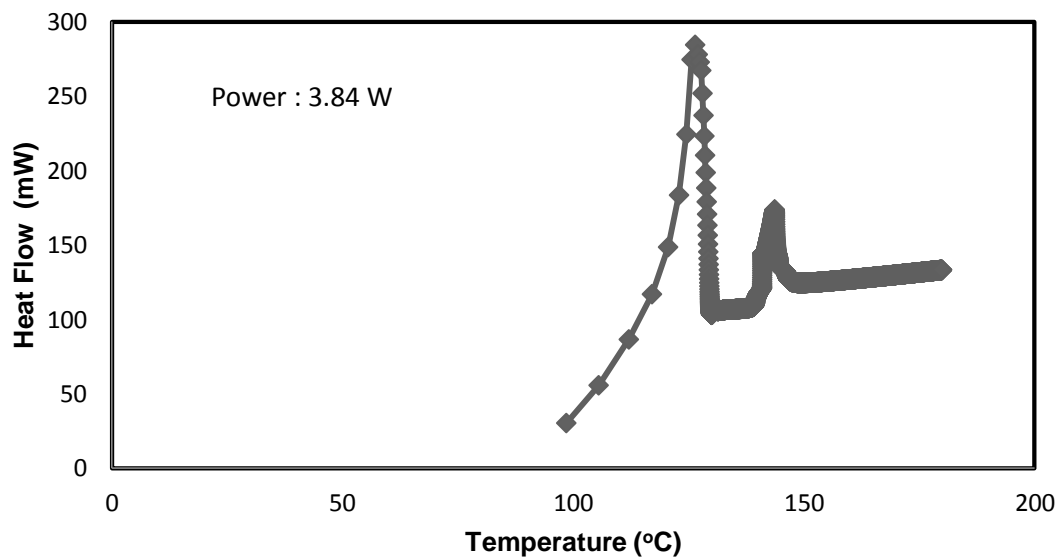


**Figure 46 Graph Showing no change in Tg for Nafion® 10% in THF Sonicated for 20 Min with Us Probe 40%AMP**

- Nafion® 10% in THF 20 Min Us Probe 40% 20hr Dry

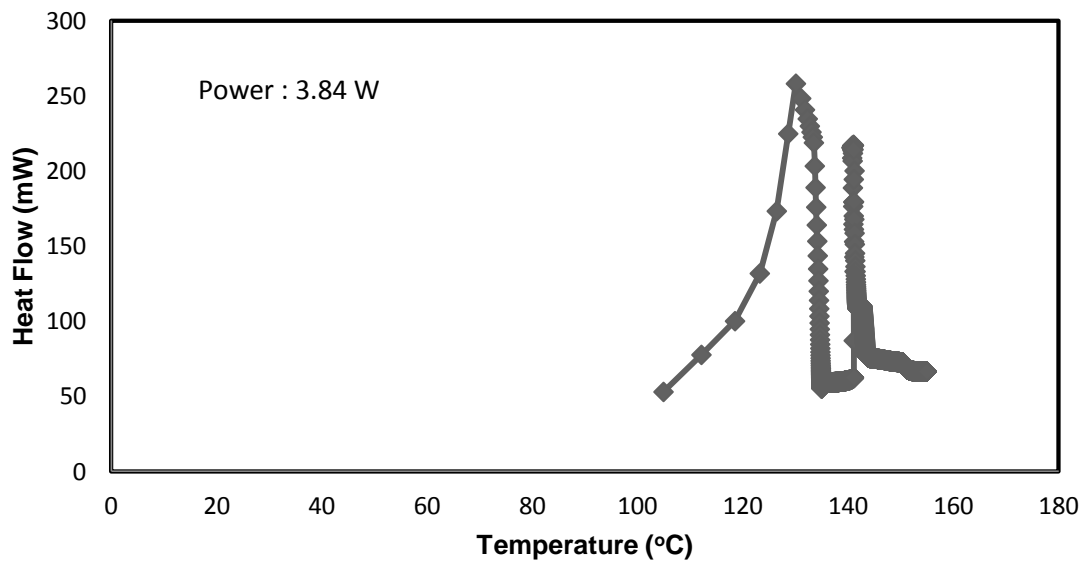


Figure 47 Graph showing no change in Tg for Nafion® 10% in THF Sonicated for 20 Min with Us Probe 40%AMP 20hr Dry

- Nafion® 10% in THF 10 Min US Bath 18hr Dry

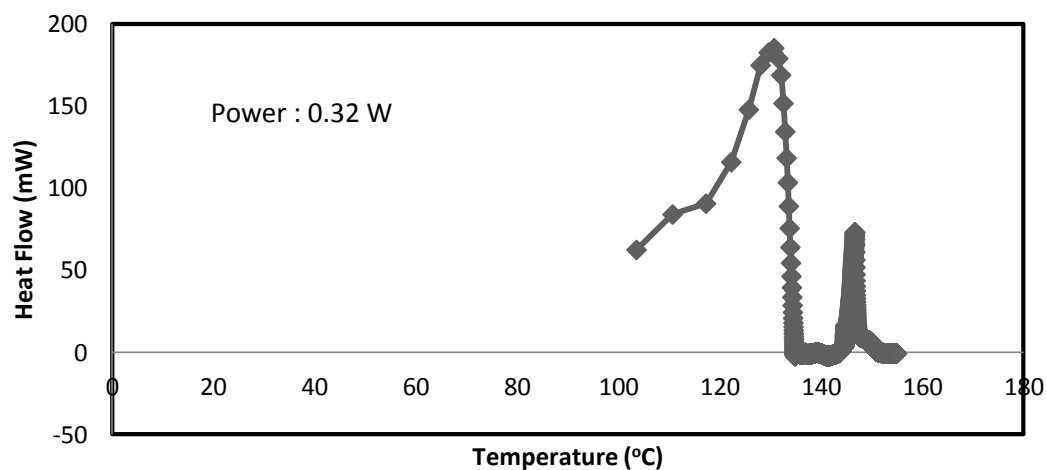


Figure 48 Graph Showing No change in Tg for Nafion® 10% in THF Sonicated for 10 Min Using US Bath 18hr Dry

- **Nafion® 10% in THF 10 Min Us Probe 40%**

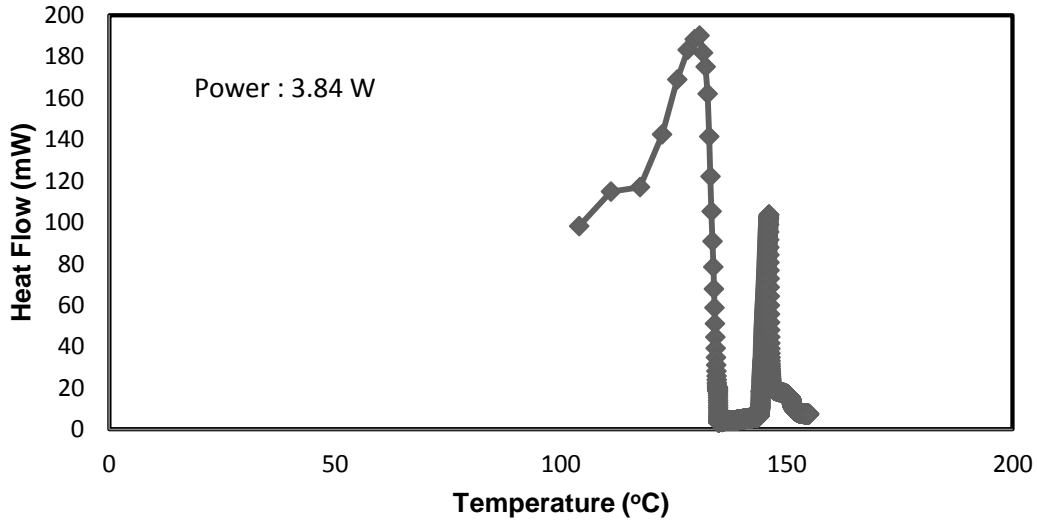


Figure 49 Graph Showing No change in Tg for Nafion® 10% in THF Sonicated for 10 Min Using Us Probe 40%AMP

**Nafion® 10% in THF 60 And 120 Min Us Probe 20% (Fig 50 to Fig 51 Decrease in Tg)**

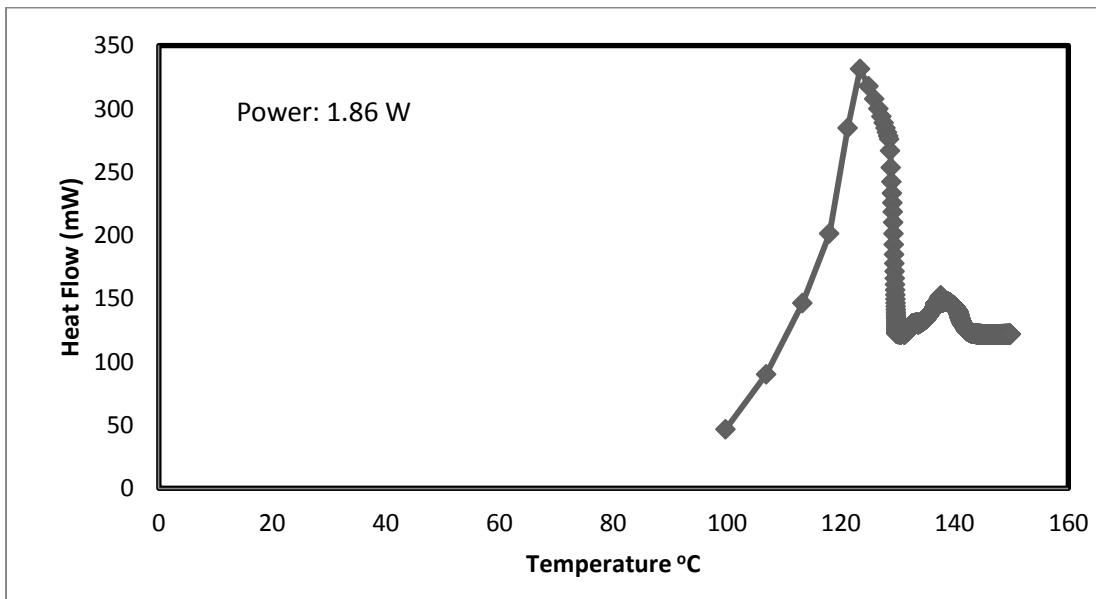
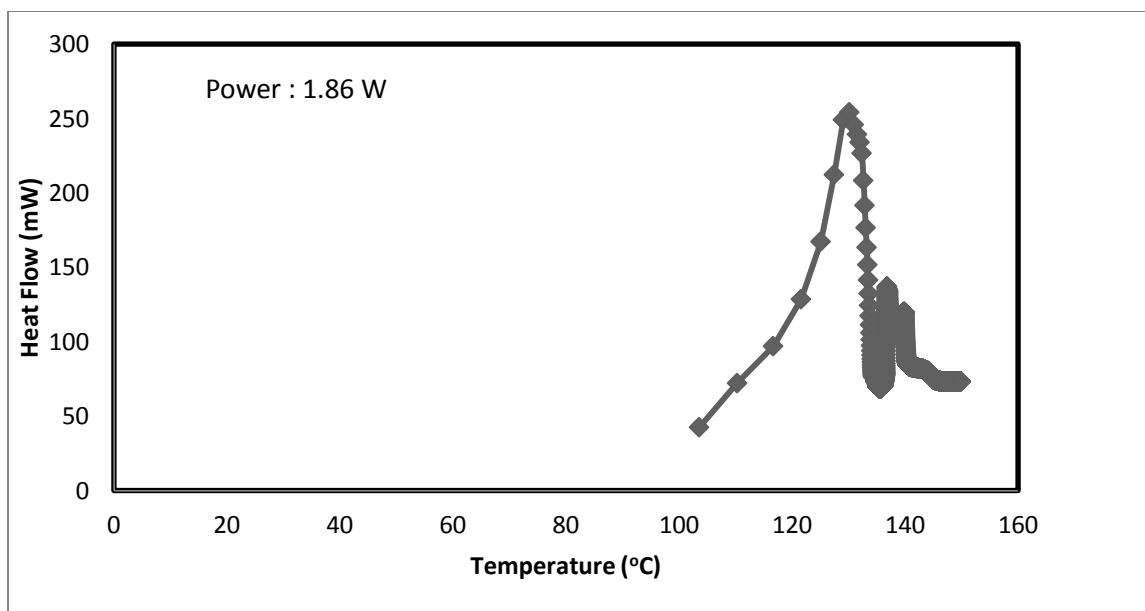


Figure 50 Graph Showing Decrease in Tg for 10% Nafion® in THF Sonicated for 120 Min Using Us Probe 20% AMP





**Figure 51 Graph Showing Decrease in Tg for 10% Nafion® in THF Sonicated for 60 Min Using Us Probe 20% AMP**

#### 4.2.10. Summary of the 4 different Nafion® concentrations at 4 different powers

Extensive range of experiments were performed on different Nafion® concentrations at various ultrasonic powers and time ranges in order to see Nafion® functionality in PEMFC's using ultrasound, and to see if ultrasound could have a beneficial effect in fuel cell operations.

From the discussion above it was seen that in all the 4 different Nafion® concentration sonicated the general trend was initial decreases in viscosity due to degradation of the polymer. However at certain ultrasound frequency the viscosity showed an increase due to the reasons explained above. Thermal and rheological studies show that the morphology of the Nafion® polymer is strongly dependent on the sonication time and frequency. As we have found in this study that at certain time and frequency of ultrasound irradiation the viscosity and glass transition temperature were shown to increase, the possible explanation for this is that Upon irradiation of ultrasound, molecules are exposed to alternate compression and expansion modes, by which bubbles are formed and eventually collapsed. On the molecular level, this implies a rapid strike to the molecules impeded by surrounding molecules cannot adjust. Thus, friction is generated which causes strain and eventually bond

rupture in the macromolecules. Therefore, it is supposed that in situ copolymers are formed from Nafion® macroradicals that occur with ultrasonic irradiation in this study. The copolymers act as a compatibilizer to improve and stabilize the morphological structure. This study enabled us to see what conditions are required to get desirable use out of ultrasound for future fabrication of Nafion®. It is noted that there is a trend between viscosity increase due to sonication at certain frequency and time and stabilisation of the polymer. In other words sonication at certain frequency and time period shows better stability of the polymer as shown by increase in Tg.

**Table 14 Table showing increase and decrease in Tg for different Nafion® samples at different experimental condition**

Nafion® Solution (conc %)	Ultrasound Power (W)	Irradiation Time (Mins)	Original Tg (°C)	Tg(°C) after sonication
5	1.86	30	148	156
5	1.86	60	148	155
10	3.84	20	148	148
10	0.32	10	148	148
10	3.84	10	148	148
10	1.86	120	148	141
10	1.86	60	148	144

From table 14 above it can be seen that the most desirable frequency and irradiation time of ultrasound is 1.86 W at 30 minutes for the 5% Nafion® solution followed by 60 minutes irradiation time. Each of the result given above was repeated 3 times in order to ensure the results were reliable. From this we can establish for the fabrication of Nafion® polymer for fuel cell use would require Nafion® to be sonicated for 30 or 60 minutes at irradiation power of 1.86 W. The increase in Tg can be explained due to the fact that When ultrasound is applied, its powerful vibration, shatter and cavitations disperse Nafion® matrix and help the molecules near the interface penetrate and entangle with each other. This ultrasonic-induced structure is beneficial to stress transfer and energy dissipation in the whole system, which may lead to improved mechanical properties. The use of ultrasound vibration showed the crystallinity of Nafion® phase was larger than that of the non sonicated sample. Ultrasound makes the molecular chains of Nafion® disentangled and orientated; it increases the degree

of order in the melt, and so increases the crystallinity of the different phases when the blend cools down. Ultrasonic vibration, is a mechanochemical method, it has found a widespread use in polymer processing. Ultrasound is evident for effects on accelerating chemical reaction, increasing productivity, and improving properties of polymer materials.

Studies have already showed that extrusion of rubber using ultrasound has showed better stability, productivity and good surface quality.(Chen 2005)

Additionally at higher ultrasound Power and amplitude the opposite effect was seen where the Tg showed a decrease in the literature value of 148°C to 141°C. The intensity of sonication is proportional to the amplitude of vibration of the ultrasonic source and, as such, an increment in the amplitude of vibration will lead to an increase in the intensity of vibration and to an increase in the sonochemical effects. To achieve the cavitation threshold a minimum intensity is required. This means that higher amplitudes are not always necessary to obtain the desired results. In addition, high amplitudes of sonication can lead to rapid deterioration of the ultrasonic transducer, resulting in liquid agitation instead of cavitation and in poor transmission of the ultrasound through the liquid media. Equilibrium should be attained between the intended effects and sonication amplitude since, as explained above, high amplitudes lead to high sonication intensities and high sonication intensities can promote some undesired effects such as degradation of polymer. (Hugo Miguel Santos 2009)

#### **4.2.11. Advantage of Increase in Tg of Nafion®**

As mentioned earlier common fuel cells contain Nafion® membrane which degrades at higher temperatures this means that the PEM fuel cells can only be operated at certain temperatures. Although higher temperatures are desirable for fuel cell operation because it reduces CO poisoning of the catalyst, therefore the use of ultrasound for the fabrication of membranes that show better thermal stability would be extremely important. As our results show increase of the Tg for certain samples following ultrasound irradiation therefore suggests that ultrasound can be of extreme importance in fabrication of Nafion® membranes. An increase in Tg means better thermal stability because the Nafion® phase change occurs at a higher temperature than the usual of 148°C.

#### 4.2.12. GC/MS Analysis of Sonicated Samples

The sonicated samples were analysed with GC/MS in order to understand the ultrasound induced degradation of Nafion® polymer. Gas Chromatography (GC) is used to separate volatile components of a mixture. A small amount of the sample to be analyzed is drawn up into a syringe. The syringe needle is placed into a hot injector port of the gas chromatograph, and the sample is injected. The injector is set to a temperature higher than the components' boiling points. This is so that components of the mixture evaporate into the gas phase inside the injector. A carrier gas, such as helium, flows through the injector and pushes the gaseous components of the sample onto the GC column. The separation of the components takes place within the column. Molecules partition between the carrier gas (the mobile phase) and the high boiling liquid (the stationary phase) within the GC column. (Hao 2007, Watanabe 2009). The Nafion® samples were prepared in the same manner and then sonicated for various time periods, including a control sample which was not sonicated to be used as reference. (Anna Carlsson 2011). The analysed samples with the GC/MS spectrums are given in appendix 1b:-

From the GC spectrums for all the 4 samples there is only one peak evident at retention time of 21.01 which corresponds to a compound known as Butylated Hydroxytoluene. This conclusion was reached by searching for the most likely compound at the specified retention time from 'The Compound Library'. This is further backed by the spectrum of MS which corresponds to the same compound. (Shertzer 1991)

The Butylated Hydroxytoluene is used as an antioxidant in the membrane and is therefore evident in all the spectrums. However from the results there are no other conclusive peaks present that show the degradation segments following ultrasound irradiation and therefore we were unable to recognize any degradation products following ultrasound treatment, there could be a number of reasons for the inconclusive information from GC/MS.

The solvent amount used might have been used in excess which results in the sample being too diluted and therefore no sample peaks can be seen. The syringe used for injecting the sample into the GC probably had air bubbles in the syringe which results in the peaks to be really small on the chart recorder. Another reason for no peaks could be that the polymer fragments might have been too big for GC/MS to detect. Because the sample to be tested needs to dissolve well in the solvent for the GC/MS analysis to show any peaks, but if it does

not dissolve than it can not show any peaks. Due to the reasons discussed and inconclusive results from the GC/MS about the degradation mechanism of Nafion® following ultrasonic irradiation, it was decided to use Solid State NMR spectroscopy for identifying the sonochemical degradation mechanism. Thermal, mechanical and chemical degradation modes have been successfully identified with Solid State NMR spectroscopy. Therefore it is considered as the best way of finding sonochemical degradation, however because the Solid State NMR facility was not available at the University of Birmingham and the duration of the course was only a year it was not possible to carry out this analysis.

## 5. CHAPTER 5 KINETICS

### 5.1. Kinetics of Degradation

In the experiments, the effect of different solution concentration at various times on the rate of degradation was investigated. Kinetics of degradation was studied by viscometry method. The calculated rate constants indicate that degradation rate of Nafion® solutions decreases with increasing of solution concentration. With increasing solution concentration, viscosity increases and it causes a reduction in the cavitation efficiency thus, the rate of degradation decreases. It was also noted that there is a steady decrease in viscosity with increase in time of sonication but at certain time and sonicating power the viscosity increased for reasons explained above.(Taghizadeh 2003)

There is no evidence that there is any interaction between the sound waves and the polymer chains. The degradation arises as a result of the effect of the ultrasound on the solvent. The passage of the longitudinal sound wave through a liquid can be described in terms of the acoustic pressure in the liquid,  $P_A$ , represented by:(Taghizadeh 2003)

$$P_A = P_M \sin(2\pi\nu t) \quad (39)$$

Where  $P_M$  and  $\nu$  are amplitude and frequency of the sound wave, respectively. When  $P_M$  is sufficient to overcome the intermolecular forces in the solution, alternate rarefaction and compression phases by sound wave that pass through a liquid cause cavitation. Formation, growth and rapid collapse of microscopic bubbles generate high temperatures and pressures during bubble collapse. Considering the collapse as an adiabatic process leads to the following for maximum temperature,  $T_{max}$ , and pressure,  $P_{max}$ , generated during cavitation:

$$T_{max} = \frac{TP_M(\gamma-1)}{P} \quad (40)$$

$$P_{max} = P \left( \frac{P_M(\gamma-1)}{P} \right) \gamma(\gamma - 1) \quad (41)$$

Where  $T$  is the ambient temperature,  $P$  the pressure in the bubble before collapse and  $c$  the polytropic ratio (the ratio of the specific heat capacities at constant pressure and volume) of the solvent vapour. These equations predict the values in the region of several thousand Kelvin and several hundred atmospheres, depending on the system. These extreme conditions are primarily responsible for sonochemical reaction. In a dilute solution, the role of the generated heat is probably of minor importance for polymer degradation. Accordingly since the hot regions are highly localized and should be quenched in less than  $1\mu\text{s}$ , the polymer molecules do not have time to diffuse and to reach these spots in such a short interval. Above a threshold sound intensity, bubbles are created and increased in size until a critical diameter of order  $250\ \mu\text{m}$  reached. The bubble becomes unstable above that size and collapses violently in a time-scale of  $20\ \mu\text{s}$ . Several mathematical treatments have been derived to describe bubble wall motion during the implosive collapse. An approximate equation describing the wall velocity,  $V_R$ , is given by:(Taghizadeh 2003)

$$V_R = \left( \frac{2P_h}{3\rho} \left( \frac{R^3 m}{R^3} - 1 \right) \right)^{0.5} \quad (42)$$

Where  $\rho$  is the solvent density,  $P_h$  is the external pressure,  $Rm$  is the maximum radius of the bubble and  $R$  is the instantaneous radius of the imploding cavity. However,  $R$  reaches a minimum radius of the order  $0.5\ \mu\text{m}$  during the final collapse. The motion of the wall of imploding bubble causes the movement of the solvent molecules around the bubbles. These movements set up large shear fields that are primarily responsible for the degradation of polymer.(Taghizadeh 2003)

## 5.2. Calculation of Rate Constants for Different Ultrasound Powers

Kinetics of polymer degradation under stress could be expressed as Eq.(43) according to Li et al, which is used in this work to describe the kinetics of ultrasonic degradation:(Li 2005)

$$\left( \frac{d(M_t - M_\infty)}{M_\infty dt} \right) = k \frac{(M_t - M_\infty)}{M_\infty} \quad (43)$$

where  $M_\infty$  and  $M_t$  are the limiting molecular weight and average molecular weight at irradiation time  $t$ , respectively, and  $k$  is the rate constant of degradation reaction.

By integrating and considering that at  $t = 0$ ,  $M_t = M_0$  (where  $M_0$  is the initial molecular weight), Eq. (44) could be expressed as:

$$M_t = (M_0 - M_\infty)e^{-kt} + M_\infty \quad (44)$$

On designating the constant  $M_0 - M_\infty = A$

$$M_t = M_\infty + Ae^{-kt} \quad (45)$$

From Eq. (45), the limiting molecular weight and the rate constant of degradation reaction could be gained. The degradation rate at ultrasonic time  $t$  ( $v_t$ ) could be expressed as the differential of Eq. (45):

$$v_t = - \frac{dM_t}{dt} = kAe^{-kt} \quad (46)$$

If the polymer degradation process is monitored in terms of the intrinsic viscosity of the polymer solution, similar equation in terms of intrinsic viscosity can be written as:

$$n_t = (n_0 - n_\infty)e^{-kt} + n_\infty \quad (47)$$

Where  $n_0$ ,  $n_t$ , and  $n_\infty$  delegate the intrinsic viscosity at ultrasonic time 0,  $t$ , and limiting intrinsic viscosity, respectively.

According to Eq. (47), the magnitude of the rate constant has been calculated for all the runs knowing the initial viscosity and the limiting intrinsic viscosity of the polymer solution by plotting a graph of  $\ln(A)$  against time where  $A = (n_0 - n_\infty) / (n_t - n_\infty)$ . (Mohod 2011)



### 5.3. Viscosity and Molecular Weight Relationship

The intrinsic viscosity number  $\eta$  of a solution is defined as:

$$[\eta] = \lim_{c \rightarrow 0} \frac{\eta - \eta_0}{\eta_0^c} \quad (48)$$

In terms of the solvent viscosity  $\eta_0$ , the solution viscosity  $\eta$  and the solute concentration  $c$ . The quantity  $[\eta]$  of a polymer solution is a measure of the capacity of a polymer molecule to enhance the viscosity, which depends on the size and the shape of the polymer molecule. Within a given series of polymer homologs,  $[\eta]$  increases with the molecular weight  $M$ ; hence it is a measure of  $M$ .(J.Brandrup 1999)

The limiting viscosity number  $[\eta]$  and molecular weight relationships for polymers in various solvents and at various temperatures are available in the literature. For example the data from literature contains the constants of the equation:(J.Brandrup 1999)

$$[\eta] = KM^a \quad (49)$$

This equation is known as the Mark-Houwink-Sakurada equation. It is now a well known fact that for linear, flexible polymers, under special conditions of temperature or solvent termed as the Flory 'theta' temperature or solvent, the above equation becomes: (J.Brandrup 1999)

$$[\eta]_{\theta} = K_{\theta}M^{0.50} \quad (50)$$

From the data in the literature where the  $\theta$  is used in the parenthesis suggests that the viscosity constants were obtained under the theta conditions. Therefore equation 50 is approximately valid over the whole molecular weight range,  $K_{\theta}$  and  $a = 0.50$  can be used without modification, outside of the molecular weight range in which they were deduced. It should be noted that  $[\eta]$  is sensitive to temperature in the vicinity of  $\theta$  importantly when  $M$  is

higher than  $5 \times 10^5$ . In usual solvents, the constants  $K$  and  $a$  obtained are valid only within a rather limited range of  $M$ . Therefore the literature relationships will be in error outside the indicated range of  $M$ . As for the effect of temperature, however, both  $K$  and  $a$  mostly become insensitive to the temperature when  $a$  exceeds about 0.70, and they may be used in a 10-degree range on either side of temperature at which the constants were determined. (J.Brandrup 1999)

#### 5.4. Sample Calculation of Rate Constant

Using the above equation the rate constant was worked out for the 2.5% ultrasound probe Nafion® solution at 20% amplitude.

$$A = (2.769 - 1.538) / (5.466 - 1.538) = 0.313$$

$$\ln A \ 0.313 = -1.162.$$

$$A = (2.769 - 1.538) / (5.415 - 1.538) = 0.3175$$

$$\ln A \ 0.3175 = -1.147$$

$$A = (2.769 - 1.538) / (5.394 - 1.538) = 0.3192$$

$$\ln A \ 0.3192 = -1.142$$

$$A = (2.769 - 1.538) / (5.318 - 1.538) = 0.32566$$

$$\ln A \ 0.32566 = -1.122$$

$$A = (2.769 - 1.538) / (1.909 - 1.538) = 7.1988$$

$$\ln A \ 7.1988 = 1.9739$$

The plot of  $\ln A$  against sonication time gives the rate constant from the graph below.

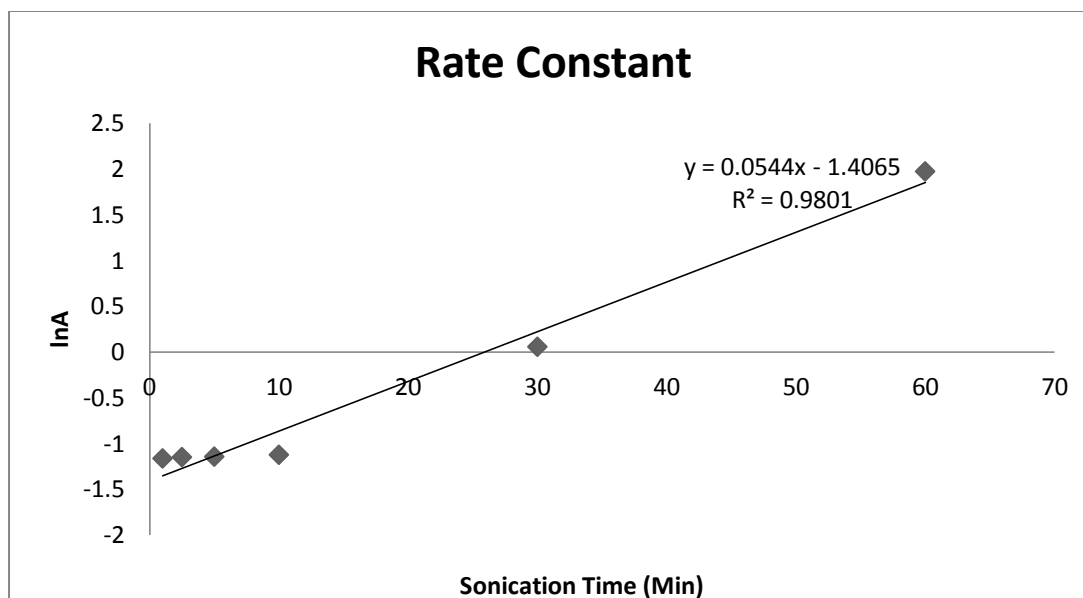


**Figure 52 graph of ln A vs Sonication time For 2.5% Nafion® Solution**

The same calculations were carried out for different Nafion® concentrations of 5, 7.5 and 10% at different ultrasound powers and then the plot of ln A against sonication time deduced the rate constant. The different rate constants are presented in the table below.

**Table 15 showing the calculated rate constants for Nafion® at various concentrations**

Rate Constant K (Min <sup>-1</sup> )	Nafion® concentration (wt %)
0.0544	2.5
0.0773	5
0.1021	7.5
0.1067	10

**Table 16 Showing reverse concentratin vs K values**

Calculated K Values k (Min <sup>-1</sup> )	Reverse Concentration (wt %)
0.0544	2.5
0.0773	5.0
0.1021	7.5
0.1067	10

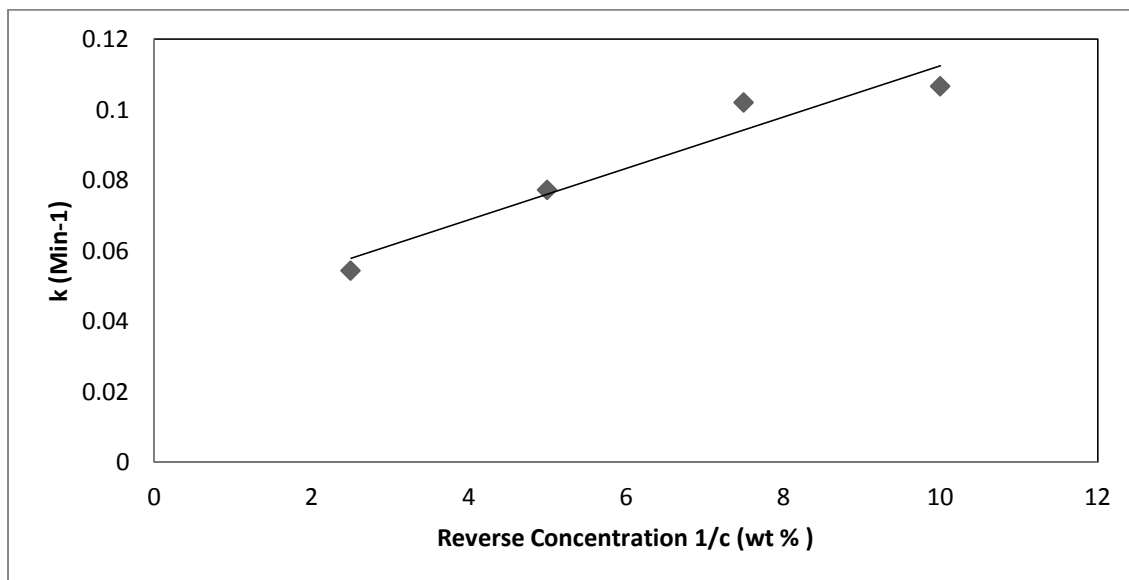


**Figure 53 Graph showing the relationship between the calculated Rate constant and Reverse Concentration**

The calculated rate constants,  $k$ , are correlated in terms of reverse solution concentration and the data indicates that, the rate constant of ultrasonic degradation decreases with increasing solution concentration. The analysis of these observations is that there is less overlap between polymer chains at low concentration. Therefore, they are more susceptible to the hydrodynamic forces generated around cavitation bubbles. This is found to be similar to work carried out in the literature by Mohammed Taghi and Abbas Mehrdad. (Taghizadeh 2003).

## 6. CHAPTER 6 FURTHER WORK

It has been shown that ultrasound causes the degradation of Nafion® polymer at certain power and irradiation time. However, under carefully chosen conditions, it is possible to initiate polymerization reactions using ultrasound, the products obtained vary depending on the functional groups present or absent. Further study is needed to see how the nature of the product and the polymerization rate changes with conditions, for example; temperature, adducts, impurities, solvents, gases, pulsing of ultrasound, intensity, frequency, etc.

### 6.1. MEA Preparation for Ultrasound Effects

To see the Nafion® polymer behaviour in the fuel cells we would need to build an MEA to see if ultrasound really does enhance the thermal stability and hence improves the general durability of the membrane. Catalyst ink will be prepared by mixing 40 wt% Pt/C (E-tek, Inc.) With isopropyl alcohol (Baker Analyzed HPLC Reagent) and then it will be sonicated for 1 h. (5 wt% Nafion® solution (Du Pont, Inc.) will be added to the catalyst ink, which will be sonicated again for 1 h. MEAs will be fabricated by a conventional method. For the conventional MEA, the prepared catalyst ink is sprayed on a wet-proofed carbon paper (Sigracet®, SGL Carbon Inc.) to make an electrode. Then, the electrodes will be placed on both sides of a pre-treated Nafion®112 membrane and hot pressed. , the active electrode area will be 25 cm<sup>2</sup> with catalyst loading of 0.3 and 0.4 mg Pt cm<sup>-2</sup> for anode and cathode, respectively, and hot pressing will be conducted at 140°C with a compaction pressure of 200 kgcm<sup>-2</sup>for 90 s. Single cells will be assembled with a prepared MEA, Teflon gaskets, and 5 channel semi-serpentine graphite blocks. H<sub>2</sub> and O<sub>2</sub> or air will be fed to the anode and cathode, respectively. The stoichiometry of H<sub>2</sub> and O<sub>2</sub> or air will be 1.5 and 3 with relative humidity of 100 and 55%, respectively. The cell temperature will be 80°C. The same fabrication procedure will be followed for the making an MEA that incorporates ultrasound treated Nafion® and instead of placing the electrodes in conventional Nafion® they will be treated with sonicated Nafion® and hot pressed.(Prasanna 2008).(Chen and Fuller 2009)

## **6.2. Testing Of MEA with Nafion® Incorporated Membrane**

Chemical and physical characteristics of the MEAs will be investigated by mercury porosimetry, X-ray diffraction (XRD), scanning electron microscopy (SEM) combined with electron probe micro analysis (EPMA), and Fourier transformation infrared spectroscopy (FTIR). Before and after long-term operation to see how the MEA made from ultrasound treated Nafion® behaves in terms of performance and stability. (Prasanna 2008)

## **6.3. Structural Changes following Ultrasonic Treatment of Nafion®**

As we know that ultrasound increases the Tg of Nafion® at various ultrasonic power and time therefore the next step would be to observe the structural changes in Nafion® following ultrasonic treatment of the polymer. This would give us an idea of how the structure is modified that results in an increase in the glass transition temperature of Nafion®. As we know an increase in Tg results in better mechanical stability therefore this can be of an extreme importance in fuel cell operation. Currently one of the issues associated with PEM fuel cells is the durability of the Nafion® in the fuel cell operation but as the results of ultrasound treatment of Nafion® shows promising results of increase in Tg therefore means ultrasound as a promising method of fabricating Nafion® membranes for fuel cell use.

The advantage of observing the structural changes for the samples that show increase in Tg will mean that the results can easily be reproduced and confirmed, also the toughness depends on morphology. A common method used for determining morphology is by using Scanning Electron Microscopy (SEM).

#### 6.4. Determination of Mechanical properties After Sonication

The mechanical properties of Nafion® should be tested after sonication to see if sonication improves mechanical properties. This is of extreme important because currently the degradation of Nafion® membrane is a big problem due to the fact that Nafion® although a perfect polymer for use in fuel cells is not durable. The mechanical properties following ultrasound irradiation needs to be investigated to see if it can enhance the durability of the Nafion® membrane in fuel cells. The tensile stress to break and young modulus versus sonication needs to be plotted by using LR5KPlus 5 kN and an impact tester (*Ceast Model 6545*). The LR5KPlus 5 kN is used for routine quality control testing or complex multi-stage tests and can perform Tensile experiments. The *Young Modulus, E* is a material property that describes its stiffness and is therefore one of the most important properties in engineering design. Therefore an enhancement in the Young Modulus can result in improved durability. From the literature it has been reported by Youngjoo Lee et al that specific ultrasound power and time can improve tensile stress to break and *Young Modulus* at short irradiation time of ultrasound but soon reached a peak and decreased. Therefore finding the right irradiation power and time seems like an interesting concept for improving the mechanical properties of Nafion® in fuel cell operation. As we already know some of the ultrasound frequencies of interest this would be an easy next task.

#### 6.5. Additional Work

It is also suggested that future work needs to be carried out on the effect of stabilisers on Nafion®. Stabilizers for polymers are used directly or by combinations to prevent the various effects such as oxidation, chain scission and uncontrolled recombination's and cross-linking reactions that are caused by photo-oxidation of polymers. Polymers are considered to get weathered due to the direct or indirect impact of heat and ultraviolet light. The stabilizers can have desirable effects for fuel cell use but the effect of other parameters after incorporation needs to be examined such as permeability across the Nafion® membrane.

## 7. CHAPTER 7 CONCLUSION

### 7.1. Conclusions

According to the results of this study it was found that ultrasound degrades the Nafion® polymer. The most extensive degradation was observed at the lowest frequency when the input power was above the cavitation threshold. There was also sudden increase in Nafion® viscosity. This was attributed to scission of polymer bonds due to ultrasound (depolymerisation) supplies new chain carriers for polymerization. Under carefully chosen conditions, it was possible to initiate polymerization reactions using ultrasound. The manufacturing of MEA using ultrasound would therefore require specific conditions to get the desired effect such as improving the mechanical toughness of the Nafion®. Normally during the production process catalysts or initiators are used to start the polymerization reaction, which also contaminate the final product. These chemicals are not required using ultrasound, as it can produce radicals in situ from the reactants, this had a desired effect in our results because at certain frequency and irradiation time where the Tg was shown to increase from the Dsc studies was also the same frequency at which polymerization was shown to occur thereby proving that ultrasound increases the Tg which is desirable in fuel cells. Therefore for the fabrication of MEA using ultrasound the required ultrasonic frequency and time would be 30 minutes ultrasound at 1.86 W using ultrasonic probe for the 5% Nafion®. At this frequency of ultrasound the Nafion® glass transition increases and therefore means the durability of the Nafion® membrane is enhanced. This has another benefit because high temperatures are desirable for a better efficiency and CO tolerance, ultrasound prepared MEA using the specific frequency and irradiation time will advance the PEM Fuel cells.

It was shown by Differential Scanning Calorimetry that at specific time and frequency of ultrasound irradiation there was an increase in the glass transition temperature of Nafion® from its original value in the literature. The fact that an increase in glass transition temperature results in better thermal stability and toughness of the polymer, it is then concluded that Ultrasound can prove to be a very advantageous method for fabrication of Nafion® as it has been for fabrication of other fuel cell materials. These results were also confirmed by some other work on different polymers.



The effect of high shear mixer on Nafion® at various speeds analogous to the use of ultrasound at different powers was also investigated to compare its effect on the polymer. However, it was found that high shear mixer resulted in a gradual decrease in viscosity of the polymer due to degradation and there were no sudden increases in viscosity. Thus it was concluded that high shear mixing only degrades the polymer and does not initiate polymerization. Furthermore the glass transition temperature from Differential Scanning Calorimetry either showed no change in Tg or decrease in Tg from its original value in the literature.

The GC/MS spectrums for various ultrasound treated Nafion® samples did not show the mode of degradation and therefore we could not conclude anything about the Sonochemical degradation of Nafion®. It is suggested to use Solid State NMR for future identification of degradation modes due to Solid State NMR being more suitable technique.

## References

Alwai, K. B. M. (2009). Thermal degradation and morphology of polymer blends comprising poly( $\epsilon$ -caprolactone) and epoxidized natural rubber with addition of phenol as catalyst. Chemistry, Mara, Universiti Teknologi. **Bachelor Of Science (Hons):** 1-24.

Carlsson, A.H. Jorissen, L. Tillmetz, W. (2011). Degradation of PFSA Membrane in Fuel Cell. Germany, Baden-Württemberg (ZSW).

Balakrishnan, R. K. Guria, C. (2007). "Thermal degradation of polystyrene in the presence of hydrogen by catalyst in solution." Polymer Degradation and Stability **92**(8): 1583-1591.

Barbir, F.(2001). PEM Fuel Cells. 27 - 51

Berlin, A. A, Dubinskaya, A. M. (1962). "Studies in the mechanochemistry of polymers—X. Initiation of polymerization by radicals formed during the ultrasonic degradation of macromolecules." Polymer Science U.S.S.R. **3**(2): 345-351.

BP (2011). "BP Statistical Review of World Energy June 2011." Retrieved 06/2011.

Booth, C. (1963). "The mechanical degradation of polymers" Polymer **4**: 471-478.

Chen, C. and Fuller. T.F (2009). "The effect of humidity on the degradation of Nafion® membrane." Polymer Degradation and Stability **94**(9): 1436-1447.

Chen, Y. Li, H. (2005). "Phase morphology evolution and compatibility improvement of PP/EPDM by ultrasound irradiation." Polymer **46**(18): 7707-7714.

Curtin, D. E. Lousenberg, R.D. Henry, T.J, Tangeman, P.C. Tisack, M.E. (2004). "Advanced materials for improved PEMFC performance and life." Journal of Power Sources **131**(1-2): 41-48.

Desai, V. Mohan, A.S. Gogate, P.R. (2008). "Degradation of polypropylene using ultrasound-induced acoustic cavitation." Chemical Engineering Journal **140**(1-3): 483-487.

Fernandes, A. C. and Ticianelli, E.S. (2009). "A performance and degradation study of Nafion 212 membrane for proton exchange membrane fuel cells." Journal of Power Sources **193**(2): 547-554.

Gareth, J.P. (2003). "Recent developments in sonochemical polymerisation." Ultrasonics Sonochemistry **10**(4-5): 277-283.

Ghassemzadeh, L . Kreuer, K.D. Maier, J. Müller, K. (2011). "Evaluating chemical degradation of proton conducting perfluorosulfonic acid ionomers in a Fenton test by solid-state <sup>19</sup>F NMR spectroscopy." Journal of Power Sources **196**(5): 2490-2497.

Goyat, M. Ray, S. Ghosh, P. K. (2011). "Innovative application of ultrasonic mixing to produce homogeneously mixed nanoparticulate-epoxy composite of improved physical properties." Composites Part A: Applied Science and Manufacturing **42**(10): 1421-1431.

Grönroos, A. Pirkonen, P. Heikkinen, J. Ihalainen, J. Mursunen, H. Sekki, H. (2001). "Ultrasonic depolymerization of aqueous polyvinyl alcohol." Ultrasonics Sonochemistry **8**(3): 259-264.

Hao, C. Xiaoming, Z. Yang, Paul. (2007). "GC-MS and HPLC-MS analysis of bioactive pharmaceuticals and personal-care products in environmental matrices." TrAC Trends in Analytical Chemistry **26**(6): 569-580.

Santos, H.M. Lodeiro, C. Capelo-Martínez, J.L. (2009). The Power of Ultrasound. Ultrasound in Chemistry: Analytical Applications. J.-L. Capelo-Martínez: 1-16.

Petit, J.R. Jouzel, J. Raynaud, D. Barkov, N.I. Barnola, J.M. Basile, I. Bender, M. Chappellaz, J. Davis, M. Delaygue, G. Delmotte, M. Kotlyakov, V.M. Legrand, M. Lipenkov, V.Y. Lorius, C. Pe´ pin, L. Ritz, C. Saltzman, E. Stievenard, M. (1999). "Climate and atmospheric history of the past 420,000 years from the Vostok ice core, Antarctica. Nature **399**.

Brandrup, J. Immergut, E.H. Grulke, E.A. (1999). Polymer Handbook, A John Wiley & Sons.

Karaman, S. Yilmaz, M.T. Ertugay, M.F. Baslar, M. Kayacier, A. (2012). "Effect of ultrasound treatment on steady and dynamic shear properties of glucomannan based salep dispersions: Optimization of amplitude level, sonication time and temperature using response surface methodology." Ultrasonics Sonochemistry **19**(4): 928-938.

King, C. J. (2009). A MODEL OF DEGRADATION IN A POLYMER ELECTROLYTE MEMBRANE. Environmental Resources Engineering. HUMBOLDT, HUMBOLDT STATE UNIVERSITY. **Masters of Science**: 1-44.

Kurniawan, D. Arai, H. Morita, S. Kitagawa, K. (2013). "Chemical degradation of Nafion ionomer at a catalyst interface of polymer electrolyte fuel cell by hydrogen and oxygen feeding in the anode." Microchemical Journal **106**(0): 384-388.

Leblanc, R. (2010). The Effect of Ultrasound on a Catalyst Ink and on Water Electrolysis. Chemical Engineering. Birmingham, University of Birmingham.

Li, J. Guo, S. Li, X. (2005). "Degradation kinetics of polystyrene and EPDM melts under ultrasonic irradiation." Polymer Degradation and Stability **89**(1): 6-14.

Li, J. Liang, M. Guo, S. Ying, L. (2004). "Studies on chain scission and extension of polyamide 6 melt in the presence of ultrasonic irradiation." Polymer Degradation and Stability **86**(2): 323-329.

Mohod, A. V. Gogate, P.R. (2011). "Ultrasonic degradation of polymers: Effect of operating parameters and intensification using additives for

carboxymethyl cellulose (CMC) and polyvinyl alcohol (PVA)." Ultrasonics Sonochemistry **18**(3): 727-734.

Nguyen, N. T. Lethiecq, M. Gerard, J.F. (1995). "Glass transition characterization of homogeneous and heterogeneous polymers by an ultrasonic method." Ultrasonics **33**(4): 323-329.

Pollet, B. G. (2010). "The use of ultrasound for the fabrication of fuel cell materials." International Journal of Hydrogen Energy **35**(21): 11986-12004.

Prasanna, M. Cho, E. A. Lim, T.H. Oh, I.H. (2008). "Effects of MEA fabrication method on durability of polymer electrolyte membrane fuel cells." Electrochimica Acta **53**(16): 5434-5441.

Price, G. J. and P. F. Smith (1993). "Ultrasonic degradation of polymer solutions: 2. The effect of temperature, ultrasound intensity and dissolved gases on polystyrene in toluene." Polymer **34**(19): 4111-4117.

Price, G. J. West, P. J. Smith, P.F. (1994). "Control of polymer structure using power ultrasound." Ultrasonics Sonochemistry **1**(1): S51-S57.

Psillakis, E. Mantzavinos, D. Kalogerakis, N. (2004). "Monitoring the sonochemical degradation of phthalate esters in water using solid-phase microextraction." Chemosphere **54**(7): 849-857.

Redl, A. Guilbert, S. Morel, M.H. (2003). "Heat and shear mediated polymerisation of plasticized wheat gluten protein upon mixing." Journal of Cereal Science **38**(1): 105-114.

Riesz, P. and Takashi, K. (1992). "Free radical formation induced by ultrasound and its biological implications." Free Radical Biology and Medicine **13**(3): 247-270.

Satterfield, M. B. (2007). Mechanical and water sorption properties of nafion and composite nafion/titanium dioxide membranes for polymer

electrolyte membrane fuel cells. . Chemical Engineering, Princeton University. **Doctor of Philosophy**: 1-224.

Shertzer, H. G. Bannenberg, G.L. Rundgren, M. Moldéus, P. (1991). "Relationship of membrane fluidity, chemoprotection, and the intrinsic toxicity of butylated hydroxytoluene." Biochemical Pharmacology **42**(8): 1587-1593.

Taghizadeh, M. T. Mehrdad, A. (2003). "Calculation of the rate constant for the ultrasonic degradation of aqueous solutions of polyvinyl alcohol by viscometry." Ultrasonics Sonochemistry **10**(6): 309-313.

Vijayalakshmi, S. P. and G. Madras (2004). "Effect of temperature on the ultrasonic degradation of polyacrylamide and poly(ethylene oxide)." Polymer Degradation and Stability **84**(2): 341-344.

Watanabe, C. Tsuge, S. Ohtani, H. (2009). "Development of new pyrolysis-GC/MS system incorporated with on-line micro-ultraviolet irradiation for rapid evaluation of photo, thermal, and oxidative degradation of polymers." Polymer Degradation and Stability **94**(9): 1467-1472.

Wei, S. Valentina, P. Schreiner, M. (2012). "Photochemical degradation study of polyvinyl acetate paints used in artworks by Py-GC/MS." Journal of Analytical and Applied Pyrolysis **97**(0): 158-163.

Weir, N.A. Buchanan, F.J. Orr, J.F. Farrar, D.F. Boyd, A. (2004). "Processing, annealing and sterilisation of poly-l-lactide." Biomaterials **25**(18): 3939-3949.

Wu, J. Yuan, X.Z. Martin, J.J. Wang, H. Zhang, J. Shen, J. Wu, S. Merida, W. (2008). "A review of PEM fuel cell durability: Degradation mechanisms and mitigation strategies." Journal of Power Sources **184**(1): 104-119.

Xie, T. and Hayden, C.A. (2007). "A kinetic model for the chemical degradation of perfluorinated sulfonic acid ionomers: Weak end groups versus side chain cleavage." Polymer **48**(19): 5497-5506.